LBL-7895
c.2

RECEIVED
LAWRENCE
BERKELEY LABORATORY

NOV 1 1978

LIBRARY AND
DOCUMENTS SECTION

TWO-WEEK LOAN COPY

This is a Library Circulating Copy
which may be borrowed for two weeks.
For a personal retention copy, call
Tech. Info. Division, Ext. 6782

Energy and Environment Division

Investigations on the Use of Anodic Stripping Voltammetry for the Analyses of Lead in Saline Environments

Charles W. Case
(Ph.D. thesis)

August 1978

Lawrence Berkeley Laboratory University of California/Berkeley
Prepared for the U.S. Department of Energy under Contract No. W-7405-ENG-48

LBL-7895
c.2

LEGAL NOTICE

This report was prepared as an account of work sponsored by the United States Government. Neither the United States nor the Department of Energy, nor any of their employees, nor any of their contractors, subcontractors, or their employees, makes any warranty, express or implied, or assumes any legal liability or responsibility for the accuracy, completeness or usefulness of any information, apparatus, product or process disclosed, or represents that its use would not infringe privately owned rights.

Investigations on the use of Anodic Stripping Voltammetry for the Analyses of Lead in Saline Environments

By

Charles Whipple Case

A.B. (San Francisco State University) 1973
M.A. (University of California) 1974

DISSERTATION

Submitted in partial satisfaction of the requirements for the degree of

DOCTOR OF PHILOSOPHY

in

Engineering

in the

GRADUATE DIVISION

of the

UNIVERSITY OF CALIFORNIA, BERKELEY

Approved:

Pat Wilde

Alex J. Horne

N. J. Monson

Committee in Charge

ABSTRACT

Investigations on the Use of Anodic Stripping Voltammetry for the Analyses of Lead in Saline Environments

By

Charles W. Case

This research modifies the anodic stripping voltammetry (ASV) analytic method in order to acquire data for lead from ambient sea water conditions, and develops a chemical model which uses these data to identify inorganic lead species for saline environments.

These modifications are made: (a) the nitrogen purge is eliminated in order to maintain both the pH of the water samples and ambient conditions for the lead species; (b) electrodes are constructed using a simplified process; and (c) an inexpensive portable instrument, which is easily moved and repaired, is assembled with standard laboratory components. This simple instrumentation and methodology allow ASV techniques to be used for trace element analysis on shipboard or in remote locations. By changing the analysis controls, including the nitrogen purge, the data reflect ambient sea water conditions rather than conditions which have been altered for analysis.

Laboratory and field samples were analyzed for lead partitioning in: (a) KCl electrolyte solutions; (b) I.A.P.S.O. Standard Sea Water; (c) sea water samples from Quatsino Sound, British Columbia; (d) a series of sea water samples from San Francisco Bay; and (e) sea water samples from the Gulf of Mexico.

The electrochemical traits of the lead species and the ASV oxidation potential expression, which are developed in detail, are the fundamental constituents of the chemical model. The model uses the data from the analyses to provide the mass balance relationships for lead partitioned among the major anions in sea water. Theoretically these partitions, or species of lead, in order of dominance include Pb^{++}, $PbCO_3^o$, $PbSO_4^o$, $PbSO_4^{++}$, $PbCl^+$, $PbOH^+$, $PbCl_2^o$, $PbCl_3^-$, $PbCl_4^=$, $Pb(OH)_2^o$, $Pb(OH)_3^-$, and $Pb(OH)_4^=$.

The laboratory analyses of KCl electrolyte and Standard Sea Water give the following results. The modified ASV method and chemical model provide information on ambient labile and non-labile inorganic lead complexes in these saline solutions down to the parts-per-billion level. No purge and the simple electrodes cause some erratic behavior and spurious potentials, but the data are reproducible. In addition to Pb^{++}, the most dominant measured lead species in order include $PbCO_3^o$, $PbSO_4^o$, $PbCl^+$, and $Pb(NO_3)_2^o$ from the lead additions solution. These results agree with recent theoretical chemical models but in a few cases disagree with other laboratory analyses, probably because of the change in the purge.

The analyses of the field samples give the following results. Samples were taken from the partially anoxic basin in Quatsino Sound, British Columbia with one successful analysis which is for somewhat normal dissolved oxygen conditions. Data show that lead is partitioned among Pb^{++}, $Pb(OH)_2^o$, $PbCO_3^o$, and $PbSO_4^o$. The analyses with purge for the San Francisco Bay water partitions lead among Pb^{++}, $PbCO_3^o$, $PbSO_4^o$, $PbCl^+$, and $PbOH^+$. With successive lead additions $Pb(NO_3)_2^o$ is decidedly the dominant species. These results agree with other recent chemical

models cited in the thesis. The samples from the Gulf of Mexico contain lead at the parts-per-trillion level which is below the level of detection for this method.

Pat Miller

ACKNOWLEDGMENT

The traditional first acknowledgment goes to Dr. Pat Wilde of the Lawrence Berkeley Laboratory for his support, encouragement, and advice on all facets of this work. Thanks are also due the other members of my thesis committee, Professors H. Frank Morrison and Alex J. Horne of the University of California. Mr. Roy N. Anaclerio, Mr. Al Hodgson, and Dr. James C. Sandusky of the Lawrence Berkeley Laboratory either collected or helped collect the sea water samples from the Gulf of Mexico and San Francisco Bay. Mr. Mark E. Tatro, also of the Lawrence Berkeley Laboratory, in addition to helping with the water sampling, advised me on laboratory techniques, and was a consoling friend when needed. Another source of both solace and much practical electrochemical information was Dr. Robert Corwin of the University of California.

A special thanks goes to Ms. Janet L. McQuillan for proof reading and typing this thesis. In particular, her late night and weekend work on the figures and tables is certainly above the normal call of duty. Another special thanks goes to Lawrence Berkeley Laboratory Energy & Environment Division Office personnel. Dr. Robert J. Budnitz (Division Head), Dr. Melvin K. Simmons (Deputy Head - now at the Solar Energy Research Institute in Golden, Colorado), and Ms. Barbara West provided encouragement and moral support, and deserve a special acknowledgment. Mr. José M. Alvarez, Ms. Janette M. Bacon, Ms. Dorothy L. Bottini, Ms. Hannah Clark, Mr. Jeff Kessel, Ms. Yvonne J. Ladson, Ms. Maria T. Ossa, and Ms. Angela P. Smothers each helped in many small and large ways

(including tolerating an uneven disposition during the final months), and I hope to return the many favors.

Finally, I include my wife, Kay, and my children, Charles, George, and Ford. Without their support I would not have set out upon this adventure some time ago, and with their support and love this adventure is now complete.

This work was supported by the U. S. Department of Energy.

CONTENTS

Acknowledgments i

Contents iii

Figures vii

Tables x

Glossary xii

Chapter I - Introduction 1

Engineering Background 2

Chemical Modeling Procedures 3

Research Emphasis 9

Historical Development of ASV 10

Lead 13

Summary of Research 16

Chapter II - ASV Theory of Applied Potential 19

Introduction 20

Components of ϕ 21

E - Electromotive Force of a Reversible Cell 21

E_{ref} - Reference Electrode Potential 27

IR_{cell} - Ohmic Potential Drop 29

E_{misc} - Miscellaneous Potentials 29

η_{conc_c} - Cathodic Concentration Over-Potential 30

η_{conc_a} - Anodic Concentration Over-Potential 37

η_{trans_c} - Cathodic Transfer Over-Potential 38

η_{trans_a} - Anodic Over-Potential 43

Reduction Potential Expression 44

Oxidation Potential Expression 48

Chapter III - ASV Techniques 54

Conventional ASV - Analysis Procedure 55

Chapter IV - Laboratory Analysis - Part I - Standard Procedures 61

Introduction 62

Instruments and Components 62

Analysis Cell 65

Reference Electrode 65

Counter Electrode 67

Working Electrode 67

Glass Purge Frit 68

Lab Stand 68

Magnetic Stirring Unit 71

Resistance Box 71

Power Supply (1) 71

X-Y Recorder 71

Sweep (Circuit Integrator) 73

Power Supply (2) 73

Digital Multimeter (1) 73

Digital Voltmeter (2) 73

Digital Voltmeter (3) 74

Timer 74

Miscellaneous Equipment 74

Analysis Techniques 74

Glass and Plasticware 75

Electrode Procedures 78

Trace Element Addition Solutions 78

A Standard Sample Analysis in KCl 79

Chapter V - Laboratory Analysis - Part II - Modified

Procedures and Chemical Model 84

Nitrogen Purge 85

Laboratory Experiments - KCl - No Purge 89

Laboratory Experiments - Sea Water - Purge 91

Laboratory Experiments - Sea Water - No Purge 97

Modeling and Partitioning of Lead in Sea Water 98

Electrochemical Traits of Certain Lead Species 105

Particulate Lead 107

Labile (unstable) Lead 107

Non-Labile (unstable) Lead 111

The Chemical Model 112

Chapter VI - Results - Chemical Modeling With Field

Samples 115

Calculations for Model - The Constant E_k 116

$E_{\frac{1}{2}cell}$ for Chemical Forms of Lead 119

Chemical Model of Laboratory Samples 130

KCl with Purge 130

KCl without Purge 137

Sea Water with Purge 140

Sea Water with Purge 140

Sea Water without Purge 146

Conclusions on Analysis of Laboratory Samples 150

Field Samples - Quatsino Sound, British Columbia 153

Field Samples - San Francisco Bay 162

San Francisco Bay Water with Purge (A) 164

San Francisco Bay Water with Purge (B) 170

San Francisco Bay Water with Purge (C) 170

San Francisco Bay Water without Purge (A, B, and C) . 179

Below the Threshold of Detection - Field Samples -

Gulf of Mexico 182

Appendices 185

Appendix A - Lead Data 186

Appendix B - Activity Coefficient Methods 189

Appendix C - Electrode Over-Potential 193

Inert Electrodes 193

Double Layer at Electrode-Solution Interface 194

Faradic and Non-Faradic Current 195

Appendix D - Sampling Techniques in San Francisco Bay .. 201

References 205

FIGURES

2-1 ASV Analysis Cell with Electrodes 26

2-2 ASV Electrode Configuration 46

3-1 Reduction and Oxidation Curve 58

4-1 Laboratory Layout 63

4-2 Plastic Tent for ASV 64

4-3 Analysis Cell and Electrode Configuration 69

4-4 Analysis Cell and Laboratory Stand 70

4-5 Component Diagram 72

4-6 KCl Analysis - Purge 80

4-7 Concentration of Lead in KCl (With N_2 Purge) 83

5-1 KCl Analysis - No Purge 90

5-2 Concentration of Lead in KCl - No Purge 92

5-3 Sea Water Analysis - Purge 94

5-4 Concentration of Lead in Sea Water - Purge 95

5-5 Concentration of Lead in Sea Water After 6 Month Storage 96

5-6 Sea Water Analysis - No Purge 99

5-7 Concentration of Lead in Sea Water - No Purge 100

6-1 Measured Potential During Stripping in KCl of Lead (with purge) 133

6-2 Current Repression of Non-Labile Lead - KCl Electrolyte (purge) 134

6-3 Measured Potential During Stripping in KCl of Lead (without purge) 138

6-4 Current Repression of Non-Labile Lead - KCl Electrolyte (no purge) 139

6-5 Measured Potential of Lead During Stripping in Sea Water (with purge) 142

6-6 Current Repression of Non-Labile Lead - Sea Water (with purge) 144

6-7 Measured Potential During Stripping of Lead in Sea Water (without purge) 147

6-8 Current Repression for Non-Labile Lead - Sea Water (no purge) 149

6-9 Chemical Forms vs. Concentrations - Electrolyte 154

6-10 Chemical Forms vs. Concentrations - Sea Water 155

6-11 Map of Quatsino Sound, British Columbia 157

6-12 Analysis of Samples from Quatsino Sound, British Columbia 160

6-13 Sampling Locations in San Francisco Bay 163

6-14 Analysis of San Francisco Bay Water - Sample (A) 165

6-15 Calibration Curve - Concentration of Lead in Bay Sample: Analysis (A) 166

6-16 Measured Potential of Lead During Stripping - San Francisco Bay Water (with purge) - Sample (A) ... 167

6-17 Current Repression of Non-Labile Lead - San Francisco Bay Water (purge) - Sample (A) 168

6-18 Analysis of San Francisco Bay Water - Sample (B) 171

6-19 Calibration Curve - Concentration of Lead in Bay Sample - Analysis (B) 172

6-20 Measured Potential of Lead During Stripping - San Francisco Bay Water (with purge) - Sample (B) ... 173

6-21 Current Repression of Non-Labile Lead - San Francisco Bay Water (purge) - Sample (B) 174

6-22 Analysis of San Francisco Bay Water - Sample (C) 175

6-23 Calibration Curve - Concentration of Lead in Bay Sample: Analysis (C) 176

6-24 Measured Potential of Lead During Stripping - San Francisco Bay Water (purge) - Sample (C) 177

6-25 Current Repression of Non-Labile Lead - San Francisco Bay Water (purge) - Sample (C) 178

6-26 Analyses of San Francisco Bay Water (without purge) . 181

C-1 Current vs. Potential Curves for Polarizable and Non-Polarizable Electrodes 197

C-2 Schematic Diagram of the Electrode Double Layer 198

C-3 Schematic Circuit Diagram of Electrode - Solution Interface 199

TABLES

1-1 Steps in the Development of a Chemical Model for Sea Water 5

4-1 ASV Components 66

4-2 Some Variables to Control in a Typical ASV Experiment 76

4-3 Miscellaneous ASV Analysis Items 77

4-4 Calibration for Pb in KCl (with purge) 81

5-1 Calibration for Pb in KCl (without purge) 89

5-2 Calibration for Pb in Sea Water (with purge) 93

5-3 Calibration for Pb in Sea Water (without purge) 97

5-4 General Partitioning of Lead in Sea Water 103

5-5 Partitioning of Lead in Sea Water with Major Anions . 104

5-6 Electrochemical Traits of Various Chemical Forms of Lead 106

6-1A $E_{\frac{1}{2}cell}$ for Chemical Forms of Lead 120

6-1B $E_{\frac{1}{2}cell}$ for Chemical Forms of Lead 123

6-2 E_{total} Without Activities for Complexes 128

6-3 E_{total} With Activities for Complexes 131

6-4 Chemical Forms of Lead in KCl Electrolyte (purge) ... 136

6-5 Chemical Forms of Lead in KCl Electrolyte (no purge) 141

6-6 Chemical Forms of Lead in Sea Water (purge) 145

6-7 Chemical Forms of Lead in Sea Water (no purge) 151

6-8 Samples from Rupert Inlet, Quatsino Sound, British Columbia 158

6-9 Chemical Forms of Lead in Sea Water - Rupert Inlet, Quatsino Sound, British Columbia 161

6-10 Chemical Forms of Lead in Sea Water - San Francisco Bay (with purge) 180

6-11 Chemical Forms of Lead in Sea Water - San Francisco Bay (without purge) 183

GLOSSARY

a = mean diameter of ions (cm)

a_j = activity of the jth component

a_j^o = experimental value dependent on the effective diameter of the jth ion in solution (cm)

A = Debye - Hückel constant characteristic of the solvent $(kg/mole)^{\frac{1}{2}}$

A_e = electrode area (cm^2)

B = Debye - Hückel constant characteristic of the solvent $(kg/mole)^{\frac{1}{2}}/Å$

C = capacitance (farads)

C_j = concentration of species j ($moles/cm^3$)

C_b = concentration of species in the bulk solution ($moles/cm^3$)

C_o = concentration of species due to oxidation ($moles/cm^3$)

C_r = concentration of species due to reduction ($moles/cm^3$)

C_s = concentration of species at the electrode surface ($moles/cm^3$)

D_j = diffusion coefficient of species j (cm^2/sec)

e = base of Napierian logarithm

e_e = electronic charge (1.6021×10^{-19} coulombs)

E = electromotive force of a reversible cell reaction (volts)

E^o = electromotive force of a reaction when all substances are at unit activity (volts)

E_{comp} = potential of components (volts)

E_e = equilibrium potential (volts)

E_k = potential constant (volts)

E_m = measured potential (volts)

$E_{misc.}$ = miscellaneous potentials (volts)

E_{ref} = potential of a reference electrode (volts)

E_t = total potential for a reaction (volts)

$E_{\frac{1}{2}}$ = electromotive force of a ½ cell reaction (volts)

f_j = fugacity of the dissolved component j

f_j^o = fugacity of the dissolved component j in the standard state

F = Faraday constant (96,487 coulombs/equivalent)

G = Gibbs Free Energy (joules)

i = current density (amps/cm^2)

i_o = exchange or equilibrium current density (amps/cm^2)

i_c = capacitor current density (non-faradic) (amps/cm^2)

i_f = faradic current density (amps/cm^2)

i_p = peak current density (amps/cm^2)

i_l = limiting current density (amps/cm^2)

i_t = total current density (amps/cm^2)

i_{anode} = anodic current density (amps/cm^2)

$i_{cathode}$ = cathodic current density (amps/cm^2)

IR_{cell} = ohmic potential drop (ohms)

I_s = ionic strength (mole/kg)

k,K = thermodynamic equilibrium constant (mole/liter)

K_c = reaction rate constant (cm/sec)

K_o = oxidation rate constant (cm/sec)

K_o^o = oxidation rate constant with E = 0 (cm/sec)

K_r = reduction rate constant (cm/sec)

K_r^o = reduction rate constant with E = 0 (cm/sec)

$K_{L(i)_n}$ = dissociation rate for a labile ligand (cm/sec)

l = mercury film (amalgam) thickness (cm)

$L(i)_n$ = uncomplexed ligand or anion

m = molality of a single electrolyte (mole/kg)

m_j = molality of the jth ion

$[M]_{total}$ = total metal concentration

$[M]$ = uncomplexed and/or hydrated metal ion concentration

$[ML(i)_n]$ = concentration of the nth order complex between the metal M and the ligand L(i)

n_j = mole fraction of the jth component in solution

n = number of the electrons involved in the reaction

N = number of Moles

N_j = flux of species j (moles/cm^2-sec)

N_o = number of moles - oxidation reaction

N_r = number of moles - reduction reaction

q = electricity passed (coulombs)

q_f = electricity passed - faradic (coulombs)

q_c = electricity passed - capacitor (coulombs)

R = gas constant (8.3143 joules/mole-deg.)

R_{cell} = cell or electrolyte resistivity (ohms)

t = transport number

t_j = transport number of the jth ion

t_s = potential sweep rate (v/sec.)

T = temperature (^oK)

u_j = mobility of species j (cm^2-mole/joule-sec)

v = fluid velocity (cm/sec)

Z_j = charge number of the jth ion in solution

α = transfer coefficient

β = coefficient for ion-ion specific interactions (kg/mole)

$\beta(i)_n$ = stability constant for a particular complex

γ_j = activity coefficient of the jth ion

γ_m = activity coefficient for the uncomplexed metal ion M

$\gamma_{L(i)}$ = activity coefficient for the uncomplexed ligand L(i)

$\gamma_{ML(i)_n}$ = activity coefficient for the complex $ML(i)_n$

δ = distance between the electrode surface and bulk solution (cm)

ε = permittivity (farads/cm)

η = over-potential (volts)

η_{conc_a} = concentration over-potential at anode (volts)

η_{conc_c} = concentration over-potential at cathode (volts)

η_{trans_a} = transfer over-potential at anode (volts)

η_{trans_c} = transfer over-potential at cathode (volts)

λ_j^o = property expressing secondary reference state (kg/mole)

μ_j = chemical or electrochemical potential of species (joule/mole)

ν = number of ions into which a molecule of electrolyte dissociates

ν_+, ν_- = number of cations and anions into which a molecule of electrolyte dissociates

ρ = density of pure solvent (g/cm^3)

ϕ = electric potential (volts)

CHAPTER I

INTRODUCTION

"The sea never changes and its works, for all the talk of men, are wrapped in mystery."

Joseph Conrad, 1902, Typhoon

Engineering Background

Present social and legal interests in the environment require the engineer to investigate more precisely the effects of human activities on the environment (National Academy of Sciences, 1971, p.2). In the marine environment in particular these efforts are hampered by the lack of information on existing or background conditions with which human contributions can be compared. Thus an important task in ocean engineering is to develop instruments and methods which can be used to provide background data sufficiently precise to detect the contributions of human activities (National Academy of Sciences, 1975, p.3; 1976, p.39). One problem of great environmental significance, but also of great analytical difficulty, is the detection and identification of the ambient species of trace elements, especially metals, in sea water (Hume, 1975; Goldberg, 1965).

The engineer can apply these species data to a wide variety of oceanic environmental problems such as: (a) contamination of sea water from ocean dumping of wastes (National Academy of Sciences, 1975, p.228); (b) contamination of sea water from industrial and municipal wastewaters (Young and others, 1972, p.22; Chow and others, 1973, p.551); (c) effects of aerial fallout (Young and others, 1972, p.35; Goldberg, 1972,p.3); (d) the solubility and kinetics of trace elements in sea water (Chow and

Patterson, 1962, p.263; Garrels and Christ, 1965); and (e) the toxic effects of the trace element species (Handbook of Geochemistry, p.82-L-4). To obtain data for solutions to these problems, the engineer must develop and use analytical methods which will: (a) be rugged and dependable for shipboard and in situ use (Riley, 1965, p.296; Hume, 1975); (b) measure trace elements in concentrations as low, or lower than, parts per billion (ppb); (c) make a distinction between the chemical species for each trace element; and (d) determine as nearly as possible the ambient species (National Academy of Sciences, 1971, p.83). Factors which make such an analysis difficult include contamination of the sea water during sampling, contamination during sample storing, chemical changes during analysis, the difficulty of in situ measurements, instrument sensitivity and dependability, and adverse shipboard conditions (Hume, 1973 and 1975). Because of these problems, another approach to obtain species data is to develop theoretical chemical models of sea water.

Chemical Modeling Procedures

"Chemical oceanography is fundamentally concerned with the chemical properties of sea water. In order to study these properties, and the interactions of sea water with other phases, we must first have some concept of what sea water is. This concept is what we will call the 'chemical model' of sea water.", (Whitfield, 1972, p.289).

In his paper on the progress towards a chemical model of sea water, Whitfield (1972) describes the progression from the early implicit models of Forchhammer (1865), Dittmar (1884), Arrhenius (1887), and

others to the recent explicit models of Sillén (1961), Garrels and Thompson (1962), Kramer (1965), and others. Table 1-1 traces this history with emphasis on the more recent work, including work occurring after Whitfield's paper.

The approach in these earlier explicit models is to derive expressions for the free and complexed ions and to insert these expressions into a mass balance equation for total metal concentration. The difficulty with these expressions is to determine with reasonable accuracy and consistency the thermodynamic activity coefficients and stability constants for the various chemical forms (Ernst and others, 1975, p.969). Also, because of the complexity of the sea water mixture, in many cases it is not valid to use these coefficients and stability constants to calculate the equilibrium concentration for a particular species. As often the correct concentration of a species is calculated only by taking into account all of the competing interactions and equilibria, and as this is a task beyond normal calculations, scientists employ computer techniques for various ionic equilibria models (Florence and Batley, 1975, p.182).

Recent work includes, as another alternative, studies in which the chemical forms of certain trace elements are modeled using values derived from the laboratory analyses of sea water for stability constants, activity coefficients, and concentrations (Bradford, 1973; Zirino and Yamamoto, 1972; Ernst and others, 1975; Batley and Florence, 1976). The problem with this method is that the values come from samples which have been chemically altered for analyses and therefore do not represent ambient conditions.

TABLE 1-1

STEPS IN THE DEVELOPMENT OF A CHEMICAL MODEL FOR SEA WATER
(EARLY MODELS)

	Author	Dissolved Components	Data Required	Comments
1.	Lavoisier (1776) (implicit)	Salt molecules	Concentration of individual salts.	Analytical procedures gave ambiguous results.
2.	Murray (1819) (implicit	Salt molecules	Concentration of acidic and basic components	Cannot combine analytical data uniquely to give composition of salts.
3.	Arrhenius (1884) (implicit)	Salt molecules plus ions	Total concentration of individual salts plus proportion of ionization.	Ionization constants ambiguous for certain electrolyte situations.
4.	Debye and Hückel (1923) (implicit)	Ions	Activities of individual ions.	Can only determine mean ion activity of neutral salt. Restricted to dilute solutions.
5.	Sillén (1961) (implicit)	Ions - minor constituents	Activities of individual ions.	Does not make quantitative analysis of reactions controlling distribution.

TABLE 1-1

(EARLY MODELS - CONTINUED)

	Author	Dissolved Components	Data Required	Comments
6.	Garrels and Thompson (1962) (explicit	Ions plus ion - pairs	Activities of individual ions plus proportion of ion pair formation.	Requires arbitrarily defined single ion activities.

(Whitfield, 1972, p.391)

(MODELS WITHIN THE LAST FEW YEARS)

	Author	Comments
1.	Kramer (1965)	"Working" equilibrium sea water model based on a series of equilibrium reactions between the major dissolved components and a limited number of solid phases.
2.	Pitzer and others (1972-1974)	A system of equations on the thermodynamics of electrolytes based on an improved analysis of the Debye-Hückel model and numerical calculations - recognition of an ionic strength dependence of the effect of short range forces in binary interactions.

TABLE 1-1

(MODELS WITHIN THE LAST FEW YEARS - CONTINUED)

	Author	Comments
3.	Zirino and Yamamoto (1972)	The approach developed by Garrels and Thompson has been expanded to include higher order complexes and applied to the trace elements Cu, Zn, Pb, and Cd. The effect of pH changes on chemical species was studied. Activity coefficients were obtained from a modified Debye-Hückel equation.
4.	Whitfield (1973)	The Brønsted-Guggenheim hypothesis of specific ionic interaction is used to develop a model for the major electrolyte components in sea water. This model results directly in the conventional total single ion activity coefficients commonly required for calculations in sea water equilibria.
5.	Bradford (1973)	Experimental work on sea water samples to establish stability constant and activity coefficients for zinc species - the results are correlated with models.
6.	Whitfield (1975)	Chemical models for sea water based on the Brønsted-Guggenheim hypothesis of specific ionic interactions and on the ionic interaction equations of Pitzer are extended to encompass a range of trace constituents.
7.	Ernst and others (1975)	Electrochemical techniques are used to characterize trace metal species and measure trace metal stability constants.

TABLE 1-1

(MODELS WITHIN THE LAST FEW YEARS - CONTINUED)

	Author	Comments
8.	Batley and Florence (1976)	The chemical forms of Cd, Pb, and Cu in sea water are examined and modeled with up to seven species for each metal. ASV determines concentrations of labile and total metals.
9.	Long and Angino (1977)	A theoretical model with various mixing solutions and ionic strengths is established to study the species for Cd, Cu, Pb, and Zn.

Research Emphasis

The research described in this thesis proposes to solve partially this modeling problem in this general manner by: (a) simplifying a standard analysis method so that many of the controls which affect ambient conditions are eliminated; (b) developing rigorously the theory of the method so that data can be extended to species detection; and (c) developing an inversion model which uses this data to give the lead partitioning of sea water for specific samples. With this method the samples remain relatively undisturbed during analysis and the data reflect, as nearly as possible, ambient conditions. These data, used in conjunction with the rigorously developed theory of the method, are inserted in the model and give lead complexing by percent for a number of saline environments.

These factors influenced my selection of the analysis system. The instrument must be simple, rugged, easily transported, and easily repaired - designed for shipboard or field work in remote areas. The method must be sensitive to the parts per billion range, must distinguish the species, and must minimize the chemical, physical, or biological alteration of samples in order to provide ambient concentration and species data. The usual graduate student nemesis, low budget, is another boundary condition, so ideally, commercially available items and standard laboratory components should comprise as much of the system as possible, and these components should double for either laboratory or field duties.

A number of different analyses systems follow these guidelines to varying degrees, but I selected anodic stripping voltammetry (ASV) because this method; (a) is theoretically simple; (b) uses a number of standard laboratory components; (c) theoretically makes species distinctions (Mancy, 1972; Zirino and Yamamoto, 1972; Bradford, 1973); (d) is sensitive to the parts per billion range (Lawrence Berkeley Laboratory, 1976); (e) does not destroy the samples; (f) is adaptable for shipboard or field use (Zirino and Lieberman, 1975, p.82); and (g) with certain changes analyzes samples without requiring the samples to be chemically altered beforehand.

Historical Development of ASV

ASV is included in the category of electrochemical analytical methods. Whitfield (1975, p.1) summarizes these methods: "Electrochemical techniques are basically simple. The working unit in all cases is a cell in which two conducting electrodes make electrical contact with the sample solution. The cell acts as a transducer which produces modified current or voltage signals in response to excitations applied to the electrodes from a controlled source. The art of electroanalytical measurements lies in the manipulation of the conditions within the cell, the structure of the electrodes and the nature of the input so that the signals transmitted by the cell are directly related to the activity or concentration of specific components."

All electrochemical procedures include this basic format with certain variations, and for ASV the variations occur with a two step reduction-oxidation process. The first step reduces and concentrates the specific trace elements as part of a mercury amalgam on a working electrode, while the second step oxidizes these elements back into the sample solution. The element type, species, and concentration is determined by measuring the current and potential developed by or required for the oxidation. The technique is "basically simple," and, although the theory is derived from fundamental areas of chemical thermodynamics and reaction kinetics, the simplicity of the theory is quickly lost in the various theoretical discussions. These discussions in varying degrees of detail are included in the extensive polarographic literature, and some of the best include: Delahay, 1954; Reilley, 1963; Shain, 1963; Barendrecht, 1967; Fried, 1973; and Whitfield, 1975.

The foundation for electrochemical techniques originated in 1834 with Faraday's Law (Faraday, 1834) which states that, "The chemical power of a current of electricity is in direct proportion to the absolute quantity of electricity which passes." Progress continued with Fick's Law of Diffusion (1885) concerning mass transport processes, Gibb's quantitative treatment of chemical equilibria, and Nernst's equation (1889) for equilibrium electrode potentials. Heyrovsky (1922), using these theories, developed the polarographic analytic techniques for measuring the current and potential during cathodic reduction of an element from a solution. Ilkovic (1934) improved the polarographic methods by deriving current diffusion equations for the dropping mercury electrode.

Christian Zbinden (1931) was the first to use the ASV variation of polarography for the more sensitive measurements of trace elements. Zbinden's ASV methods received sporadic attention for the next two decades until Delahay (1954) published his book on the principles of electrochemical instrumentation. The electrochemical methods described in this book could be performed with the improved electronic current and voltage measuring devices available then (Enke and Baxter, 1964). Scientists and engineers experimented with ASV during the next few years, and some of their publications include: Shain (1963) and Barendrecht (1967) specifically on ASV; Reilley and Murray (1963), and Reilley (1963) and Adams (1963) on electrochemistry and electrode processes; Matson, Roe, and Carritt (1965) and Roe and Toni (1965) on the theory and development of solid carbon electrodes; Enke and Baxter (1964) on instrumentation; and Perone and Birk (1965) on derivative techniques. A list of authors writing on ASV analyses for specific elements include: Perone - Ag (1963), Perone and Kretlow - Hg (1965), Florence - Fe (1970), Sinko and Dolezal - Cu, Cd, Pb, Zn (1970), Mancy - speciation (1192), Zirino and Healy - Zn (1970), Zirino and Yamamoto - Cu, Cd, Pb, Zn (1972), Ellis - Cu, Cd, Pb (1973), and Gilbert and Hume - Bi (1973), Clem (1973 and 1975), Sluyters - Rehbach and Sluyters (1975), Stulik and Hora (1976), Subramanian and Rao (1976), and Zirino and Lieberman (1974) have done recent work on electrodes, instrumentation, and in situ techniques.

Lead

Lead in sea water is a trace or non-conservative element; that is, its concentration varies with location and time, unlike the conservative, major constituents of sea water. A few of the sources for lead in sea water include: (a) groundwater runoff with the natural products of physical and chemical weathering and erosion of soils, rocks, and ore deposits (Fleischer, 1972, p.3; Handbook of Geochemistry, 1974, p.82-I-1); (b) direct introduction into oceans through hydrothermal water, hot brines, and volcanic outgassing (Handbook of Geochemistry, 1974, p.82-I-1): (c) industrial contamination from manufacturing, milling, mining, and smelting (Wixon and others, 1972, p.21): (d) municipal and industrial wastewaters (Young and others, 1972, p.21); (e) ocean dumping of refinery wastes, chemical wastes, filter cake, oil drilling wastes, refuse and garbage, radioactive wastes, military explosives, and miscellaneous wastes (National Academy of Sciences, 1976, p.5; and Young and others, 1972, p.21): (f) aerial fallout including lead from industrial and automobile emissions (Young and others, 1972, p.21; Cantwell and others, 1972; p.95; Goldberg, 1972, p.3; and Chow and others, 1973, p.551). Major lead "sinks" in the sea include: (a) biological uptake and concentration by marine organisms; (b) precipitation of lead hydroxides, phosphate, and/or carbonate; and (d) ion exchange processes (Chow and Patterson, 1962; Martin, 1972, v.II, p.307; Handbook of Geochemistry, 1974).

These are a few of the chemical and physical characteristics of lead:

Atomic weight - 207.19 (Pauling, 1970, p.92)

Atomic number - 82 (Pauling, 1970, p.92)

Standard potential of single ions:

a. $Pb = Pb^{++} + 2e^{-}$ $E_{\frac{1}{2}} = 0.126$ (Pauling, 1970, p.528)

b. $Pb^{++} = Pb^{4+} + 2e^{-}$ $E_{\frac{1}{2}} = -1.7$ (Pauling, 1970, p.528)

Concentration in sea water - parts per trillion to parts per million (Goldberg, 1965, p.163)

Activity coefficients in sea water (with an ionic strength of 0.67):

a. 0.34 (Zirino and Yamamoto, 1972)

b. 0.2 (Sillén, 1961)

c. 0.075 (Whitfield, 1973)

Residence time in the ocean - 3500 years (Handbook of Geochemistry, 1974, p.83-I-3).

Potential supply in 600g of rock - 10mg/kg of sea water (Handbook of Geochemistry, 1974, p.83-I-1).

(The Appendix contains additional data on concentrations, activity coefficients, entropies, heat of formation and free energy of formation for lead, lead compounds and complexes, and major anions.)

The major reason the ocean engineer is concerned with lead concentrations and speciation is because of its toxicity. The Handbook of Geochemistry (p.82-L-4) describes lead toxicity: "Lead is taken up by animals by ingestion and inhalation. Adsorbed and carried by the blood, mammals accumulate Pb in liver, kidney and bones. Animal muscles are usually low in lead.

"Under average conditions man takes up lead at approximate daily rates of 300 to 400 μg. About 10% of the ingested lead is absorbed gastro-intestinally. The major Pb proportion in the diet comes from vegetable and meat. Except for fish, aerial precipitates are a prime cause of dietary lead. The threshold concentration of Pb in the diet is assumed to be near 600 μg/day. The degree of absorption of inhaled Pb by the blood depends largely on particle size. Particles $> 0.6\mu$ reach the alveoli and are deposited (about 75% particulate Pb from automobile combustion is $< 1\mu$). The lead level in human blood and urine responds to exposures to extra-ordinary aerial Pb. A 'normal' lead content seems to range between 10 and 20 μg Pb per 100g blood (tentative threshold concentration: 30 μg Pb/100g blood often approached by parking and gasoline station workers, policemen, etc.). A reasonable limit for aerial concentration of Pb is believed to be 2 to 10 $\mu g/m^3$ based on inhalation of 15 m^3 of air per day; under these conditions intake is expected to match excretion of Pb.

"Ingestion of toxic amounts of lead from sources besides those already mentioned can originate from plumbing, ceramics with lead pigments in kitchenware, leaded paint, etc.

"Lead poisoning, starting with convulsions and anemia, may proceed to peripheral nerve disease, gout, chronic nephritis, encephalophathy and death."

I selected lead and confined my ASV research to this element for the following reasons. (a) Lead is highly toxic, and a large number of man's industrial and energy producting activities are a source of this

toxic lead. (b) I am interested in ocean anoxic basin chemistry, and the reduction processes in these basins affect the sulphides - a major anion which forms complexes with lead. (c) The standard potential of lead ions falls within the ASV reduction range. (d) The kinetic and diffusion characteristics of lead ions enhance the ASV reduction and oxidation processes, and these characteristics also give the multiple current peak shifts and repressions necessary for complex distinction. If other elements are analyzed, these peaks are lost in the noise. (e) These procedures developed for the analysis of lead can be applied to other metals.

Summary of Research

In summary, the emphasis of my research is on: (a) simplifying ASV instrumentation and methods so that ambient sea water conditions are more nearly duplicated and so that the methods are more suited for shipboard and field use; (b) fully developing the theory of the method to facilitate the changes and the data interpretation; (c) developing a chemical model to use this data for profiles of chemical forms; and (d) testing this system with a variety of saline samples from the laboratory and the field. The laboratory samples include KCl electrolyte and I.A.P.S.O. Standard Sea Water, and the field samples include sea water collected in Quatsino Sound, British Columbia; San Francisco Bay; and the Gulf of Mexico.

The following chapters describe this research in this fashion.

1) Chapter I - Introduction: This chapter includes a brief statement of the problem of detecting trace element concentrations and speciation, the history and problems of chemical models, the research objectives in consideration of these problems, a definition of electrochemical methods, the history of ASV, and a discussion of the properties of lead.

2) Chapter II - ASV Theory of Applied Potential: The precise potentials for ASV oxidation and reduction reactions identify the trace elements and the speciation partitioning of these elements. This chapter presents the theoretical development of the oxidation and reduction potentials. Without this precise development of the oxidation potential, species distinction cannot be made.

3) Chapter III - ASV Techniques: The current flow during ASV reduction reactions is a function of specific trace element concentrations and, in some cases, a function of the species. This chapter describes current, exchange current, and the limiting current as they pertain to ASV. Some descriptions are brief as certain parts are documented in the polarographic literature. The chapter also describes a conventional ASV analysis in order to show how current is a function of concentration and how potential is a function of the trace element and the species.

4) Chapter IV - Laboratory Analysis - Part I - Standard Procedures:

This is the first of two chapters describing the instruments and methods for the laboratory analyses. This chapter is the instrumentation chapter and describes the ASV equipment and components which have been adapted to meet the requirements of this project, the various

analysis techniques, and the standard analyses of electrolytes and sea water before equipment modifications.

5) Chapter V - Laboratory Analysis - Part II - Modified Procedures:

This chapter describes the changes made in the equipment and methods in order to provide more accurate species detection. Discussions include the theoretical basis for experimental elimination of the nitrogen purge, simplification of electrode processes, calibration of the instrument, and species detection as a function of oxidation potential and current.

6) Chapter VI - Results - Chemical Modeling with Field Samples:

This chapter developes the numerical value for the important potential constant term, includes tables for interpreting the analysis data, describes the sampling conditions and the sample analyses, and presents results and conclusions.

7) Appendices: The Appendices contain; (A) lead data, (B) discussions of activity coefficient methods, (C) electrode over-potential descriptions, and (D) more detailed descriptions of the engineering studies during which the water samples were taken.

CHAPTER II

ASV - THEORY OF APPLIED POTENTIAL

Introduction

This section develops expressions for the two steps in ASV analysis for the potential from an external source which must be applied between two electrodes in a sample cell in order either to reduce a specific trace element in solution onto a working electrode, as part of a mercury amalgam, or to oxidize this element from the amalgam back into solution. Trace element concentration and species detection depends on these expressions, specific terms therein, and the current expression developed in the next chapter. Additionally, the oxidation potential expression is a fundamental part of the chemical model for lead.

According to Kirchhoff's voltage law (Desoer and Kuh, 1969, p.6): "For any lumped electric circuit, for any of its loops, and at any time, the algebraic sum of the branch voltages around the loop is zero." Therefore the total applied potential from an outside source may be expressed as the sum of the individual potential terms from the various components of the ASV system:

$$\phi = \sum_{k=1}^{n} E_{comp_k} = 0 \qquad (2\text{-}1)$$

or:

$$\phi = \sum_{k=1}^{n} E_{comp_k}$$

with: ϕ = the applied potential (volts)

E_{comp} = component potentials (volts)

The sum of the potential terms gives the expression for the total external applied potential and includes these specific terms:

$$\phi = \sum_{k=1}^{\omega} E_{comp_k} = E + E_{ref} + IR_{cell} + E_{misc} + \eta_{conc_c} + \eta_{conc_a} + \eta_{trans_c} + \eta_{trans_a} \tag{2-2}$$

with:

E = electromotive force of a reversible cell (volts)

E_{ref} = reference electrode potential (volts)

IR_{cell} = ohmic drop in the cell (volts)

E_{misc} = miscellaneous potentials (volts)

η_{conc_c} = cathodic concentration over-potential (volts)

η_{conc_a} = anodic concentration over-potential (volts)

η_{trans_c} = cathodic transfer over-potential (volts)

η_{trans_a} = anodic transfer over-potential (volts)

The next few sections of this chapter discuss these terms in order. The Appendix contains supporting material for the over-potential terms.

Components of ϕ

1) E - Electromotive Force of a Reversible Cell

The term E is the potential derived from the relationship between the electromotive force of a reversible cell reaction, the electromotive force of a reaction when all substances involved are at unit activity, and the equilibrium constant:

(2-3) $$E = E^{o} + \frac{RT}{nF} \ln K$$

with:

E = electromotive force of a reversible cell (volts)

E^{o} = electromotive force of a reaction when all substances are at unit activity (volts)

K = thermodynamic equilibrium constant (mole/liter)

R = gas constant (8.314 joules/mole-deg)

T = temperature (^{o}K)

n = number of electrons involved in the reaction

F = Faraday constant (9.6487×10^{4} coulombs/equiv)

This relationship is a common one in electrochemical literature (Klotz, 1961; Pitzer and Brewer, 1965; Garrels and Christ, 1965; Reilley, 1965) and is not derived here.

The law of Mass Action defines K, the equilibrium constant: "The product of the activities of the reaction products, each raised to the power indicated by its numerical coefficient, divided by the product of the activities of the reactants, each raised to a corresponding power, is a constant at a given temperature.", (Garrels and Christ, 1965, p.6).

(2-4) $$K = \frac{a_D^{d} \, a_E^{e}}{a_B^{b} \, a_C^{c}}$$

The reaction of b moles of B with c moles of C comes to an equilibrium with the products of d moles of D and e moles of E: $bB + cC = dD + eE$. By substitution equation (2-3) is written as:

$$E = E^o + \frac{RT}{nF} \ln \frac{a_D^d \, a_E^e}{a_B^b \, a_C^c} \tag{2-5}$$

Garrels and Christ (1965, p.60) define the activity coefficient, a_j, as:

$$a_j = \frac{f_j}{f_j^o} \tag{2-6}$$

with: a_j = activity of the jth component

f_j = fugacity of the dissolved component j

f_j^o = fugacity of the jth component ~~in its standard state~~ (Standard state is defined as the pure liquid at the specified temperature and at 1 atmosphere total pressure.)

For an ideal solution in which the equilibrium vapor pressure of the component j of the solution equals the product of the mole fraction of that component in the solution and the equilibrium vapor pressure of the pure substance (Raoult's Law), the activity equals the mole fraction in the solution:

$$a_j = n_j \tag{2-7}$$

with: n_j = mole fraction of the jth component in solution

For other than ideal solutions the activity is:

(2-8) $$a_j = n_j \gamma_j$$

with: γ_j = activity coefficient of the jth ion.

A number of methods determine activity coefficient values for components in dilute electrolyte solutions: (a) by experiments with an analytical tool such as the glass electrode, for example, (Wilde and Rodgers, 1970); (b) by equations such as the Debye Hückel equation and others (Pitzer and Brewer, 1961; Pitzer and Kim, 1974; Whitfield, 1975; Long and Angino, 1977); or (d) by measurements of variables such as the freezing point or the vapor-pressure (Newman, 1973, p.95). The Appendix contains details of the Debye-Hückel relationship and other activity coefficient expressions.

The term E^o is the electromotive force of a reaction when all substances are at unit activity. E^o is determined experimentally as the electromotive force of a cell for a ½ cell oxidation or reduction reaction referred against a standard hydrogen electrode. The electromotive force values for various elements are in standard tables such as in Pitzer and Brewer (1961, p.371).

For example, the oxidation of lead in solution ($Pb = Pb^{++} + 2e^-$) requires a ½ cell potential, measured against a standard hydrogen electrode of -0.126 volts at 25°C. Theoretically when all substances are at unit activity lead ions in a KCl electrolyte solution are reduced to metallic lead on an inert electrode (one not entering into the reaction) in a cell with a potential of -0.126 volts applied between this electrode and a hydrogen reference electrode (See Figure 2-1).

By definition, the cathode is the electrode at which reduction occurs, and the anode the electrode at which oxidation occurs:

Cathode: $Pb^{++} + 2e^- = Pb$

Anode: $Zn = Zn^{++} + 2e^-$

Adding the corresponding ½ cell potentials gives the value for E, the electromotive force of a reversible cell reaction. There is some ambiguity in the literature as to the sign convention, but engineers (Uhlig, 1971) use the positive sign for the oxidation reaction and the negative sign for the reduction reaction. This is the sign convention used here. For example, in a cell with Zn being reduced at the cathode and Pb being oxidized at the anode:

$$Pb + Zn^{++} \rightarrow Pb^{++} + Zn \tag{2-9}$$

By substituting numerical values for the ½ cell potentials in expression (2-3):

$$E = E_{Zn} - E_{Pb} = 0.962 - 0.126 + \frac{RT}{2F} \ln \frac{[Pb^{++}]\,[Zn]}{[Pb]\,[Zn^{++}]} \tag{2-10}$$

FIGURE 2-1

ASV ANALYSIS CELL WITH ELECTRODES

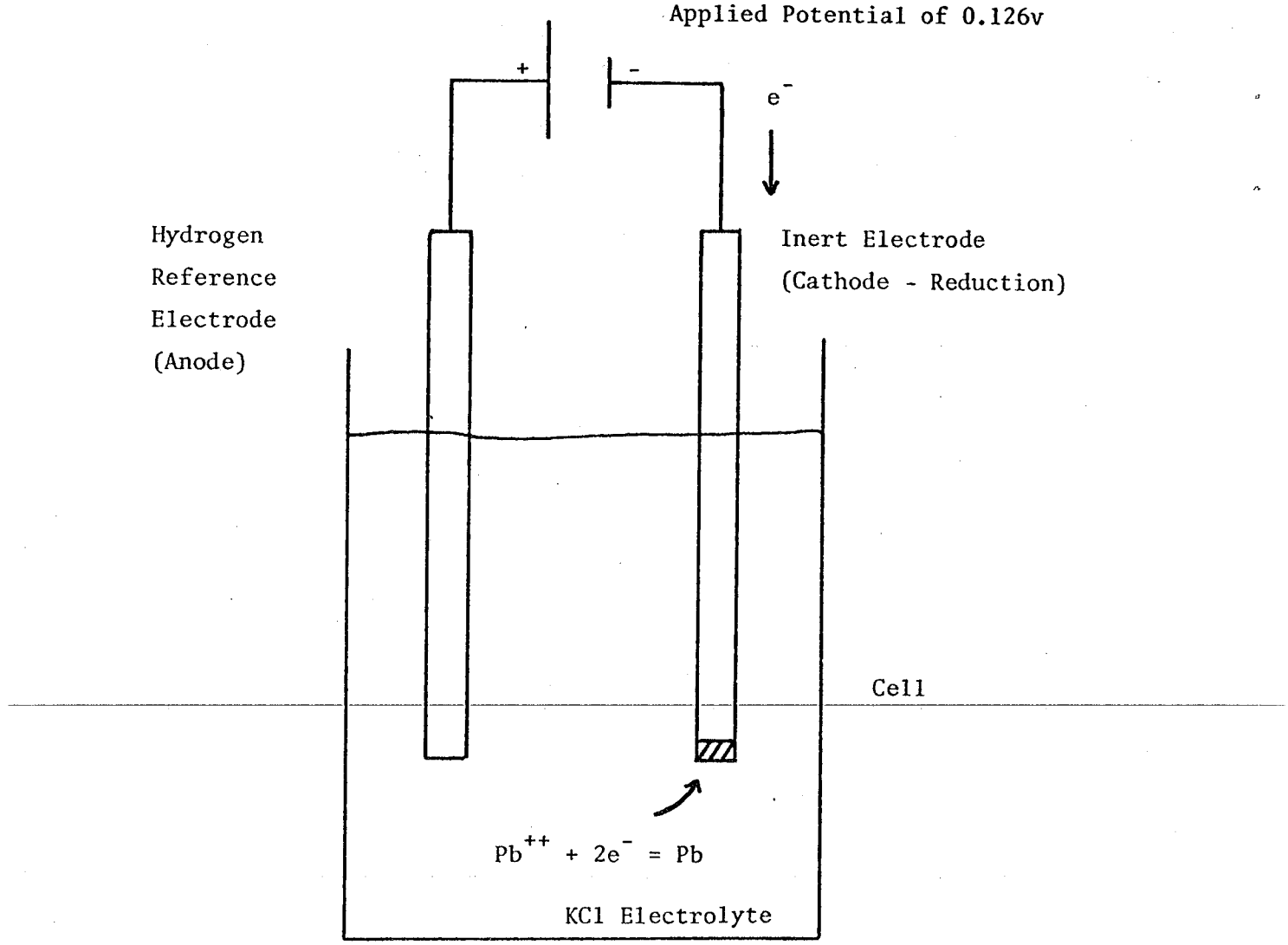

With: brackets [ ] = activities

(2-11) $$E = +\ 0.736 + \frac{RT}{2F} \ln \frac{[Pb^{++}]\ [Zn]}{[Pb]\ [Zn^{++}]}$$

The positive sign for E indicates that negative current flows in the cell from the cathode to the anode.

E represents either the ½ cell potential for an oxidation or reduction reaction, or the full cell potential for both an oxidation and reduction reaction. Therefore $E_{\frac{1}{2}}$ is the notation for the ½ cell potential while E without subscript is the total cell potential. In summary:

(2-12) $$E = E_{\frac{1}{2}\text{anode}} - E_{\frac{1}{2}\text{cathode}}$$

(2-13) $$E_{\frac{1}{2}\text{anode or cathode}} = E^{o} + \frac{RT}{nF} \ln K$$

2) E_{ref} - Reference Electrode Potential

In the preceding section the standard hydrogen electrode is the zero potential reference electrode to determine $E_{\frac{1}{2}}$ for various elements. Usually other types of reference electrodes are used because the hydrogen electrode is both cumbersome and dangerous to manipulate.

A reference electrode is ideally non-polarizable and should acquire the equilibrium potential rapidly and maintain this potential over long periods of time, even during passage of small currents. (Appendix C discusses polarization. Also refer to Ives and Janz, 1961, for a

detailed dissertation on reference electrodes.) The electrode reaction should be rapid and reversible, have zero resistance, and provide a constant voltage at a given temperature.

A number of electrodes, besides the hydrogen electrode fulfill this criteria to varying degrees. Two of these electrodes are: 1) the saturated calomel electrode (SCE) - also called the mercury-mercurous chloride electrode and described by Cl^-/Hg_2Cl_2,Hg in saturated KCl solution*; and the 2) silver-silver chloride electrode - described by Cl^-/AgCl,Ag.

The ½ cell reaction for the SCE (Garrels and Christ, 1965, p.127) is:

(2-14) $2Hg + 2Cl^- \rightleftharpoons Hg_2Cl_2 + 2e^-$ (at 25°C, E_{ref} = 0.244 volts)

For the silver-silver chloride electrode, the ½ cell reaction (Garrels and Christ, 1965, p.140) is:

(2-15) $Ag + Cl^- \rightleftharpoons AgCl + e^-$ (at 25°C, E_{ref} = 0.222 volts)

This discussion is confined to the SCE as this electrode is the one most commonly used in ASV work. By using the SCE electrode as a reference for measuring ½ cell oxidation or reduction such as in Figure 2-1, the SCE ½ cell potential of 0.244 volts is included in the total measured potential.

* Notation: (/) represents a liquid junction with electron transfer, and
(,) represents a phase difference with no electron transfer.

3) IR_{cell} - Ohmic Drop

The next potential term is IR_{cell}, with:

I = current passing between the electrodes (amps)

R = cell (electrolyte resistivity) (ohms)

This term represents ohmic potential drop due to cell conduction between the reference electrode and the electrode where the ½ cell reaction is measured. In cases of high solution resistivity, high current densities, or large electrode separation this potential can be significant, but, as shown below, for most electrochemical analysis in sea water IR_{cell} can be ignored:

Specific conduction of sea water at $25^{o}C$ and salinity of $35^{o}/o^{o}$ = $0.05\ ohm^{-1}cm^{-1}$

Current density = 1×10^{-6} amps cm^{-1} (electrode area = 1 cm^2)

Electrode separation ≅ 1 cm:

(2-16) $$IR_{cell} = (0.05\ ohm^{-1}cm^{-1})-1(1\ cm)(1 \times 10^{-5}\ amps\ cm^{-2})$$

$$IR_{cell} = 2 \times 10^{-8}\ volts$$

4) $E_{misc.}$ - Miscellaneous Potentials

This term includes the other various potentials which may arise during the analysis. The values for these potentials are extremely difficult to measure or to determine theoretically either because of their diminutive size or because of experimental variables which are

difficult to control. The following list shows the sources of a few of these potentials (MacInnes, 1961):

(a) potential from the varying magnetic field of the magnetic stirring unit;

(b) the energy change from the heat generated by the stirring;

(c) stray potentials from the operation of the pH meter;

(d) streaming potential from the stirring;

(e) zeta potential at the electrode double layer;

(f) change in potential generated by internal and external cell temperatures;

(g) noise from improperly guarded electrical connections;

(h) reaction over-potential at working electrode.

Because of the difficulty in determining these values, the total value of $E_{misc.}$ is included in the ± 5% experimental error term. Based on various ASV analyses and computations with the model, and on comparison of the model results with the literature, this approach seems reasonable.

5) η_{conc_c} - Cathodic Concentration Over-Potential

"When an electric current is passed through an electrolyte bounded by metal electrodes, the accumulation of the ions at the electrodes produces the phenomenon called Polarization, which consists of an electromotive force acting in the opposite direction to the current, and producing an apparent increase of the resistance." (Maxwell, 1891, p.387)

The derivation of the specific term, η_{conc}, as a function of current or concentration, depends on charge-transfer processes between electrodes in an electrolyte solution. (Appendix C discusses overpotential.) A dissolved species in a solution may be transported by three processes; migration, diffusion, and convection. The Molar Flux Law expresses the flux of each dissolved species (Newman, 1967, p.89 and 1973, p.217):

$$N_j = -Z_j u_j F C_j \nabla\phi - D_j \nabla C_j + C_j v \tag{2-17}$$

with:

N_j = flux of species j (moles/cm^2 - sec)

Z_j = charge of species j in solution

u_j = mobility of species j (cm^2-mole/joule-sec)

F = Faraday's constant (9.6487 x 10^4 coulombs/equivalent)

C_j = concentration of species j (moles/cm^3)

ϕ = electrostatic potential (volts)

D_j = diffusion coefficient of species j (cm^2/sec)

v = fluid velocity (cm/sec)

Newman (1967, p.90) states: "In this equation, N_j, the flux of a species j, is a vector quantity which indicates the direction in which the species is moving and the number of moles going per unit time across an area of 1 cm^2 oriented perpendicular to the flow of the species."

The first term ($-Z_j u_j F C_j \nabla\phi$) represents the flux due to motion of a charged species in an electric field. This is the migration term, particular to electrolyte solutions, and carries a negative sign because the electrostatic gradient is the negative of the electric field. The sub-term, $A_j u_j F$, is the ionic mobility.

The second term ($-D_j \nabla C_j$), the diffusion term, describes either electrolyte or non-electrolyte solutions. The same is true of the third term ($C_j v$), the convection term. All three terms together represent the flux of an ionic species in an electrolyte solution due to migration, diffusion, and convection.

The current density in the solution is expressed in terms of the sum of the specific species fluxes:

(2-8) $$i = F\Sigma_j Z_j N_j$$

with: i = current density (amps/cm^2) (The other terms have been described.)

Substituting (2-18) into the Molar Flux Law (2-17) gives:

(2-19) $$i = F^2 \nabla\phi \Sigma_j Z_j^2 u_j C_j - F\Sigma_j Z_j D_j \nabla C_j + Fv \Sigma_j Z_j C_j$$

Each of these three mass transport terms are simplified. First, in the migration term, let t equal the transfer or transport number and let t_j represent the transport number for a particular ionic species j.

Then $t_j i$ is the fraction of current carried by the ionic species j due to the migration, and:

$$t_j i = -F^2 Z^2_j u_j C_j \nabla\phi \tag{2-20}$$

In a supporting electrolyte the transfer number for a specific trace metallic ion approaches zero as t for the solution approaches 100. Therefore in a conductive supporting electrolyte the migration term for a specific trace metallic ion is eliminated.

In a solution where there is no net fluid velocity between the two electrodes, v is zero, and the convection term also is eliminated. The Molar Flux Law for a metallic species in a supporting electrolyte with no convection is:

$$i = -FZ_j D_j \nabla C_j \tag{2-21}$$

By letting C_b equal the concentration of a species in the bulk of the solution, C_s equal the concentration at the electrode surface, and δ being the distance between the two (See Figure 2-2), the diffusion term becomes:

$$i = \frac{-Z_j F D_j \ (C_b - C_s)}{\delta} \tag{2-22}$$

The limiting current of a particular charge-transfer reaction is the maximum current which flows during this reaction and is a function of the diffusion term (2-21). For i to be the limiting current, δ should be at a minimum (i.e., the diffusion gradient should be at a maximum). Stirring the solution directly beneath the electrode accomplishes this. To increase the diffusion gradient, C_s should approach zero. As D_s approaches zero, i is the limiting current, and:

$$(2\text{-}23) \qquad i_L = \frac{-Z_j F D_j C_b}{\delta}$$

Or for a particular ionic species:

$$(2\text{-}24) \qquad i_L = \frac{-ZFDC_b}{\delta}$$

The current then is a function of the mass transportation of the species by diffusion through the diffuse layer at the electrode-solution interface. The limiting current or current maximum occurs when the species concentration at the electrode surface and the double layer distance are both at a minimum. This limiting current is related to the concentration over-potential in the following manner.

For the ideal case when the mass transfer rate is infinite and diffusion is not a controlling factor, over-potential η is:

$$(2\text{-}25) \qquad \eta = \text{irreversible potential} - \text{reversible potential}$$

For finite mass transportation the activities of the reactants at the electrode surface differ from the corresponding activities in the bulk of the solution. Therefore the equilibrium potential differs from the potential developed by the species concentration in the bulk of the solution. This potential difference is the concentration over-potential.

Generally an electrochemical reaction occurring without any measurable over-potential (of any type) is reversible, while an electrode process involving considerable over-potential is irreversible (Delahay, 1954, p.38). This distinction between reversible and irreversible reactions is not so clear in the case of stirred solutions where the diffuse layer is controlled, and the mass transport is finite. Because of these factors, I consider η_{conc} reversible for the over-potential for a stirred solution.

For a reversible process due to a concentration difference, a modified Nernst equation (Delahay, 1954, p.219) expresses the over-potential as:

$$(2\text{-}26) \qquad \eta = \frac{RT}{nF} \ln \frac{C_s}{C_b}$$

From (2-22) and (2-23) the expressions for current and limiting current are written as a function of diffusion, letting 1 equal the sum of the over-potential at both the cathode and the anode:

(2-27) $$\frac{C_s}{C_b} = 1 - \frac{i\delta}{DZFC_b}$$

(2-28) $$\frac{C_s}{C_b} = 1 - \frac{i}{i_L}$$

Unlike the potential terms from earlier sections, the expression is for a potential at a specific electrode, the cathode. In order to be consistent with the cathodic sign notation, a minus sign is used for this specific expression. Therefore, by combining (2-26) with (2-28) and by using the proper sign notation, the concentration over-potential at the cathode is:

(2-29) $$\eta_{conc_c} = -\frac{RT}{nF} \ln\left(1 - \frac{i}{i_L}\right)$$

The cathodic over-potential occurs in both of the ASV reduction and oxidation steps but is most important in the reduction step when a specific element is reduced from the solution onto the working electrode surface as part of the mercury amalgam. This over-potential is of minor importance during the oxidation step when this same element is oxidized into the solution at the electrode. As this second step is an oxidation process there must be a corresponding reduction at the inert electrode, but it is inconsequential because the potential is measured between the working electrode and the reference electrode.

The literature often refers to another type of concentration over-potential called reaction over-potential. This potential occurs when the charge-transfer step is preceded or followed by a slow or strongly retarded chemical reaction which decreases the concentration of the transfer step reactant and increases the concentration of the product in the electrode vicinity. Frequently the overall electrode process involves these chemical steps, but the steps are fast and rarely become rate determining.

6) η_{conc_a} - Anodic Concentration Over-Potential

η_{conc_a} is the potential term for concentration over-potential at the anode. For cathodic concentration over-potential the controlling factor is the rate of diffusion of the ionic species, involved in the charge-transfer process, from the bulk of the solution to the electrode surface. At the surface the species is reduced, and electrons transfer from the electrode to the species. (The next two sections discuss the over-potential from this transfer or activation process, η_{trans}.) By definition oxidation is the anodic reaction. Therefore, at the anode the reverse charge-transfer process occurs, and the anode acts as an electron "sink." Anodic concentration over-potential occurs during both of the reduction and oxidation steps. During the reduction step, it is part of the accompanying oxidation-reduction reaction, is of minor importance, and can be discounted. This over-potential cannot be discounted during the second (oxidation) step though. Now the controlling, or limiting, factor for the charge-transfer process is the rate of

diffusion of the oxidized ionic species from the electrode surface into the bulk of the solution, and is a mass transport limited reaction. The limiting current is developed in the same manner as η_{conc}, and the same expression for η_{conc} is used. After making the proper changes for the anodic sign and after summing over the entire reaction, anodic concentration over-potential is:

$$\eta_{conc_a} = \frac{RT}{nF} \ln \left({}^{i}/_{i_L} \right) \tag{2-30}$$

7) η_{trans_c} - Cathodic Transfer Over-Potential

η_{trans_c} represents transfer over-potential at the cathode. A number of authors including Delahay (1954 and 1965), Fried (1973), Mohilner (1966), and Newman (1973) discuss in detail transfer (or activation) over-potential. Newman (1967, p.111) points out the distinction between transfer and concentration over-potential, "'Activation polarization' (herein called transfer over-potential) refers to the slowness of the chemical step or the charge transfer at the electrode. Concentration polarization refers to the fact that the electrode potential shifts because the concentration at the electrode is different from that in the bulk of the solution as a result of limited rates of mass transfer."

Transfer over-potential includes four specific types classified according to origin: (a) specific activation over-potential caused by slow electron transfer from electrode to solution (or solution to electrode); (b) crystallization over-potential caused by a retarded rate

of incorporation of the reduced substance into the lattice at the electrode surface; (c) nucleation over-potential which appears on inert electrodes during the continuous formation of new phases on the electrode surface; and (d) resistance over-potential which is the separate potential term IR_{cell}. All of these over-potentials are irreversible to certain degrees, and all, except for resistance over-potential, are included in the following general derivation of transfer over-potential.

The rate of reaction, expressed in terms of moles of the ionic species transformed by electron transfer at the electrode surface per unit of time and per unit of area, is (Delahay, 1954, p.33):

$$-\frac{dN_o}{dt} = \frac{dN_r}{dt} = k_o C_o - k_r C_r \tag{2-31}$$

with:
- N_o = number of moles - oxidation reaction
- N_r = number of moles - reduction reaction
- C_o = concentration due to oxidation reaction (moles/cm^3)
- C_r = concentration due to reduction reaction (moles/cm^3)
- K_o = oxidation rate constant (cm/sec)
- K_r = reduction rate constant (cm/sec)

This relationship is written in terms of α, the transfer coefficient. Delahay (1954, p.33) describes this coefficient: "It is recognized that a substance which undergoes a chemical transformation has to overcome an energy barrier. This principle is applicable to any type of reaction, but in the case of an electrochemical reaction

it is necessary to take into account the effect of the electrical field at the interface of the electrode-solution. This field favors the electrochemical reaction in one direction and hinders the reaction in the other direction. If E is the electrode potential referred to the normal hydrogen electrode, the fraction α E of this potential favors the cathodic reaction. ...likewise, the fraction (1- α)E favors the anodic reaction. The parameter α introduced in this manner is the transfer coefficient for the electrode process."

α also is known as the symmetry factor, and for most symmetrical reactions the value is 0.5. The potential for activation energy applies equally to both electrodes.

The rate constants, K_r and K_o, are written in terms of the transfer coefficient (Fried, 1973, p.44):

(2-32) $$k_r = k_r^o \exp\left\{ \frac{-\alpha n F}{RT} E \right\}$$

(2-33) $$k_o = k_o^o \exp\left\{ \frac{(1-\alpha) n F}{RT} E \right\}$$

with: K_r^o = reduction rate constant for E = 0 (cm/sec)

K_o^o = oxidation rate constant for E = 0 (cm/sec)

Equations (2-32) and (2-33) are the Butler-Volmer equations and were derived, "Early in the history of the study of electrode processes following the experimental observations by Tafel (in 1905) that the current density is proportional to the exponent of potential,

when E is not too near the equilibrium potential," (Fried, 1973, p.44). (The electrochemical literature, including Fried, 1973, and Uhlig, 1971, thoroughly discusses Tafel's work.)

The total oxidation-reduction reaction is written in the general form:

(2-34) Red = Ox + ne

reduction = oxidation plus the number of electrons involved in the reaction

Therefore the Butler-Volmer equations are written as:

$$k_r^\circ \exp\left\{ \frac{-\alpha n F}{RT} E_e \right\} = k_o^\circ \exp\left\{ \frac{(1-\alpha) n F}{RT} E_e \right\} \tag{2-35}$$

with: E_e = equilibrium potential (volts)

At dynamic equilibrium the exchange current is the net flow of current in a single direction (Reilley, 1963, p.2123). At equilibrium the cathodic and anodic currents are equal to each other and to the exchange current. The expression for the exchange current is:

$$i_o = n F k_r^\circ \exp\left\{ \frac{-\alpha n F E_e}{RT} \right\} = n F k_o^\circ \exp\left\{ \frac{(1-\alpha) n F E_e}{RT} \right\} \tag{2-36}$$

The total current density, i, is the combination of the cathodic current density, $i_{cathode}$, and the anodic current density, i_{anode}, ($i = i_{anode} - i_{cathode}$).

Current written as the time derivative of Faraday's Law becomes:

(2-37) $$i = dq/dt = nFdM/dt$$

with: q = electricity passed (coulombs)

Combining these various expressions, the total current density is:

(2-38) $$i = nFA_e \left\{ C_o k_o^o \exp\left[\frac{(1-\alpha)nFE}{RT}\right] - C_r k_r^o \exp\left[\frac{-\alpha nFE}{RT}\right] \right\}$$

~~with: All terms as previously defined and A_e = electrode area (cm^2).~~

If the transfer over-potential is low for both the general and specific terms, $\eta_{trans} \ll \frac{RT}{nF}$ or $\eta_{trans} <$ 0.05 - 0.1 volts, as it is for most polarographic and anodic stripping voltammetry work, the exponential terms are expanded in the form of $e^{-x} \cong (1-x)$. By eliminating all terms but the first, equation (2-28) becomes:

(2-39) $$i = i_{anode} - i_{cathode} = i_o (\alpha + 1 - \alpha) \frac{nF}{RT} \eta$$

With the transfer coefficient and reduction rate coefficients eliminated, the specific cathodic linear relationship between current and transfer over-potential is:

$$\eta_{trans} = -\frac{RT}{nF}\left(\frac{i_{cathode}}{i_o}\right) \tag{2-40}$$

This expression has a minus sign in order to be consistent with the cathodic sign notation. Also, this term, when written as $i_o\eta = -\frac{RT}{nF} i_{cath.}$ defines the effective resistance imposed at the electrode surface by the finite rate of the electron-transfer process.

8) $\eta_{trans\,a}$ - Anodic Transfer Over-Potential

Transfer over-potential occurs at the anode during both the reduction and oxidation steps. $\eta_{trans\,a}$ is the equivalent transfer over-potential term for the anode.

The preceding paragraphs show that because of the low anodic stripping voltammetry transfer over-potential ($\eta_{trans} < 0.05 - 0.1$ volts), only the first term in a series expansion of (2-38) is used:

$$i = i_{anode} - i_{cathode} = i_o(\alpha + 1 - \alpha)\frac{nF}{RT}\eta \tag{2-41}$$

The specific expression for the anodic transfer over-potential is:

$$\eta_{trans\,a} = \frac{RT}{nF}\left(\frac{i_{anode}}{i_o}\right) \tag{2-42}$$

Reduction Potential Expression

The preceding paragraphs develop these individual potential terms:

a) $$E_{1/2\ \text{anode or cathode}} = \left\{ E^{\circ} + \frac{RT}{nF} \ln k \right\}$$

with: $$k = \frac{a_D^d \, a_E^e}{a_B^b \, a_C^c}$$

b) $$E_{ref.} = \left\{ E^{\circ} + \frac{RT}{nF} \ln k \right\}$$ (With values inserted for particular reference electrodes.)

c) $$IR_{cell} \cong 2.0 \times 10^{-8}\ \text{volts}$$ (For an ASV analysis in sea water.)

d) $$E_{misc.} = \pm 5\% \left(E_{measured} \right)$$

---

e) $$\eta_{conc_c} = -\frac{RT}{nF} \ln \left(1 - i/i_L \right)$$

or in terms of concentrations:

$$\eta_{conc_c} = -\frac{RT}{nF} \ln \left(\frac{C_s}{C_b} \right)_{\text{reduction}}$$

f) $$\eta_{conc_a} = \frac{RT}{nF} \ln \left(i/i_L \right)$$ or in terms of concentrations:

$$\eta_{conc_a} = \frac{RT}{nF} \ln \left(\frac{C_s}{C_b} \right)_{\text{oxidation}}$$

g) $$\eta_{trans_c} = -\frac{RT}{nF} \left(\frac{i_c}{i_o} \right)$$

h) $$\eta_{trans_a} = \frac{RT}{nF} \left(\frac{i_a}{i_o} \right)$$

Combining these terms, the total applied potential expression is:

$$(2\text{-}43)\quad \phi = \left\{ E^{\circ} + \frac{RT}{nF} \ln k \right\} + \left\{ E^{\circ} + \frac{RT}{nF} \ln k \right\}_{ref.} + IR_{cell} + \left\{ -\frac{RT}{nF} \ln \left(\frac{C_s}{C_b} \right)_r \right\} + \left\{ \frac{RT}{nF} \ln \left(C_s/C_b \right)_{ax.} \right\} + \left\{ -\frac{RT}{nF} \left(\frac{i_c}{i_o} \right) \right\} + \left\{ \frac{RT}{nF} \left(\frac{i_a}{i_o} \right) \right\} \pm 5\% \left(E_{meas.} \right)$$

Only the ½ cell reaction is considered in deriving the expression for the applied potential necessary to reduce a trace metallic element onto a working electrode. A three electrode configuration is used for applying and measuring the potential. These electrodes include; (a) an inert working electrode upon which the element is reduced during the first step and oxidized from during the second, (b) an inert platinum electrode which is the anode during the reduction step and the cathode during the oxidation step, and (c) a reference electrode for measuring the applied potential. Figure 2-2 depicts a schematic representation of this system. The electrode configuration shows that only the ½ cell potential of the working electrode is measured. Therefore during reduction, expression (2-43) is modified by eliminating the anodic over-potential terms. The IR_{cell} term also is eliminated because the potential is several orders of magnitude less than the other component potentials. For the ½ cell reduction reaction expression (2-43) is:

$$(2\text{-}44)\quad E_{1/2\,red} = \left\{ E^{\circ} + \frac{RT}{nF} \ln k \right\}_{1/2\,cell} + \left\{ E^{\circ} + \frac{RT}{nF} \ln k \right\}_{ref} + \left\{ -\frac{RT}{nF} \ln \left(C_s/C_b \right) \right\} + \left\{ -\frac{RT}{nF} \left(\frac{i_c}{i_o} \right) \right\} \pm 5\% \left(E_{meas.} \right)$$

FIGURE 2-2

ASV ELECTRODE CONFIGURATION

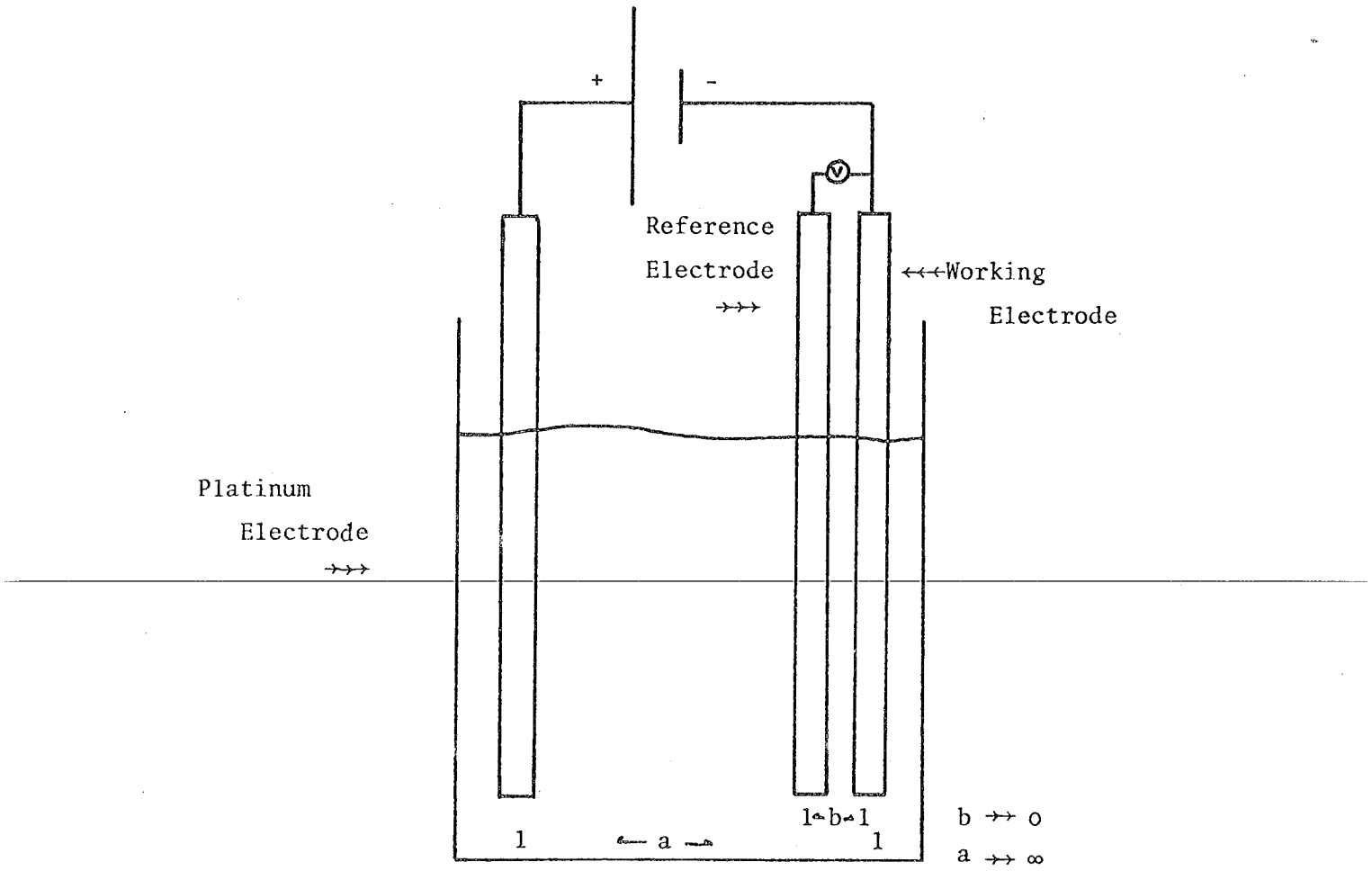

A common reference electrode for ASV analysis is the saturated calomel electrode, and the ½ cell reaction for this electrode at 25°C with unit activity is -0.244 volts (Garrels and Christ, 1965, p.127). This value is substituted for the reference potential term.

For example, the ½ cell potential for the reduction of Pb^{++} ions at 25°C with unit activity is -0.126 volts. By substituting this value for the ½ cell potential term, equation (2-44) becomes:

$$(2\text{-}45)\quad E_{1/2\ red.\ Pb^{++}} = (-0.126\,v) + (-0.244\,v) + \left\{-\frac{RT}{nF}\ln\left(\frac{C_s}{C_b}\right)\right\} + \left\{-\frac{RT}{nF}\left(\frac{i_c}{i_o}\right)\right\} \pm 5\%\ (E_{meas.})$$

Due to the low concentration of trace elements in either the electrolyte or sea water samples (parts per billion range) the cathodic current density during the reduction approaches the exchange current. The transfer over-potential is approximated as:

$$(2\text{-}46)\quad \left\{-\frac{RT}{nF}\left(\frac{i_c}{i_o}\right)\right\} \cong -\frac{0.0257\,v}{n} = -0.0129\,v$$

The concentration over-potential is a function of the ratio of the element concentration at the electrode surface to the concentration in the bulk solution. The cathodic shift of potential is equal to 0.0592/n for each order of magnitude that the ratio C_s/C_b increases above unity. During the reduction process, the concentration is in the order of parts per billion in solution to parts per million in the amalgam at the electrode surface. For lead the over-potential is:

$$(2\text{-}47)\quad \eta_{conc} \cong \left\{-\frac{0.0592}{n}\log\left(\frac{1\times10^{3}}{1}\right)\right\} = -0.0888\,v$$

The total applied potential term is now:

$$E_{1/2\,red.\,Pb^{++}} = (-0.126\,v) + (-0.244\,v) + (-0.013\,v) + (-0.089\,v) \pm 5\%\ (E_{near.}) \tag{2-48}$$

$$= -0.472\,v \pm 5\%\ (E_{near.})$$

The potential of -0.472 volts must be applied from an external source across an inert platinum electrode and an inert working electrode in an ASV cell for lead (in parts per billion concentration in a stirred electrolyte solution) to be reduced as part of a mercury amalgam onto the working electrode.

Oxidation Potential Expression

A one-step polarographic reduction procedure suffices for doing quantitative analysis for elements in concentrations above parts per million. Because of the higher concentrations, at a particular reduction potential there is a concentration gradient at the working electrode. As explained in the preceding paragraphs the limiting current is a function of the trace element concentration in the bulk solution, or:

$$i_L = \frac{-zFDC_b}{\delta} \tag{2-49}$$

The limiting current is a measure of the concentration, and the reduction potential is a function of the specific element. For parts per billion concentrations, the limiting current is too low to give precise, reproducible, quantitative measurements. For this reason

the single step polarographic procedure does not work at the parts per billion concentration level. By using the two-step anodic stripping procedure the mercury amalgam concentrates the element during the reduction process, and then current and voltage measurements are made during the oxidizing or stripping step. The concentration of the reduced element is increased sufficiently in the amalgam, from the parts per billion to the parts per million, to provide a measurable limiting current during oxidation.

The specific oxidation potential identifies the element. This section develops the oxidation formula for specific elements, although the preceding section discusses most of the terms.

The general oxidation equation form is the same as the one for reduction:

$$E_{app\,oxid.} = \eta_{conc_c} + \eta_{transf_c} + E_{1/2} + IR_{cell} + E_{ref.} + \eta_{conc_a} + \eta_{transf_a} + E_{misc.} \tag{2-50}$$

Again, certain terms are not included for the ½ cell reaction: IR_{cell} because the potential is insignificant compared to the total measurable applied potential; and the cathodic over-potential terms, η_{conc_c} and η_{transf_c}, for this anodic electrode reaction. Equation (2-50) is written as:

$$E_{app\,oxid.} = E_{1/2} + \eta_{conc_a} + \eta_{transf_a} + E_{ref} + E_{misc.} \tag{2-51}$$

By making the appropriate substitutions, the equation is rewritten as:

$$(2\text{-}52)\quad E_{applied} = \left\{ E^{\circ} + \frac{RT}{nF} \ln(k) \right\}_{1/2\,cell} + \left\{ E^{\circ} + \frac{RT}{nF} \ln(k) \right\}_{ref.} + \left\{ \frac{RT}{nF} \ln\left(\frac{C_s}{C_b}\right) \right\} + \left\{ \frac{RT}{nF} \left(\frac{i_a}{i_c}\right) \right\} \pm 5\%\, E_{bear.}$$

This equation gives a fixed specific oxidation potential. During ASV oxidation, though, for reasons which the next section discusses, the potential varies linearly from approximately -1.25 to 0.00 volts. The oxidation for specific elements occurs at various potentials within this range. The two over-potential terms in equation (2-52) are changed to include the effects of this linear sweep.

The concentration over-potential term, η_{conc_a}, is rewritten completely. The literature describes two different derivations of the oxidation potential as a function of the linear sweep; one by Randles and Sevcik (1948) for hanging drop mercury electrodes, and the other by Roe and Toni (1965) for thin mercury film electrodes.

For thin mercury film electrodes, Roe and Toni establish a model based on the homogeneous dispersion of the element in the mercury film deposited on the graphite working electrode. Diffusion in the mercury film is ignored. From this model they derive a solution for flux of the element out of the mercury film as a function of time. A variation of Fick's Law of Diffusion is used:

$$(2\text{-}53)\quad \frac{\ell\, \ell\, (C_s - C_s(t))}{\ell t} = \frac{D_o C_b(0,t) - C_b^{\circ}}{\delta}$$

with: C_s = concentration of the element in the mercury after deposition (moles/cm^3)

ℓ = mercury film thickness (cm)

D_o = diffusion coefficient in the bulk solution (cm^2/sec)

C_b = concentration in the bulk solution ($moles/cm^3$)

δ = distance between the electrode surface and the bulk solution (cm)

Substitutions into this equation are made from a rewritten form of the Nernst equation (Newman, 1973):

$$\frac{C_b}{C_s} = \exp\left\{\left(\frac{nF}{RT}\right)\left(E_t - E_{1/2}\right)\right\} \tag{2-54}$$

with: E_t = total potential for this particular derivation (volts)

Equation (2-53) with substitutions is integrated. Separation of variables is possible by following standard procedures. Boundary conditions are:

$$\frac{C_s(0,t)}{C_b(t)} = \frac{C_s}{C_b} \exp\left\{\frac{nFt_s t}{RT}\right\} \tag{2-55}$$

with: t_s = potential sweep speed (cm/sec)

and:

$$C_s(\delta, t) = C_s \tag{2-56}$$

After various manipulations a relationship is established between current and flux. An expression for flux as a function of the potential sweep speed for maximum current is derived. The result is substituted

into the Nernst equation:

$$(2\text{-}57) \qquad E_T = E_{1/2} + \frac{RT}{nF} \ln \left\{ \frac{\delta Q t_s n F}{D_a RT} \right\}$$

The last term in this expression is substituted into the equation for anodic concentration over-potential:

$$(2\text{-}58) \qquad \eta_{conc_a} = \frac{RT}{nF} \ln \left\{ \frac{\delta Q t_s n F}{D_a RT} \right\}$$

The general oxidation expression then is:

$$(2\text{-}59) \qquad E_{appoxid.} = \left\{ E^\circ + \frac{RT}{nF} \ln (k) \right\}_{1/2\,cell} + \left\{ E^\circ + \frac{RT}{nF} \ln (k) \right\}_{ref.} + \frac{RT}{nF} \ln \left\{ \frac{\delta Q t_s n F}{D_a RT} \right\} + \left\{ \frac{RT}{nF} \left(\frac{i_a}{i_o} \right) \right\} \pm 5\% \; E_{near.}$$

By replacing the η_{conc_a} term in (2-52) with (2-59), by writing the equation specifically for the oxidation of lead (with unit activity for reactants and products), by using a saturated calomel reference electrode, and by using the same value for transfer over-potential (2-46), the relationship is:

$$(2\text{-}60) \qquad E_{1/2\,oxid.\,Pb^{++}} = (-0.126\,v) + (-0.244\,v) + \frac{RT}{nF} \ln \left\{ \frac{\delta Q t_s n F}{D_a RT} \right\} + (-0.013\,v) \pm 5\% \; (E_{near.})$$

$$(2\text{-}61) \qquad E_{1/2\,oxid.\,Pb^{++}} = (-0.383\,v) + \frac{RT}{nF} \ln \left\{ \frac{\delta Q t_s n F}{D_a RT} \right\} \pm 5\% \; (E_{near.})$$

For each specific element or complex, the potential sweep controls the oxidizing potential. With a fixed sweep speed the diffusion term, D_o, in the linear sweep expression is constant (Bradford, 1973, p.758), and therefore the sweep term itself is constant.

The oxidation value then is a function of either the specific element or the complex:

$$E = E^{\circ} + \frac{RT}{nF} \ln \frac{a_D^d \, a_E^e}{a_B^b \, a_C^c} \tag{2-5}$$

Chapter V, Laboratory Analysis - Part II - Modified Procedures - continues the discussion of this term.

CHAPTER III

ASV TECHNIQUES

Conventional ASV - Analysis Procedure

The following description of conventional ASV analysis procedures is brief as most of these standard procedures are thoroughly covered in the literature.

A hard glass or Teflon cell, usually 100 ml or smaller, with a tight fitting Teflon top contains the solution to be analyzed. Four holes are machined in the top, three holes for the electrodes and a fourth for a glass gas purge frit. A precision laboratory stand, which is raised or lowered into fixed positions, supports the cell. Directly under the cell is a synchronous magnetic stirring unit which rotates a magnetic Teflon bar in the cell. (For a variation in the stirring mechanisms see Clem, 1973; and Clem and others, 1973.)

The three electrode configuration consists of these electrodes. For the working electrode a spectroscopic graphite electrode is impregnated with a high grade wax under vacuum (Matson and others, 1965). The tip is cut and polished to a mirror-like finish with #6 grade emery paper. Usually the electrode is plated with mercury in situ during the reduction process (Florence, 1970). Electrode variations include glassy carbon electrodes (Florence, 1970), hanging mercury drop electrodes (Barendrecht, 1967), rotating disc electrodes, and Cobalt-60 irradiated graphite electrodes (Clem and Sciamanna, 1975). For differential ASV a second working electrode is used for a total of four electrodes (Perone and Birk, 1965; and Zirino and Healy, 1972). The other two electrodes in the three electrode configuration include a standard laboratory platinum counter electrode (PCE) and the saturated calomel electrode (SCE).

A number of different power sources apply the potential between the electrodes, such as commercial units (Clem, 1973) or units constructed from standard laboratory components (constant voltage power supplies, circuit integrators, etc.). An X-Y recorder measures the current-voltage. Standard laboratory instruments, such as a Keithley Electrometer®, calibrate the system.

For the analysis, first the solution is placed in the cell, and a small amount of mercury is added for in situ plating (2×10^{-5}M $Hg(NO_3)_2$- Ellis (1973). Then the solution is purged of dissolved oxygen by running purified nitrogen gas through the glass frit for fifteen minutes or so before the analysis. After purging, with the nitrogen gas still flowing, the frit is moved to just above the solution. For the reduction of the element as a mercury amalgam, a sufficient potential, given by the reduction equation (2-43), is applied for a specified period of time (five to thirty minutes or longer) between the platinum and the working electrodes. The potential is usually from -1.00 to -1.40 volts depending on the electrolyte and the element to be analyzed. This potential is sufficient to reduce specific elements but is less than the electrolyte "breakdown" potential. During this step the solution is stirred at a fixed rate. The stirring increases the limiting current, controls the concentration gradient at the electrode surface, and maintains a constant deposition rate.

After the reduction step, the potential is kept at the specified level, the stirring unit is turned off, and the solution comes to rest. During the rest period the element concentration becomes homogeneous throughout the mercury film. The amalgam concentration

becomes homogeneous within a few seconds, but, to be on the safe side, the solution rests for thirty seconds (Barendrecht, 1967, p.65). The current drops almost immediately to zero because of the increase in the double layer thickness (δ) and the lack of concentration gradient. (There is still a small amount of electro-deposition during this rest period and during the beginning of the stripping.)

A number of procedures are used for the stripping step but certainly the most common one is to apply a fast linear voltage sweep (Barendrecht, 1967). The potential is linearly changed from the reduction potential to a zero or plus voltage. (See Figure 3-1 which shows current and voltage as a function of the reduction and oxidation steps.) The X-Y unit records the current and voltage. At specific potentials (equation 2-60) the trace elements in the amalgam are oxidized, and a faradic current flows. During the sweep the solution is not stirred.

The current peak during the stripping process is a function of the concentration of the element in the mercury film, and, therefore, a function of the concentration in the solution, assuming a constant deposition (reduction) rate and a homogeneous film. Roe and Toni (1965) have derived an equation for the current peak:

$$i_p = \frac{n F A_e Q C_s t_s}{R T e} \tag{3-1}$$

with: i_p = peak density (amps)

A_e = electrode area (cm^2)

l = amalgam film thickness (cm)

FIGURE 3-1

REDUCTION AND OXIDATION CURVE

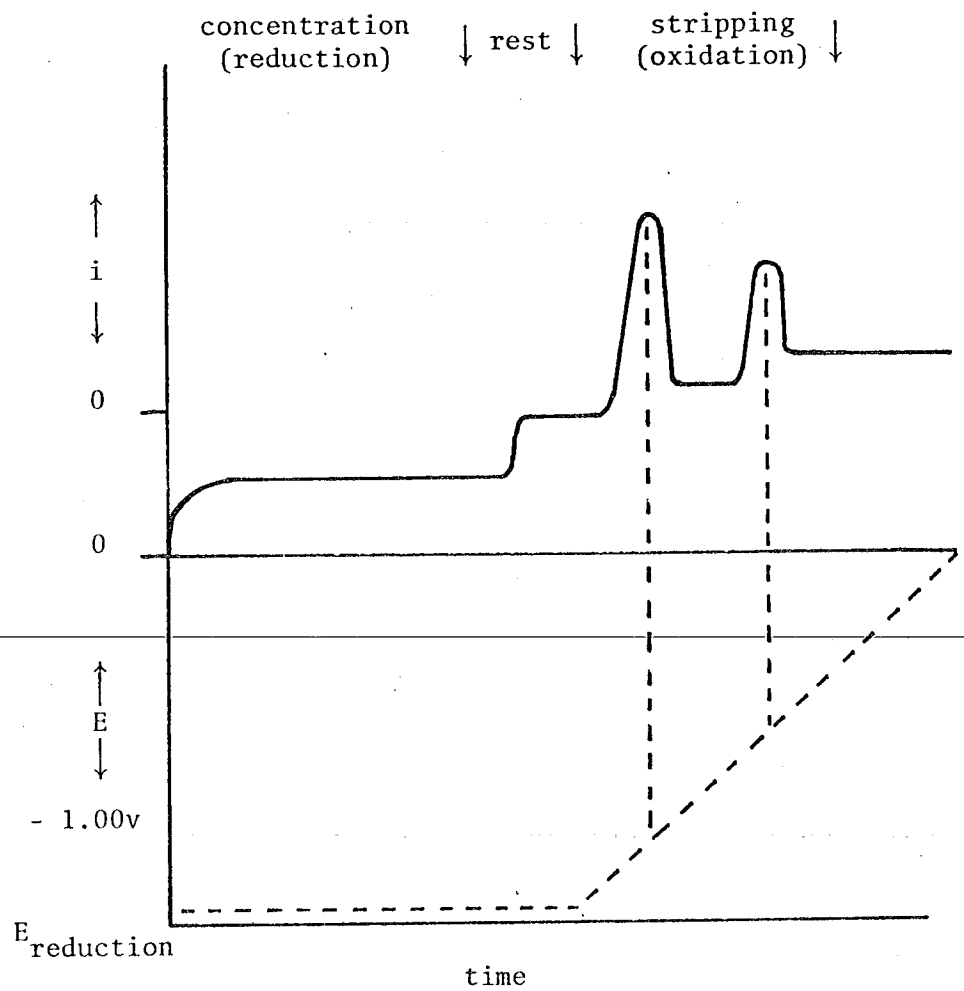

(From Barendrecht, 1967, p.57)

t_s = potential sweep rate (v/sec)

e = base of Napierian logarithms

(For details of this equation, see Roe and Toni, 1965. The derivation is similar to the derivation of expression (2-58) and is based on the potential developed by a concentration gradient and Fick's First Law of Diffusion: flux = $\frac{-D\partial c}{\partial x}$, with: D = diffusion coefficient, C = concentration, and x = distance.)

These observations are made from the peak current expression:

a) The peak current is directly proportional to the initial element concentration in the mercury film;

b) The amalgam film thickness (1) affects the peak current. Experimental values for 1 are for the order of 10^{-4} cm (Roe and Toni, 1965);

c) The peak current is directly proportional to the potential sweep rate. The faster the rate, the greater the peak, but with too fast a rate there may not be a resolution between peaks if more than one element is being stripped. A rate in the range of 2 mv/sec is used most often;

d) The peak current does not depend on the stirring rate;

e) An analysis does not require either the total amount of the element in the solution be deposited on the electrode or the entire amount, which has been reduced onto the electrode, be oxidized during the stripping step. Partial reduction and partial oxidation are sufficient;

f) Peak height may also be a function of complex type. The next chapter discusses this function (Batley and Florence, 1976, p.357).

Before an analysis, a blank is run with no reduction step in order to give a base to measure current peaks against (See Figure 3-1). (Even though the oxidation potentials at the beginning of the sweep are sufficient for reduction, the concentration in the solution is too low for faradic current to be measured on the X-Y recorder.) Two methods determine concentration from current peaks. (a) The area or height is measured and substituted into expression (3-1), or (b) the area of height is compared to calibration curves from standard additions. Peak area is often used rather than peak height because of resolution problems from the scan rate. The calibration curve method may be superior to formula calculations as the formula requires an estimate of the mercury film thickness. It is best to obtain calibration graphs for metals over a wide range of additions for each sample (Batley and Florence, 1976, p.357).

CHAPTER IV

LABORATORY ANALYSIS - PART I - STANDARD PROCEDURES

Introduction

These are the guidelines for designing and arranging the laboratory and equipment: (a) The laboratory arrangement should be similar to the field type which might be set up in an area with limited supplies. (b) The laboratory facilities and equipment should be adaptable for work at sea (rugged, easily repaired, etc.). (c) Equipment and modifications must be either purchased or made on a limited budget.

The laboratory for these experiments is a wet laboratory originally designed for geochemical work. The only item which might not be found in a field laboratory is a negative pressure hood. Figure 4-1 shows the laboratory layout. The laboratory was thoroughly cleaned, and all pipes and metal fixtures were cleaned and stripped with naval jelly. I applied two or three coats of mixed Mira-Plate® Epoxy Coating 683-00 Hi-Lustre Hardner and Mira-Plate® Epoxy Coating 617-00 white paint to these fixtures. Ring stand holders, junction boxes, parts of the counter, and miscellaneous metal parts were also stripped, cleaned, and painted.

I built a simple, inexpensive analysis tent to sit on the laboratory counter top (Figure 4-2). The tent cover is plastic with the seams sealed with filament tape. The upper corners have intake vents for positive pressure from nitrogen or filtered air. The tent contains the analysis cell, certain small ASV components, and glassware.

Instruments and Components

There are a number of commercial ASV units available, but as I plan to do species analysis for anoxic basins in British Columbia, and as

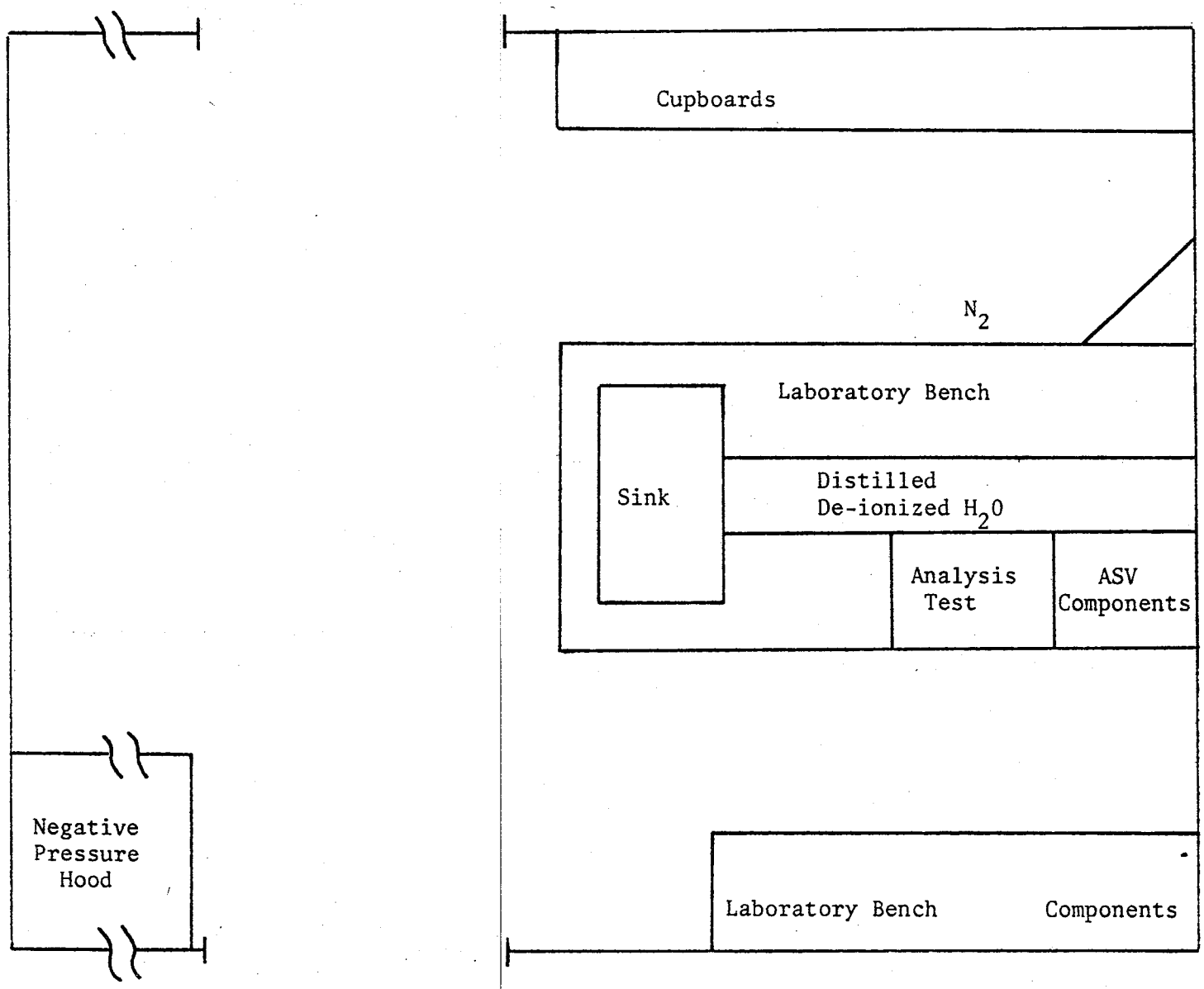

FIGURE 4-1
LABORATORY LAYOUT

FIGURE 4-2

PLASTIC TENT FOR ASV

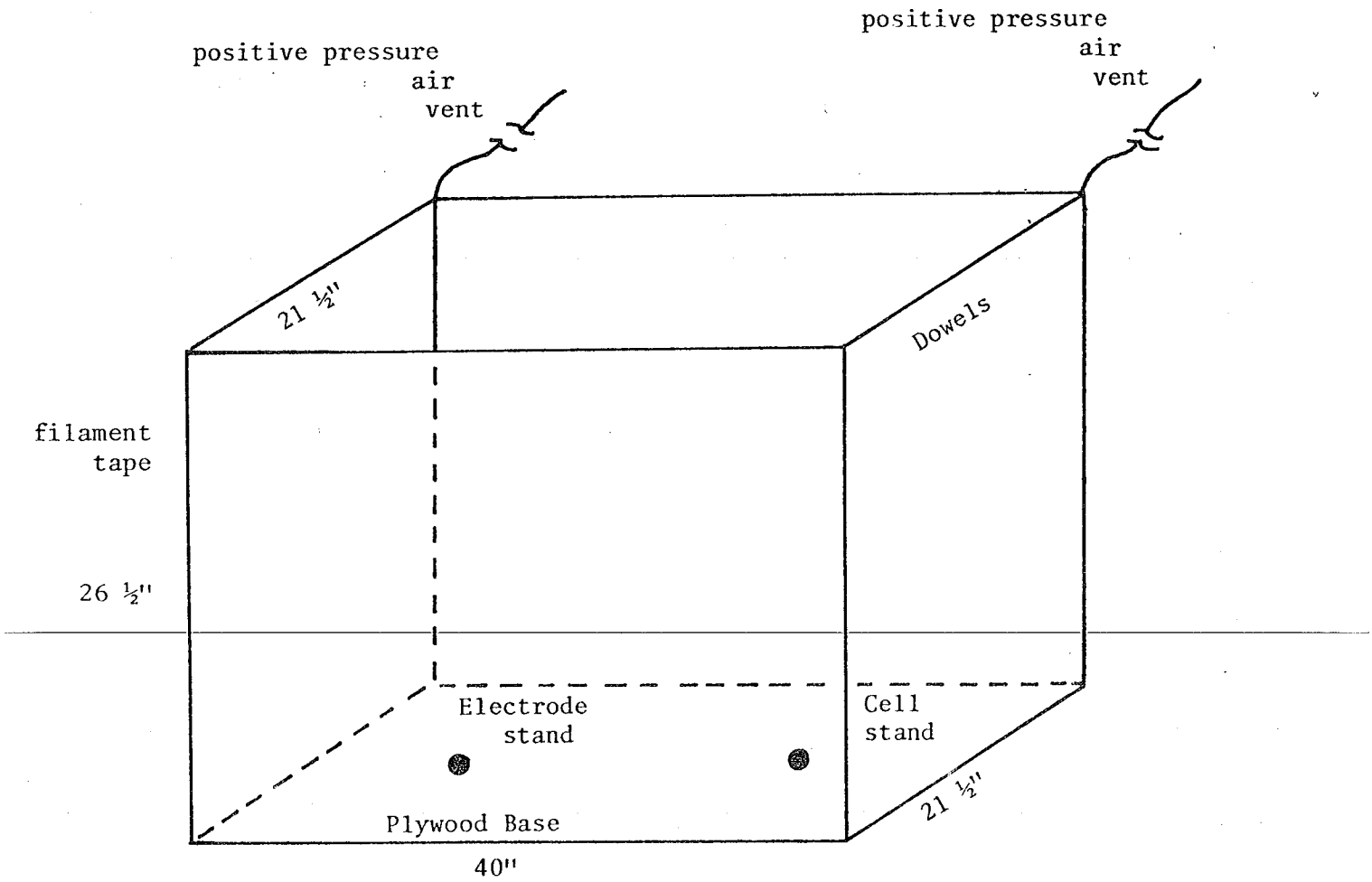

these basins are not easily accessible, it is important the ASV instrument be simple, and easily repaired, and disassembled, moved, and assembled. Therefore I decided to construct a composite unit from commercially available standard components. These components are standard laboratory items and are used for other purposes, which is important for field work. The following is a brief description of the ASV components. These components are listed in Table 4-1.

1) Analysis Cell

The analysis cell is a 150 ml Pyrex® container with a linear polyethelene (LP) plastic screw top. An epoxy painted ring clamp supports the cell. Four holes are drilled in the plastic top, which fits snugly on the cell with a Nalgene® "O" ring. The holes are for the three electrodes and the N_2 purge frit (Figure 4-3).

2) Reference Electrode

The first electrode in the three electrode configuration is the reference electrode. The section on reference electrodes discusses the various types. For most of my experiments I use a Beckman Saturated Calomel Ceramic Junction Reference Electrode Model #39402A. This is a common reference electrode and develops a potential of -0.244 volts at 25°C. When I measure both potential and pH, a Sensorex Combi® reference-pH electrode replaces the Beckman SCE.

TABLE 4-1

ASV COMPONENTS

Beckman Saturated Calomel Ceramic Junction Reference Electrode Model #39402

Beckman Platinum Counter Electrode Model #39002

Union Carbide National Spectroscopic Carbon Electrodes

Corning Tube Gas Dispersion Cylinder (frit) Model #12EC FJ-06

Precision Scientific Co. Big Jack®

Sargent-Welch 600 Synchronous Magnetic Stirring Unit Model #S764922

Heathkit Decade Resistance Box Model #1N-17

Hewlett-Packard Constant Current - Constant Voltage Power Supply Model #6216A

Hewlett-Packard X-Y Recorder Model #7035B

Hewlett-Packard Time Base Model #17108A

Hewlett-Packard Constant Voltage Power Supply Model #6215A

Valhalla Scientific Digital Multimeter - Counter Model 4440

Dana Laboratory, Inc. Danameter® voltmeter

Data Precision Voltmeter Model #245

Dimco - Gray Co. Gralab® Timing Mechanism

3) Counter Electrode

The second electrode in the configuration is the platinum counter electrode (PCE) which acts as the anode during reduction and the cathode during oxidation. I use the Beckman Platinum Counter Electrode Model #39002, a common laboratory electrode.

4) Working Electrode

The ASV literature describes an assortment of electrode types, each prepared differently (Matson, Roe, and Carritt, 1965; Roe and Toni, 1965). All electrodes show erratic behavior at times as there are uncontrollable factors such as electrode surface, purity, and contamination which produce various over-potentials. Often electrodes must be replaced, and possibly new ones must be constructed in the field. Therefore I used techniques simpler than those in the literature. These electrodes, even without certain controls, give reproducible results and certainly seem sensitive enough for my work. Many of the problems others have experienced with electrodes come from analyses in acidic solutions, which is not a factor in my work.

I constructed my electrodes in this manner. The electrodes are Union Carbide National Spectroscopic Carbon Electrodes, 1 cm in diameter and 30.5 cm long. The impurity level of the carbon is 6 parts per million (ppm) maximum total spot impurities and 2 ppm maximum spot impurity per element. These electrodes are divided in half into equal lengths and are immersed in liquid American Oil Company Parowax® for approximately 15 minutes or until the Parowax® permeates the electrodes, and a thin coat forms on the electrode surfaces. After cooling,

Parowax® is scraped from the electrode tips, and the tips are polished with #6 grade emery paper. The tips are examined under a microscope for surface blemishes and then are polished to a mirror-like finish with Scott Micro-wipes®. If an electrode becomes contaminated, the tip is broken off, and the new tip is repolished. These electrodes cannot be polished to the same finish as the glassy carbon electrodes which are now available. The surface blemishes and porosity are the source of noise after prolonged use (Batley and Florence, 1974, p.25).

5) Glass Purge Frit

A Corning Tube Gas Dispersion Cylinder (frit) Model #12EC FJ-06 purges the solution of dissolved oxygen during some experiments. The frit is placed in the cell with the electrode configuration, shown in Figure 4-3, and connects with a cylinder of Hi-Pure Nitrogen.

6) Lab Stand

An epoxy painted ring holder, connected to a Precision Scientific Co. Big Jack® laboratory stand, supports the analysis cell. This stand is painted with epoxy, and the height is adjustable. The cell height is adjusted so that the electrode configuration and glass frit, which are held at fixed positions by epoxy painted ring holders and stands, are immersed in the solution (Figure 4-4). For each analysis, the electrodes are in the same position in the cell and in relation to each other.

FIGURE 4-3

ANALYSIS CELL AND ELECTRODE CONFIGURATION

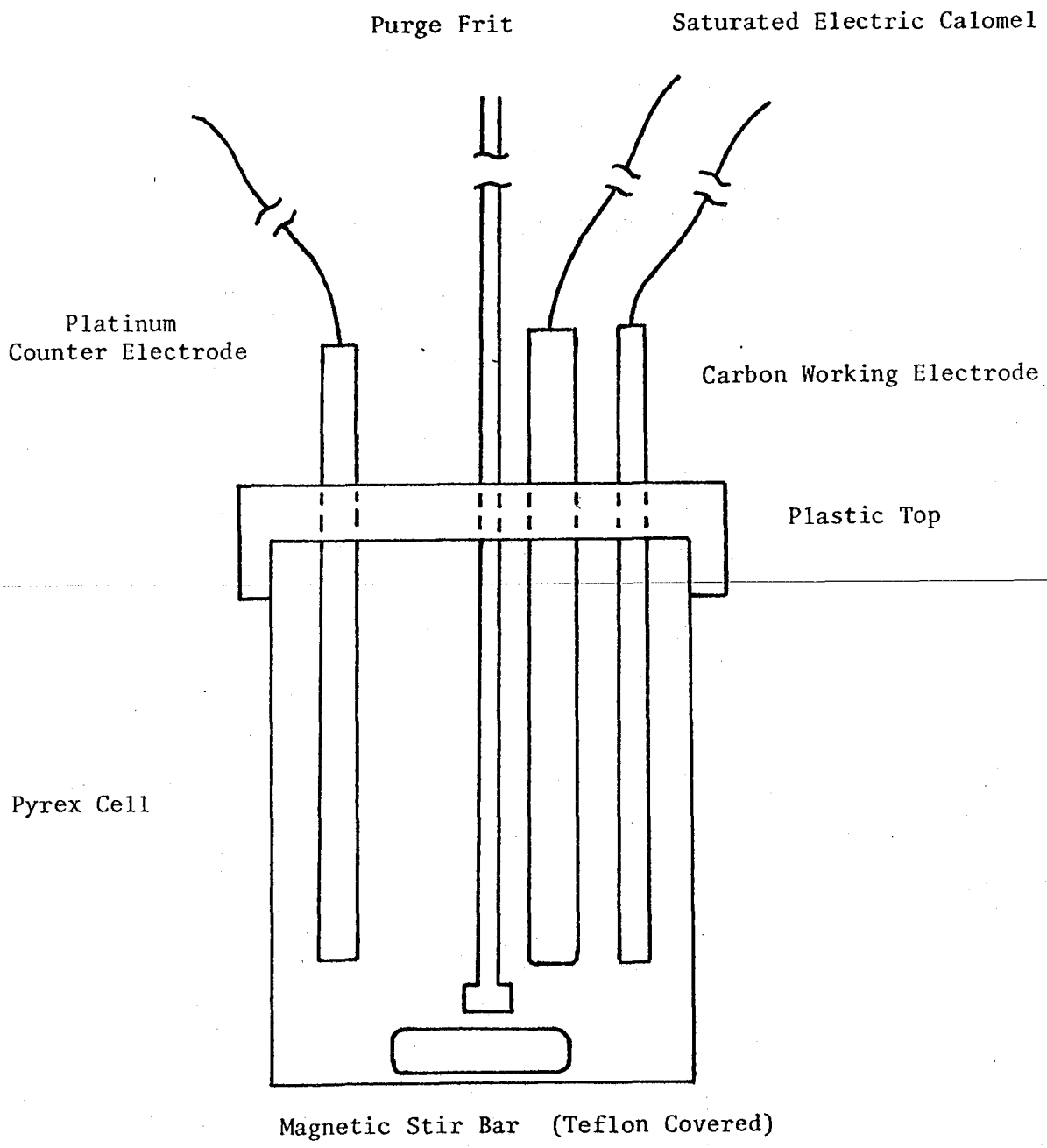

FIGURE 4-4

ANALYSIS CELL AND LABORATORY STAND

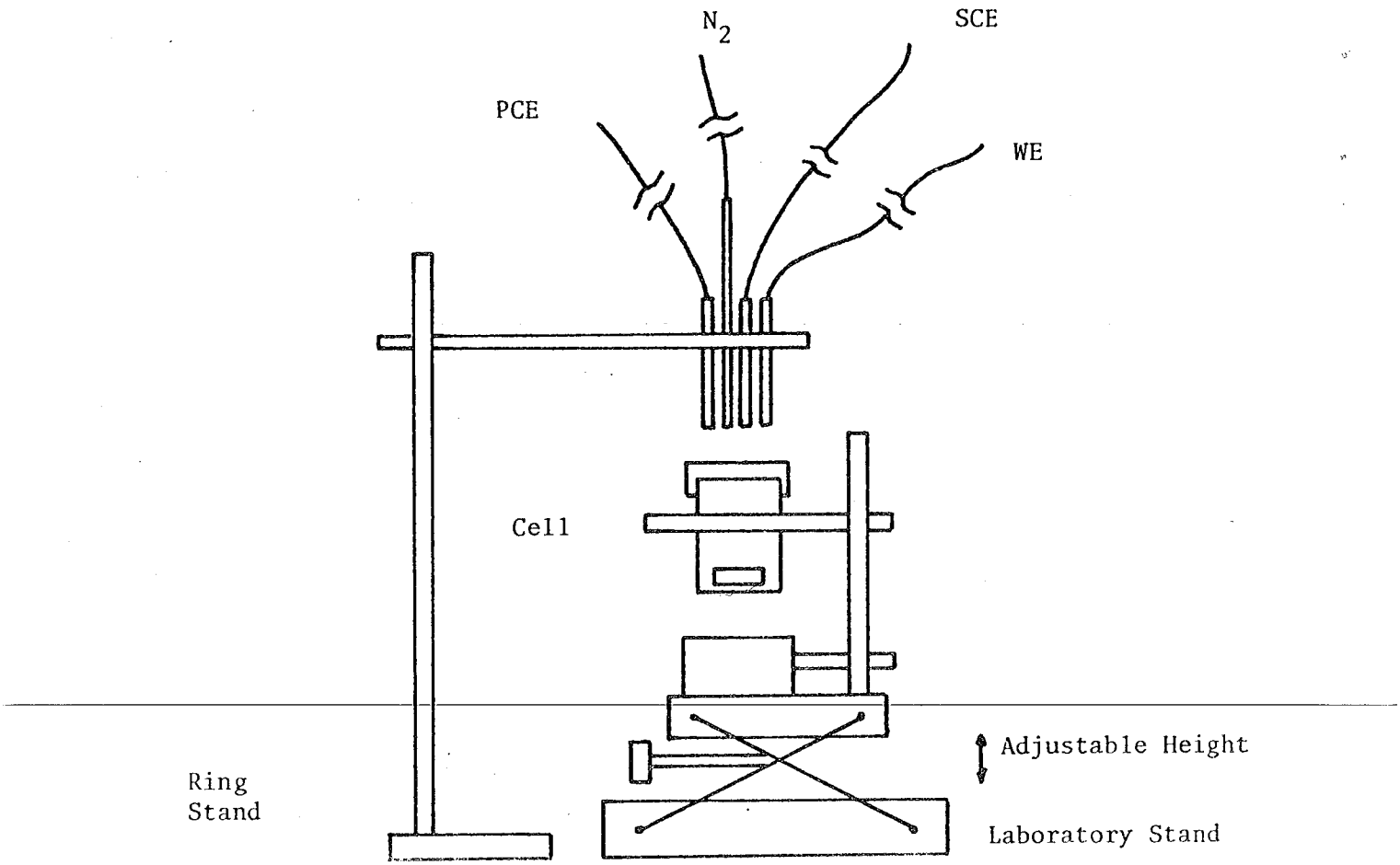

7) Magnetic Stirring Unit

Figure 4-4 shows a Sargent-Welch 600 synchronous magnetic stirring unit attached to the laboratory stand and positioned directly under the cell. The rotating magnetic field from the stirring unit rotates a Teflon coated magnetic bar in the cell at 600 rpms.

8) Resistance Box

Current is monitored across a Heathkit Decade Resistance Box Model #1N-17. Figure 4-5 shows the components and electrical connections. If the resistance is increased, the slope of current-voltage traces on the X-Y recorder increases. A 1000 ohm resistance gives the current peak with the optimum slope.

9) Power Supply (1)

A Constant Current-Constant Voltage Hewlett-Packard Power Supply Model #6216A provides the controlled potential between the working electrodes and the PCE. The potential is adjusted for the proper potential during the reduction step and is varied linearly by the sweep (circuit integrator) during the oxidation step. The potential is from -1.00 to -2.00 volts, depending on the elements which are being reduced.

10) X-Y Recorder

A Hewlett-Packard X-Y Recorder Model #7035B records the current and voltage during the oxidation step. The Y axis records the current, and the X axis records the voltage. Sensitivity of the Y scale is changed depending on the trace element concentration.

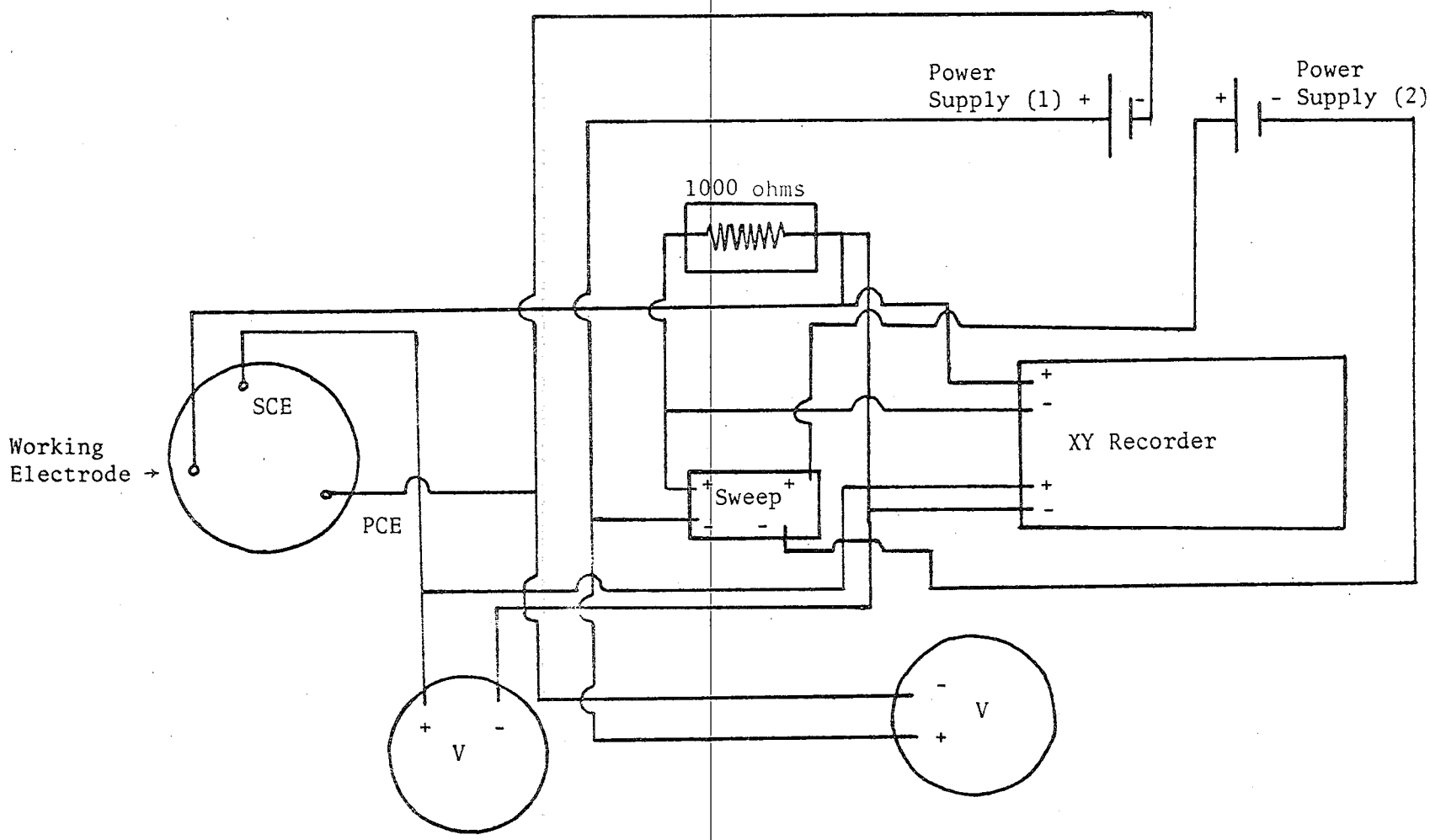

FIGURE 4-5
COMPONENT DIAGRAM

11) Sweep (Circuit Integrator)

A Hewlett-Packard Time Base Model #17108A is a simple circuit integrator for varying linearly the voltage during the oxidation reaction. The potential is a ramp function and varies from -1.00 to +0.20 volts. The range depends on the elements being stripped. The sweeping rate is varied - an important factor as the current peak and oxidation potentials are functions of this rate. The recorder may not respond to sudden current fluctuations with too fast a sweep though. I found that a rate of 5 sec/inch, or 10 mv/sec, compromises best between peak height and recorder response.

12) Power Supply (2)

A Hewlett-Packard Constant Voltage Power Supply Model #6215A provides 12.5 volts to operate the circuit integrator.

13) Digital Multimeter (1)

A Valhalla Scientific Digital (high impedance) Multimeter Counter Model #4440 monitors the potential between the SCE and the working electrode. (The X-Y recorder records the same potential during oxidation.)

14) Digital Voltmeter (2)

A Dana Laboratories, Inc. Danameter® monitors the potential between the platinum counter electrode and the graphite working electrode. This potential is the total potential, E_t, applied across the cell. The Valhalla multimeter measures the reduction or oxidation ½ cell potential, $E_{\frac{1}{2}red}$ or $E_{\frac{1}{2}oxid}$.

15) Digital Voltmeter (3)

A high impedance digital Data Precision Voltmeter Model #245 measures directly the potential from the Hewlett-Packard Power Supply (1). This is the constant potential from the power supply.

16) Timer

The timer for controlling the purge, reduction, and rest steps is a Dimco-Gray Co. Gralab® Timing Mechanism. This unit connects to the magnetic stirrer and automatically stops the stirrer after a specified time.

17) Miscellaneous Equipment

The equipment includes these miscellaneous items:

a) I have tried a number of different Teflon coated magnetic stir bars in the cell. For most of the early experiments I used a 3 cm long, 0.75 cm diameter, Teflon coated cylindrical bar. I replaced this bar with a Nalgene® star head stir Model #6600-0010 to minimize the uncontrolled turbulence and the vortex.

b) The usual laboratory connecting wires complete the various circuits between the components. Electrical tape or tin foil isolate exposed electrical connections in order to reduce noise and stray electric fields.

Analysis Techniques

A large number of experimental variables, not including sampling techniques, affect the measured potential and current. Important

variables are listed in Table 4-2. These variables must be controlled because of the sensitivity of the analysis and to achieve reproducible results. Some of the laboratory items and experimental techniques described in this section control these variables. Table 4-3 lists these miscellaneous laboratory items.

1) Glass and Plasticware

The glassware includes the standard laboratory Pyrex® flasks, beakers, etc. All glassware is washed in a 1:1 solution of HNO_3 which remains in the glassware overnight. Then the glassware is rinsed five times with distilled-deionized water.

Almost all of the plastics are the conventional polyethelene (CP) type. The most common items are the VWR CP Nalgene® 500 ml narrow mouth bottles, Model #2003-0016. These bottles store sea water samples, trace element additions, and miscellaneous solutions. Other plastic items include wash bottles, cell top, tubing, beakers, etc.

I clean the plastics by two different methods. (a) The plastics are washed in a 10% HCl solution and rinsed five times with distilled-deionized water. (b) Approximately 50 ml of concentrated HCl are poured into the 500 ml CP bottles, and the bottles stand for 24 hours. Then the bottles are rinsed with distilled-deionized water; filled with a 2% HCl solution made from G. Frederick Smith Chemical Co., 6M, Ultra HCl; and placed in a 60°C oven for at least 48 hours. Then the bottles are rinsed five times again. Although time consuming, this second method is the best. After cleaning, all glass and plasticware are wrapped in plastic wrap material and stored either in the analysis

Table 4-2

SOME VARIABLES TO CONTROL IN A TYPICAL ASV EXPERIMENT

1) Equipment cleanliness
2) Equipment storage
3) Chemical purity
4) Additions solution mixing (for calibration)
5) Reproducibility of additions techniques (for calibration)
6) Working electrode surface geometry
7) Platinum counter electrode surface
8) Reproducibility of saturated calomel electrode
9) Electrode position in relation to each other
10) Electrode depth in cell
11) Cell height above stirrer
12) Stirring rate in cell
13) Stir bar position
14) N_2 purge rate
15) Purge glassware position
16) Amount of solution in cell
17) Electrolyte strength
18) Solution temperature in cell

(These variables do not include the variables of sea water sampling and storage techniques.)

TABLE 4-3

MISCELLANEOUS ASV ANALYSIS ITEMS

Nalgene Star Head Stir Bar Model #6600-0010

Manostat Mini-Pet® 10 ml variable volume repeatable pipettes - with stainless steel tip

VWR Grumbaum® Pipet 100 µl (1% accuracy, 0.1% reproducibility)

Beckman pH meter Model #76

Scott Micro-wipes® Model #05310

Kimberly-Clark Kimwipes® Model #34150

VWR CPE Nalgene Bottles - 500 ml - narrow mouth - Model #2003-0016

Markson Finnpipette® 5-50 µl with disposable tips - Model #FP11

Standard Laboratory Pyrex® Glassware

tent or in the negative pressure hood. I handle all items during analysis with plastic disposable gloves.

2) Electrode Procedures

All electrodes are cleaned continually by rinsing in distilled-deionized water. Periodically I clean the platinum electrode by alternating the electrode for 10 seconds, first as a cathode then as an anode in a weak HNO_3 solution with a +1.0 volt potential applied across the cell. After each analysis I clean the graphite working electrode by polishing the tip with #6 grade emery paper and with Micro-wipes® or Kimwipes®. Occasionally a fresh surface in the graphite electrode is prepared by snapping off the tip and polishing the new surface.

3) Trace Element Addition Solutions

I prepare the trace element addition solutions by diluting to various strengths the J. T. Baker Dilut-It® Analytical Concentrations. These solutions, stored in 1000 ml CP containers, are added to the cell by using:

(a) Manostat Mini-Pet® 10 ml variable volume repeatable pipettes with stainless steel tips, or;

(b) VWR Grumbaum® 100 µl pipettes, or;

(c) a 5-50 µl Markson Finnpipette® Model #FP11, with disposable tips

I prefer the Markson Finnpipette® because of its control and non-contaminating tips.

A Standard Sample Analysis in KCl

I designed a series of experiments to test the modified equipment, the analysis methods, and the chemical model for lead species. These experiments include the analyses of; (a) KCl electrolyte, (b) I.A.P.S.O. sea water, (c) sea water from Quatsino Sound, British Columbia, (d) sea water from the San Francisco Bay, and (e) sea water from the Gulf of Mexico.

This chapter describes the first experiment using standard equipment, and the next chapter describes subsequent experiments with the new methods. The following experiment with KCl is typical of a variety of experiments which I did with electrolyte solutions.

I poured 150 ml of 0.5M KCl electrolyte solution into the analytical cell and added 20 ml of a 0.1 Hg solution, prepared from a J. T. Baker Dilut-It® mercury standard. The cell was positioned just above the stirrer (Figure 4-4), and, with the stirring unit off, the glass frit was inserted into the solution. The solution was gently purged with nitrogen for 30 minutes.

The purge was left on but positioned above the solution, the stand was raised immersing the electrodes, and a blank was run with no reduction step. This blank establishes a calibration baseline for subsequent lead additions. I used a sweep range of -1.03 to +0.80 volts, a sweep speed of 5 sec/in, and a "normal" calibration on the X-Y recorder. Two sweeps were made for each analysis, and in each case the first one was recorded. Figure 4-6 shows the X-Y recorder plots of the sweeps.

FIGURE 4-6

KC1 ANALYSIS - PURGE

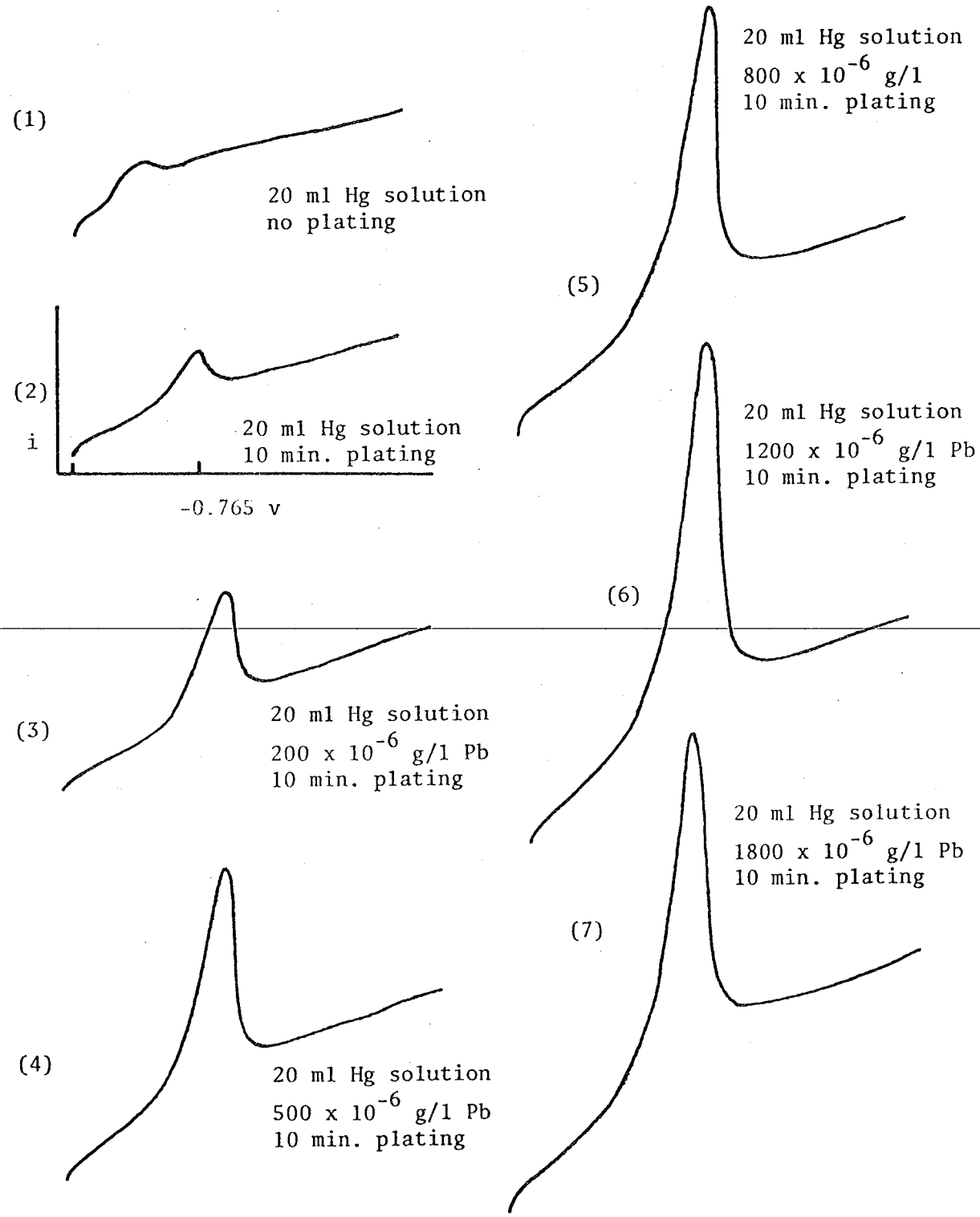

Using this same solution with no additions, I simultaneously reduced the mercury and the trace amounts of lead in the solution onto the working electrode by applying the $E_{\frac{1}{2}red}$ of -1.22 volts. (The stirring unit was turned on, and the purge, with a gentle flow of nitrogen, remained just above the solution.) After ten minutes, the stirring unit was turned off, the potential was maintained at the same level, and the solution was allowed to rest for 30 seconds. I ran two sweeps with the same conditions as the blank. The first one was recorded (Figure 4-6 - (2)) and shows a slight peak at -0.765 volts.

A series of calibration sweeps were run using successive lead additions in order to determine the lead concentration from this current peak. Table 4-4 shows the total amount of lead added to the solution for each calibration sweep:

TABLE 4-4

CALIBRATION FOR Pb IN KC1 (with purge)

Calibration Sweep Number (two sweeps for each step)	Pb Added ($x\ 10^{-6}$ g/1)	Total Pb in Solution ($x\ 10^{-6}$ g/1)
(1)	-	(x)
(2)	-	(x)
(3)	200	(x + 200)
(4)	300	(x + 500)
(5)	300	(x + 800)
(6)	400	(x + 1200)
(7)	600	(x + 1800)

Figure 4-7 shows the graph of these values with the peak height of the current plotted on the abscissa and concentration on the ordinate. Peak area is often the most reliable indicator of element concentration, but in this case, because of the well defined peaks and because of similar peak shapes, the peak height is plotted. The error flags on this graph include experimental error from noise, lead additions, instrumentation, and electrode contamination. The current-concentration relationship for lead concentrations less than about 1×10^{-3} g/l appears to be linear, thus agreeing with the theoretical linear expression (3-1):

$$i_p = \frac{nF^2 A Q C_s t_s}{R T_e} \qquad (3\text{-}1)$$

By using this linear calibration line, the concentration of lead in the KCl electrolyte, before additions, is $130 - 190 \times 10^{-6}$ g/l. Various complexes of lead cause this relationship to deviate from the linear function. This deviation is one of the tools for complex distinction and is described in the next chapter.

FIGURE 4-7

CONCENTRATION OF LEAD IN KCl (WITH N_2 PURGE)

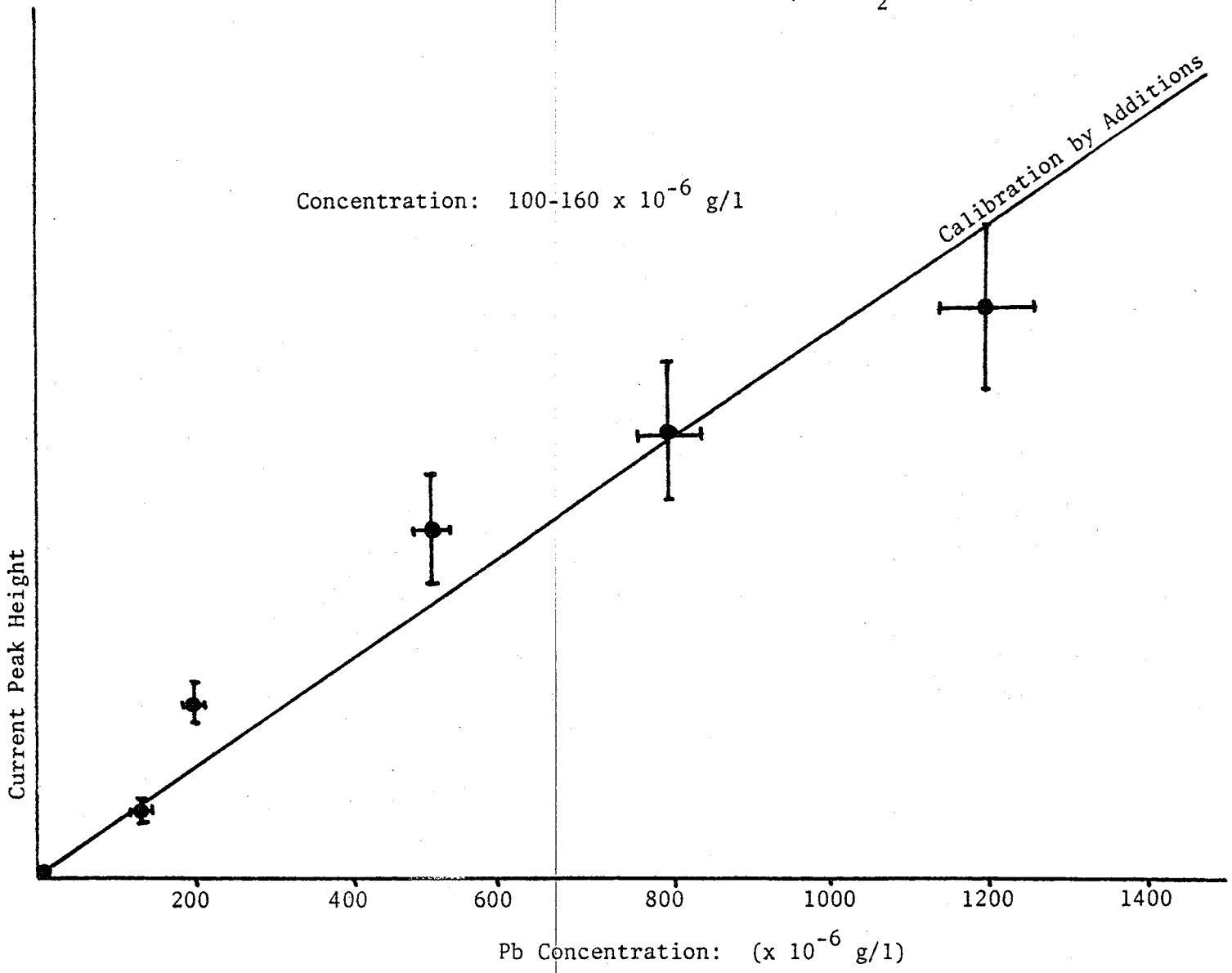

CHAPTER V

LABORATORY ANALYSIS - PART II- MODIFIED PROCEDURES AND CHEMICAL MODEL

"I thought it was absolutely necessary to know with precision the composition of the present ocean in order to form an opinion about the action of that ocean ...."

Forchhammer, 1865, p.203

Nitrogen Purge

Traditionally the experimenter has always removed oxygen from the solution prior to polarographic or ASV analyses. The polarographic literature documents the reasons for this (Shain, 1963; Barendrecht, 1967) and includes this brief synopsis by Bond (1973, p.1141). "Problems arise both from the voltammetric behavior of oxygen itself and from the associated chemical reactions that can take place with oxygen or its reduction products. Oxygen gives two polarographic waves. The first is due to the reduction of oxygen to hydrogen peroxide or hydrogen peroxide and hydroxide (depending on the pH)":

(5-1) $2e^- + O_2 + 2H^+ \rightleftharpoons H_2O_2$ (acid media)

with: $E_{\frac{1}{2}} = -0.05$ volts vs. SCE

(5-2) $O_2 + 2H_2O + 2e^- \rightleftharpoons H_2O_2 + 2OH^-$ (neutral or alkaline media)

The second involves the reduction of hydrogen peroxide to hydroxide or water:

(5-3) $H_2O_2 + 2H^+ + 2e^- \rightleftharpoons 2H_2O$ (acid media)

with: $E_{\frac{1}{2}} = 0.5$ to -1.2 volts vs. SCE

(5-4) $H_2O_2 + 2e^- \rightleftharpoons 2OH^-$ (neutral or alkaline media)

Two types of complications arise if oxygen is not removed from the solution. The hydrogen peroxide produced from the first reaction produces invidious effects on other electroactive species present in solution as it functions as both an oxidizing agent and a reducing agent. More specifically, however, pH changes occur in the vicinity of the working electrode due to the reduction of oxygen. The resultant increase in pH in the vicinity of the dropping mercury electrode can precipitate heavy metal ions and thus diminish their diffusion currents. Also, those species (i.e., organics) whose reduction involves hydrogen ions will be already affected due to the localized increase in pH at the dropping mercury electrode.

According to Bond (1973, p.1140) the reasons for removing oxygen before analyses are: "The oxygen can be removed chemically, but is most frequently displaced with nitrogen, argon, or hydrogen. Most reviews and textbooks on the analytical use of polarography stress, with reasons, the need for doing this, and the removal of oxygen has probably become so firmly entrenched in the polarographic literature that for users of the technique it is probably a routine and unquestioned point in the procedure. This assertion is made on the grounds of the paucity of examples in the literature where authors have discussed or

shown whether the removal of oxygen is in fact necessary for their particular analytical procedure."

The traditional method of removing the oxygen from the solution is to purge the unstirred solution with purified nitrogen, introduced into the cell by a glass frit for about 30 minutes prior to the analysis. The inert nitrogen replaces the oxygen, but in doing so also purges other dissolved gases from the solution, and for sea water, one of these gases is carbon dioxide.

The carbon dioxide system in sea water, through the following reversible reactions, provides, along with the silicon and boron systems the important pH buffering function (Sverdrup and others, 1942, p.181; Goldberg, 1965, p.228; Pytkowicz, 1967, p.63):

(5-5) CO_2 (gas) $\rightleftharpoons$ CO_2 (solution)

(5-6) CO_2 (solution) + $H_2O \rightleftharpoons H_2CO_2$

(5-7) $H_2CO_3 \rightleftharpoons HCO_3^- + H^+$

(5-8) $HCO_3^- \rightleftharpoons CO_3^- + H^+$

(5-9) $Ca^{++} + CO_3 \rightleftharpoons CaCO_3$

Schmitt (1962, p.177) and Garrels and Christ (1965, p.236) show by Eh-pH diagrams that the partitioning of lead compounds in solution is a function of both the oxidation-reduction potential and the pH of the solution.

During the first experiments with ASV, I found that, despite traditional procedures, the solution does not need to be purged of oxygen in order to obtain satisfactory results. There are a number of reasons for this. First of all, in most solutions oxygen is reduced at certain potentials applied to the working electrode, and the change in pH because of this reaction may precipitate certain heavy metal ions, thereby affecting the diffusion currents (Bond, 1973, p.1141). According to Bond this may be the most significant adverse effect of oxygen. With sea water, though, the pH will not change because of the natural buffering system. Therefore the oxygen reduction reaction should not affect the diffusion currents from the heavy metals in a buffered media.

Secondly, an additional current flows during the oxygen reduction reaction in a similar fashion to the flow of current during the metal stripping step. This current, as shown by Bond (1973, p.1142), instead of masking the trace element current peak, causes a shift in the entire X-Y plot. This shift does not change the relative peak height from the stripping current, and, at least for measuring single peaks, should not be a problem. This might not be the case for certain multiple peak analyses.

Finally, as mentioned by Fried (1973, p.168), voltammetry oxidation is usually done in potentials negative to the reduction of oxygen so in most cases there should be no interference.

(5-10) $O_2 + 2H_2O + 2e^- \rightleftharpoons H_2O_2 + 2OH^-$ (neutral or alkaline media)

with: $E_{\frac{1}{2}} = -0.05$ volts vs. SCE (Bond, 1973, p.1141)

Laboratory Experiments - KCl - No Purge

This experiment duplicates the one described in the last chapter except that the KCl solution is not purged. I poured 150 ml of 0.5M KCl solution into the cell and added 20 ml of the 0.1 Hg solution. The purging step was eliminated, and a blank was run without the reduction step. I swept the voltage at the same speed, 5 sec/in, with the same range, -1.03 to +0.80 volts, and with the usual "normal" calibration on the X-Y recorder. Two sweeps were made in order to eliminate any slight oxygen interference. The second sweep was recorded. Figure 5-1 shows the X-Y recorder plots of these sweeps.

After running the blank, I applied a potential of -1.42 volts across the cell for ten minutes. The stirring unit was turned off for 30 seconds, the two oxidizing sweeps were made, and these procedures were repeated for successive additions of lead in order to establish the calibration curve. Table 5-1 shows the amounts of lead added.

TABLE 5-1

CALIBRATION FOR Pb in KCl (without purge)

Calibration Sweep Number (two sweeps for each step)	Pb Added ($x\ 10^{-6}$ g/l)	Total Pb in Solution ($x\ 10^{-6}$ g/l)
(1)	blank	(x)
(2)	-	(x)
(3)	200	(x + 200)
(4)	300	(x + 500)
(5)	300	(x + 800)
(6)	400	(x + 1200)

FIGURE 5-1

KC1 ANALYSIS - NO PURGE

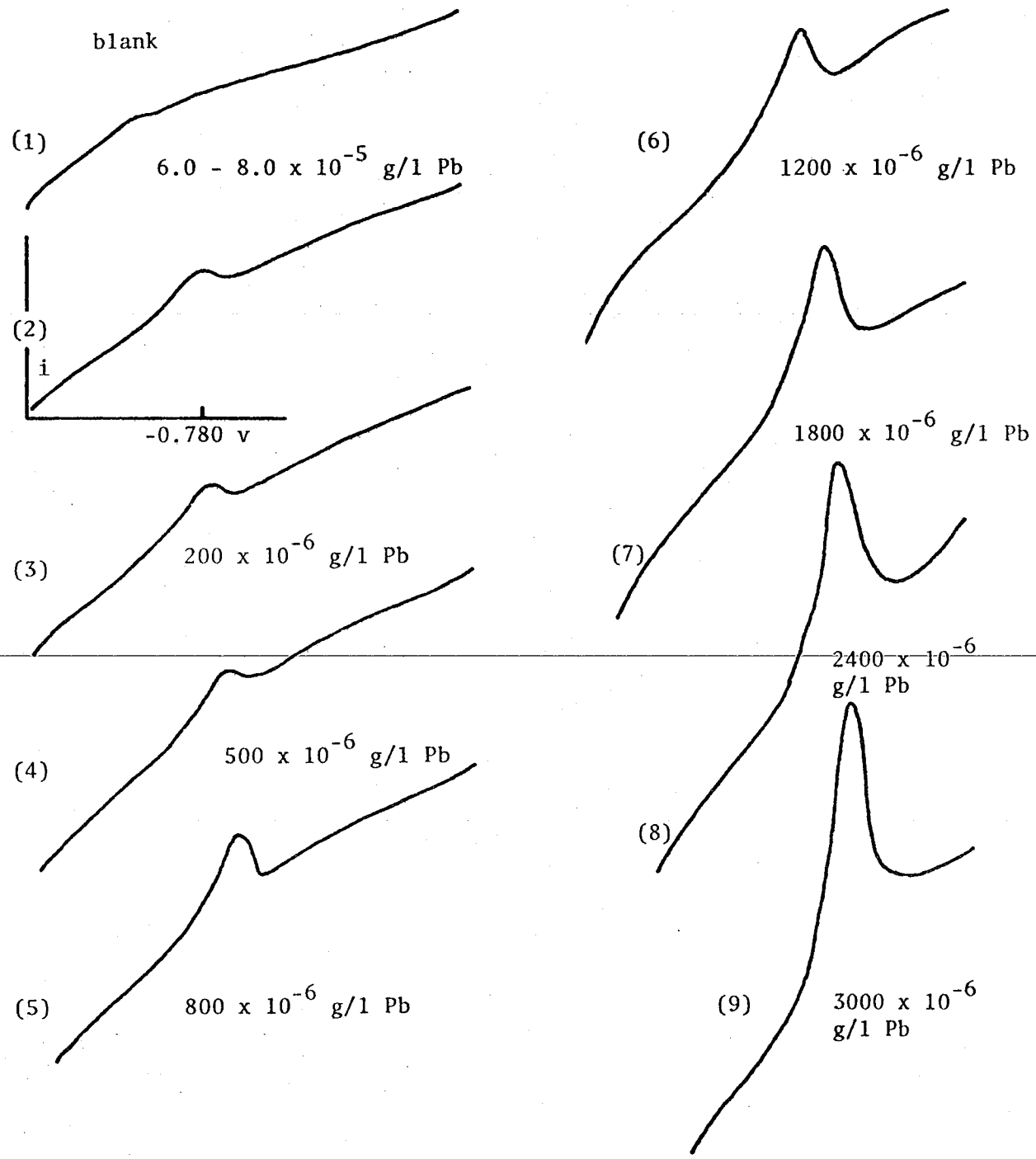

(7)	600	(x + 1800)
(8)	600	(x + 2400)
(9)	600	(x + 3000)

Figure 5-2 shows the graph of these values with the peak height of the current peak plotted on the abscissa and the lead concentration plotted on the ordinate. Peak height is used rather than area because of the distinct and similar shapes of the curves. Error flags are for the same experimental variables discussed in the previous chapter. The analysis shows a lead concentration of 6.0 - 8.0 x 10^{-5} g/l from sweep (2) on the calibration curve. Despite the somewhat diminished peaks, which appear to be from oxygen reduction noise, the curves are distinct, and the calibration curves are easily plotted. Once again the curve is linear, this time for concentrations lower than about 4.0 x 10^{-3} g/l. All analyses without the purge yield slightly diminished peaks, but this is not a problem except with extremely low lead concentrations (Bond, 1973, p.1145).

Laboratory Experiments - Sea Water - Purge

These next experiments compare the results of lead analysis in sea water with and without the nitrogen purge. A number of experiments were run in order to validate the results. For a typical experiment with the purge, the cell held 150 ml of the I.A.P.S.O. Standard Sea Water P_{57}, $^{8-9}$/l 1972, along with 20 ml of the 0.1 Hg solution. Nitrogen purged the solution for thirty minutes. I recorded the blank and added successive increments of lead in similar fashion to the other

FIGURE 5-2

CONCENTRATION OF LEAD IN KC1 (no purge)

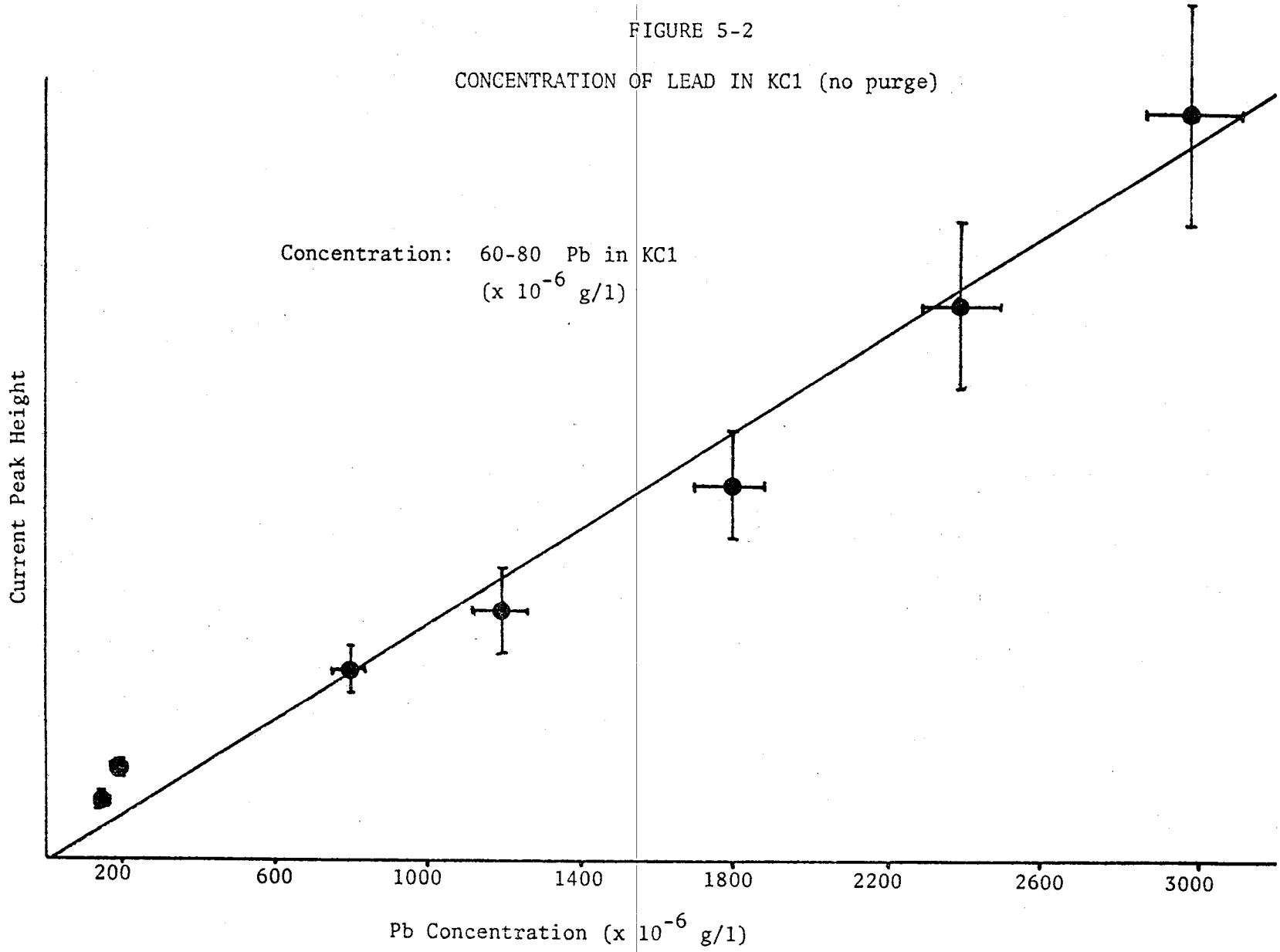

experiments, using a ten minute plating time, an applied potential of -0.77 volts, and a thirty second rest time between the reducing and oxidizing steps. Each analysis had two oxidizing sweeps in order to minimize residual currents caused by other trace metals in the sea water with reducing potentials close to that of lead. For the first sweep a fast rate of 1 sec/in is the most effective for reducing the noise, and a slower speed of 5 sec/in for recording the second sweep for lead as it is oxidized. Table 5-2 shows the lead additions.

TABLE 5-2

CALIBRATIONS FOR Pb IN SEA WATER (with purge)

Calibration Sweep Number (two sweeps for each step)	Pb Added ($x\ 10^{-6}$ g/l)	Total Pb in Sea Water ($x \cdot 10^{-6}$ g/l)
(1)	(blank)	(x)
(2)	-	(x)
(3)	200	(x + 200)
(4)	300	(x + 500)
(5)	600	(x + 1100)
(6)	600	(x + 1700)

Figure 5-3 shows the X-Y plot of the peaks, and Figure 5-4 shows the calibration curve for the original lead concentration in the sample. I used peak height instead of area for the calculations. The calibration curve is a best fit curve and is not linear due to partitioning changes at these concentrations. The next section discusses this event in detail. Figure 5-5 shows this same analysis performed after the

FIGURE 5-3

I.A.P.S.O. SEA WATER,
SEA WATER ANALYSIS - PURGE

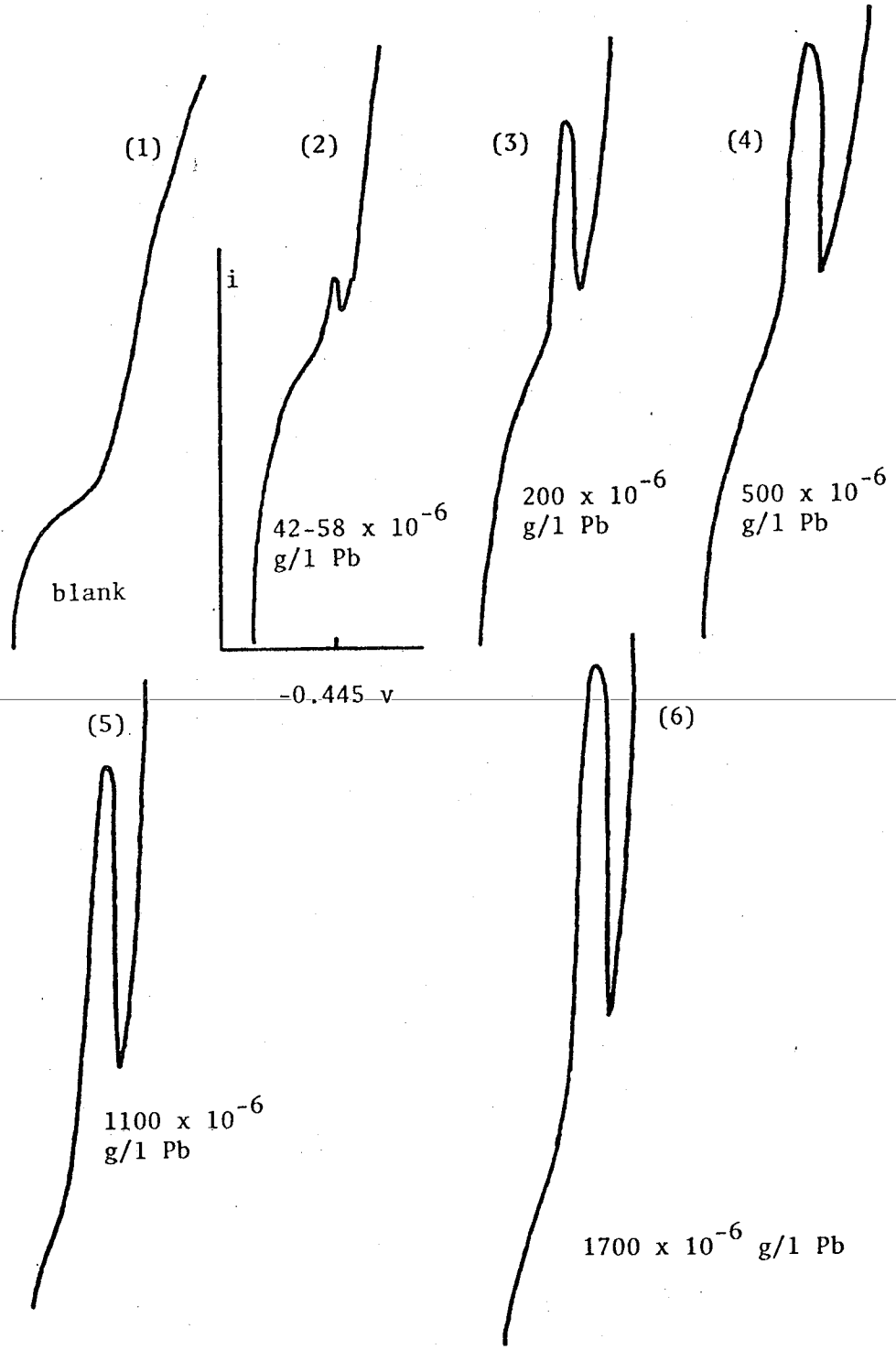

FIGURE 5-4

CONCENTRATION OF LEAD IN SEA WATER - PURGE

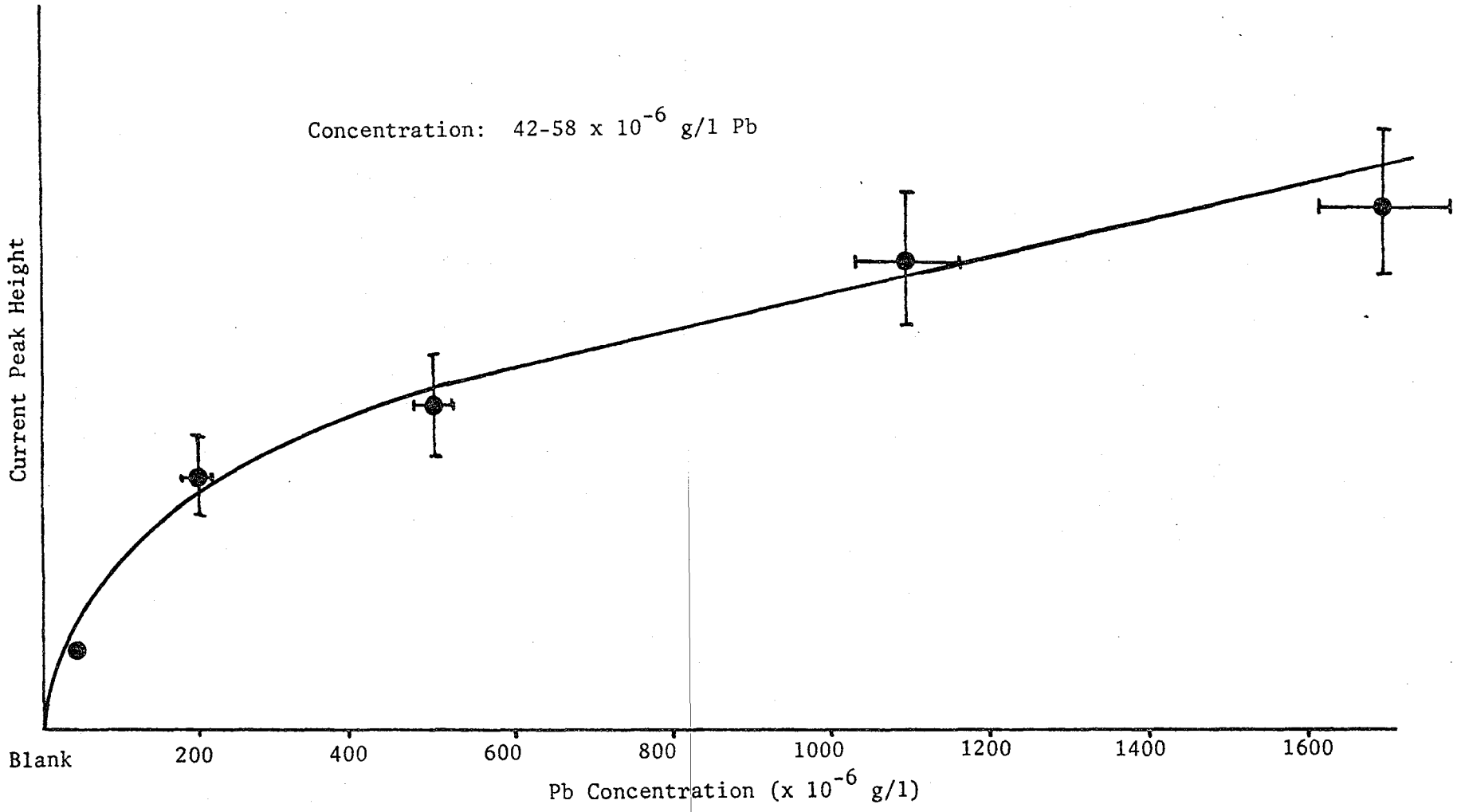

FIGURE 5-5

CONCENTRATION OF LEAD IN SEA WATER - PURGE
(Non-Acidified Sample - 6 Month Storage in Glass Container)

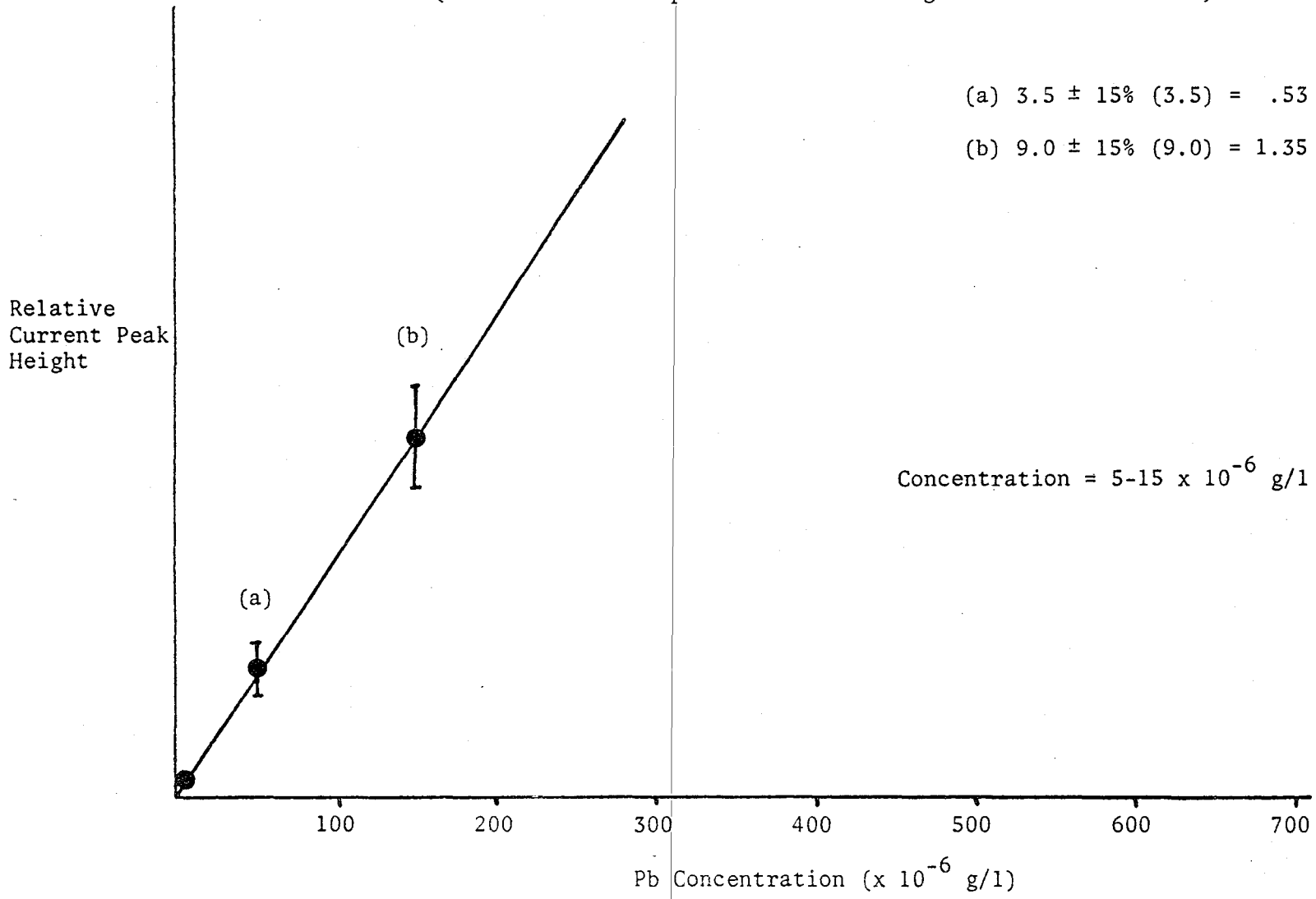

sample had been stored in an ordinary hard glass citrate bottle for six months. The lead concentration has dropped from 4.2 - 5.8 x 10^{-5} g/l to 0.5 - 1.5 x 10^{-5} g/l. This difference may be from experimental error but most likely it is from the glass scavenging the lead ions.

Laboratory Experiments - Sea Water - No Purge

I repeated the previous experiments but this time did not purge the solution. Again the cell held 150 ml of I.A.P.S.O. Standard Sea Water P57, $^{8-9}$/1 1972 along with 20 ml of the 0.1 Hg solution. The solution was not purged, and the blank was run immediately. I recorded the blank and added successive increments of lead, using the usual two minutes plating time, an applied potential of between -0.80 and -0.90 volts, and a one minute rest between the reducing and the oxidizing steps. (The one minute rest appears to give better resolution than the thirty second rest in some cases.) I swept the voltage twice, the first at 1 sec/in to eliminate the residual currents and the second at 5 sec/in to record the current peak height. Table 5-3 shows the lead additions.

TABLE 5-3

CALIBRATION FOR Pb IN SEA WATER (without purge)

Calibration Sweep Number (two sweeps for each step)	Pb Added (x 10^{-6} g/l)	Total Pb in Sea Water (x 10^{-6} g/l)
(1)	(blank)	(x)
(2)	-	(x)
(3)	200	(x + 200)
(4)	300	(x + 500)
(5)	300	(x + 800)

Figure 5-6 shows the X-Y plot of the peaks, and Figure 5-7 shows the calibration curve. The multiple peaks of Figure 5-6 are a function of the species and are discussed in the next section. I did not plot the peaks from additional concentrations of lead because of residual current noise from intermetallic reactions with the mercury on the electrode surface. This noise occurs upon occasion with ASV sea water analysis and with high trace element concentrations in most types of electrolytes (Batley and Florence, 1974, p.36). Without the purge, the lead concentration, 2.5 - 3.5 x 10^{-5} g/l, is slightly lower than the concentration determined by the analysis with the purge, but this may be a function of the species.

Modeling and Partitioning of Lead in Sea Water

The next paragraph describes the general method for my species model, and the next few sections expand on this method and describe the theoretical features of ASV and the chemical forms of lead which make this method possible.

This thesis models lead in sea water by comparing the theoretical $E_{oxid.}$ for lead with a measured $E_{oxid.}$ from the simplified ASV system and attributing the potential difference to a potential shift caused by labile forms of lead. The theoretical $E_{oxid.}$ depends on the exact oxidation equation (2-59) and considers lead to be a free ion, Pb^{++}. Within experimental error, which includes $E_{misc.}$, the difference from $E_{measured}$ is caused by labile complexing of lead ions. In addition, the theoretical total lead concentration which is derived from the ASV analysis with the lead additions method is compared to the non-linear

FIGURE 5-6

SEA WATER ANALYSIS - NO PURGE
(150 ml I.A.P.S.O. Sea Water, No Purge)

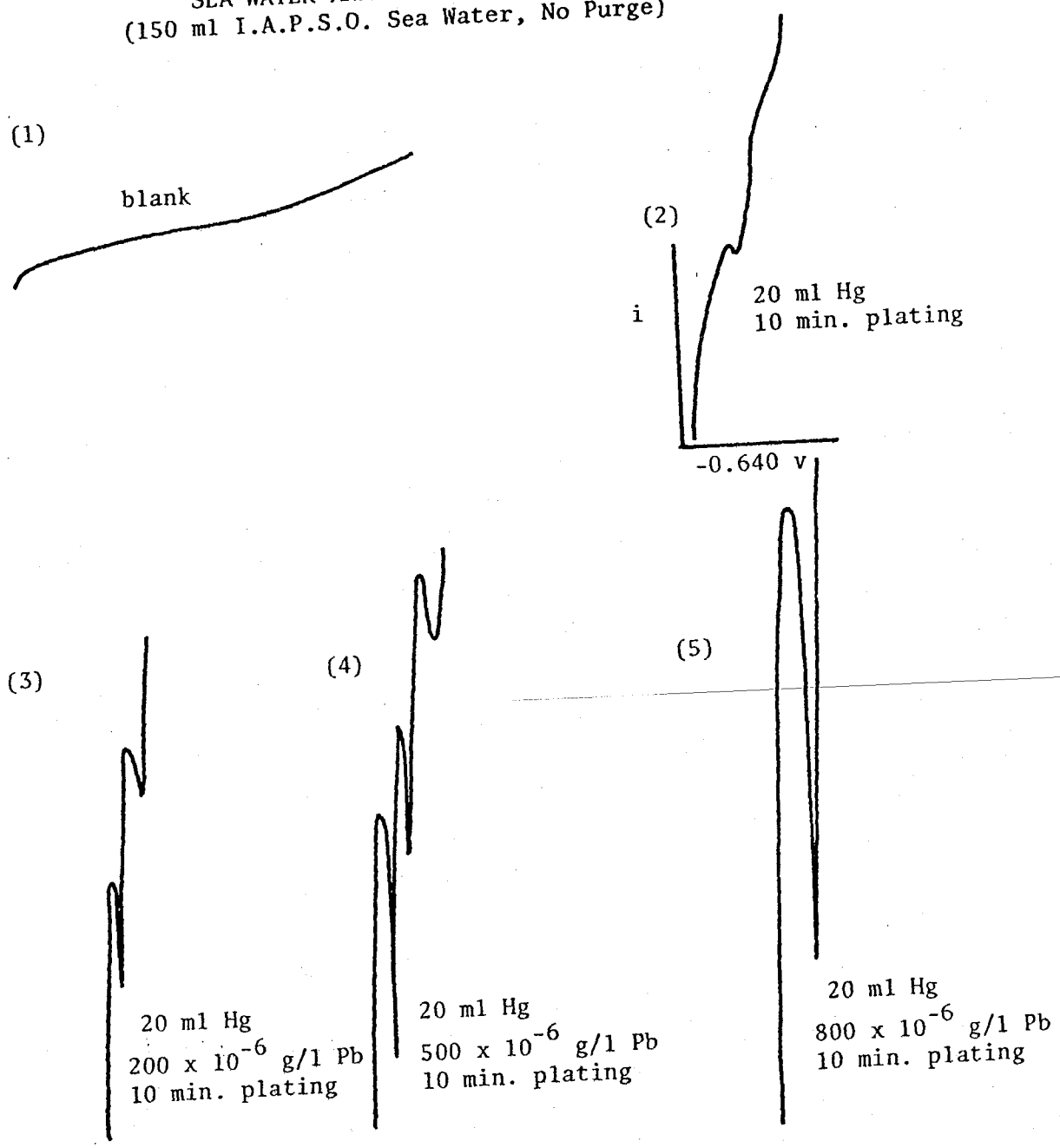

FIGURE 5-7

CONCENTRATION OF LEAD IN SEA WATER - NO PURGE

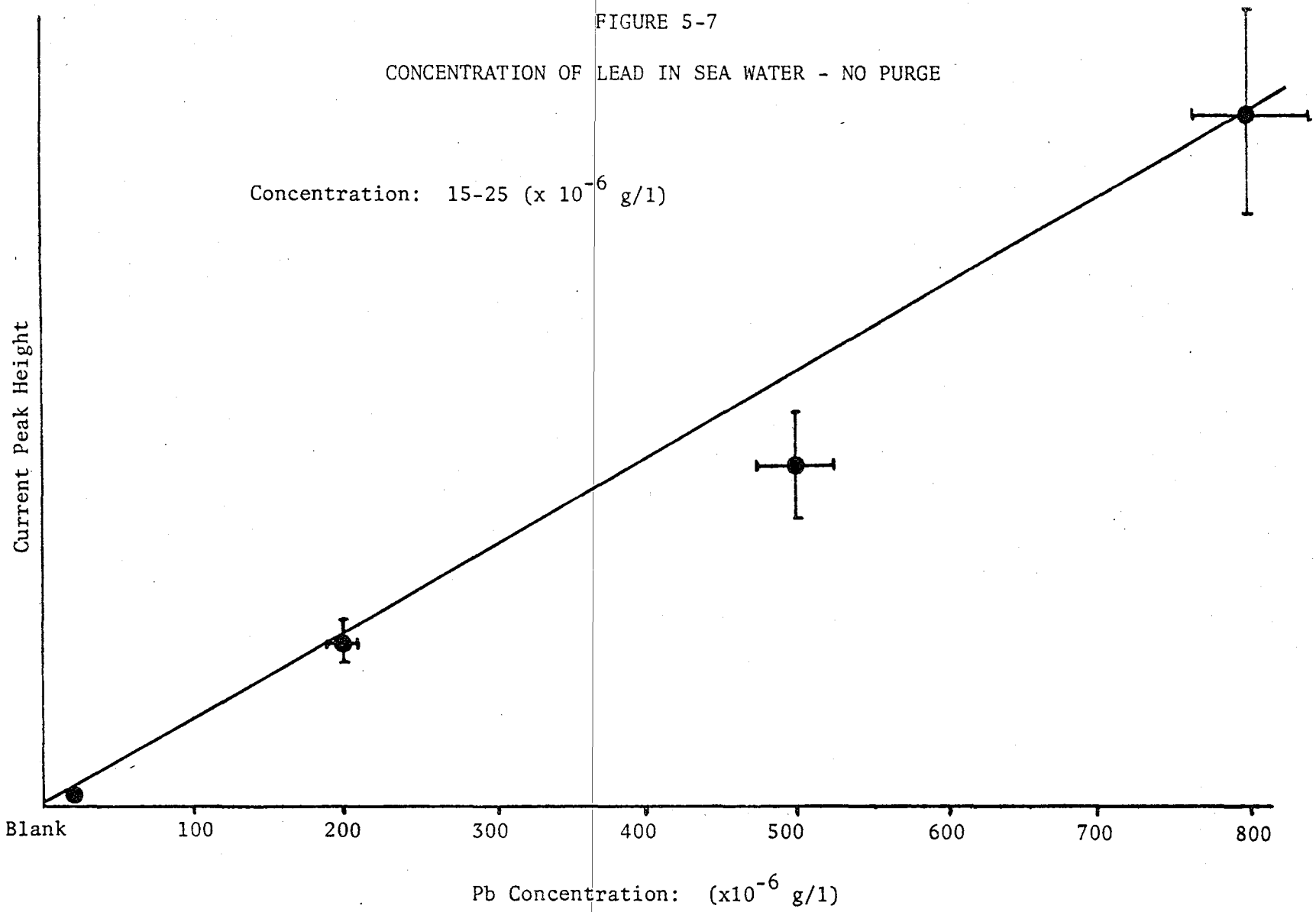

current peak heights, and the difference is attributed to non-labile lead complexes. These chemical forms are combined into a chemical model with lead partitioned according to percentages of the total lead content.

First, the mass balance equation is written for the particular metal in order to calculate the total distribution of the chemical species (Garrels and Thompson, 1962, p.62; Goldberg, 1965, p.163; and Zirino and Yamamoto, 1972, p.662):

$$(5\text{-}11) \quad [M]_{total} = [M] + \sum_{n=1}^{4} \sum_{i=1}^{j} [M\,L(i)_n]$$

with: $[M]_{total}$ = total metal concentration

$[M]$ = uncomplexed and/or hydrated metal ion concentration

$[M\,L(i)_n]$ = concentration of the nth order complex between the metal M and the ligand L(i)

j = total number of ligand types (anions) included in the model

The concentration of the complex $[M\,L(i)_n]$ is expressed in terms of the stability constant $\beta(i)_n$ (Zirino and Yamamoto, 1972, p.663):

$$(5\text{-}12) \quad [M\,L(i)_n] = \beta(i)_n\,[M]\,[L(i)]^n \; \frac{\gamma_M\,\gamma^n_{L(i)}}{\gamma_{M\,L(i)_n}}$$

with: $\beta(i)_n$ = overall stability constant for the complex

γ_M = thermodynamic activity coefficient of the uncomplexed metal ion M

$\gamma_{L(i)}$ = thermodynamic activity coefficient of the uncomplexed ligand L(i)

$\gamma_{ML(i)_n}$ = thermodynamic activity coefficient of the complex $ML(i)_n$

Table 5-4 diagrams the various forms in which lead may be partitioned in sea water (Batley and Florence, 1976, p.352). For sea water the chemical model limits the chemical forms to percent particulate and soluble lead partitioned as free ions, as hydrated ions, or among several of the major conservative anions (Garrels and Thompson, 1962, p.58). Along with Na^+, K^+, Mg^{++}, and Ca^{++}, these ions make up more than 99% of the dissolved solids in sea water (Sverdrup and others, 1942, p.166). According to Garrels and Thompson (1962, p.58), "Enough chemical data are available for these species to make possible the assessment of the most important interactions, and thus to calculate the proportion of each that exists as the free ion, as well as the proportion present as complexes." For soluble lead then, and for complexes with coordination numbers of one to four, the mass balance equation is:

$$Pb_{total} = [Pb^{++}] + [PbCO_3^o] + [PbCl^+ + PbCl_2^o + PbCl_3^- + PbCl_4^=] + [Pb(SO_4)^+ + Pb(SO_4)_2^=] + [PbHCO_3^+] + [Pb(OH)^+ + Pb(OH)_2^o + Pb(OH)_3^- + Pb(OH)_4^=] \quad (5\text{-}13)$$

Table 5-5 shows a schematic diagram of these chemical forms of lead in sea water based on this equation.

TABLE 5-4

GENERAL PARTITIONING OF LEAD IN SEA WATER

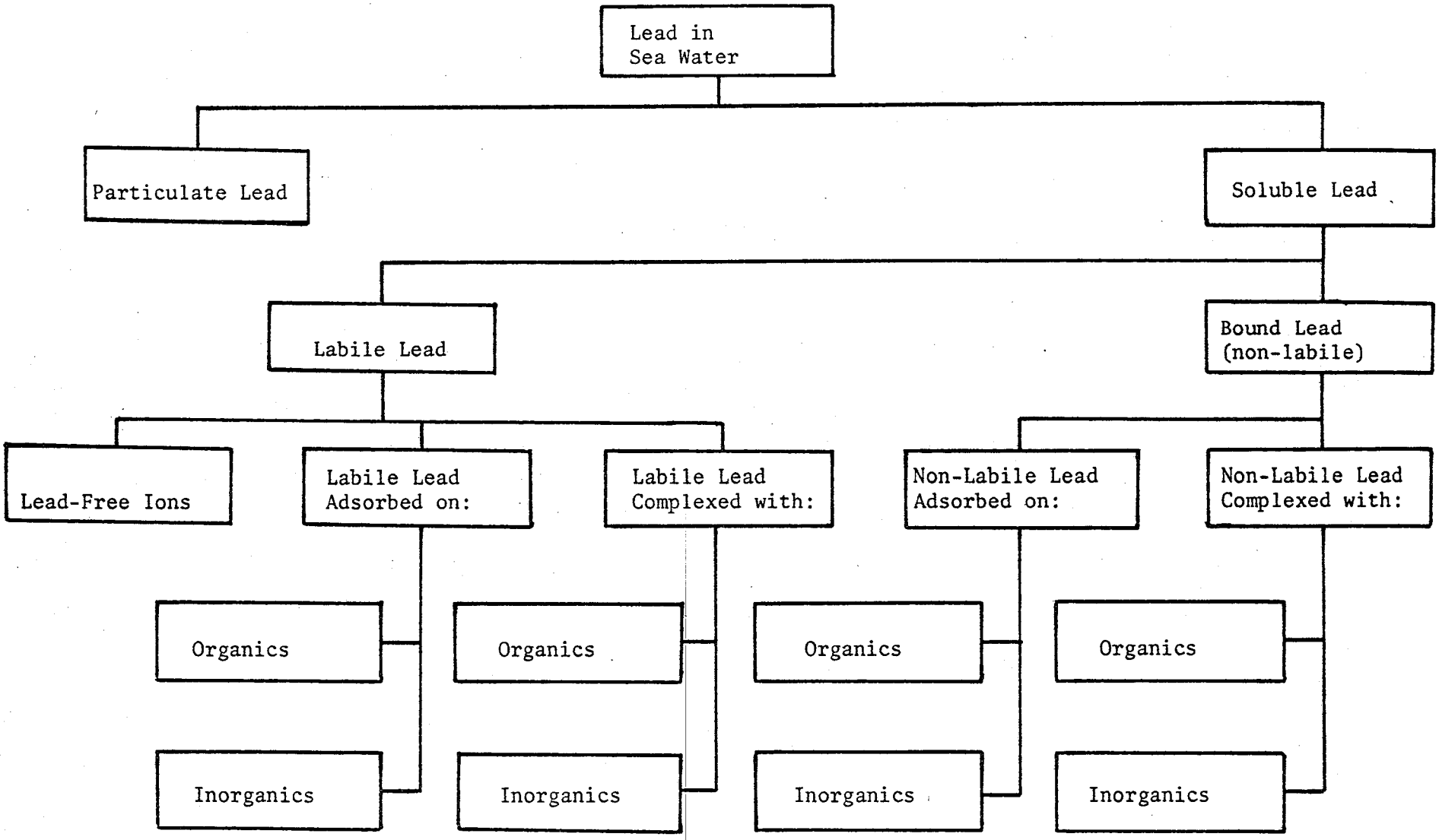

TABLE 5-5

PARTITIONING OF LEAD IN SEA WATER WITH MAJOR ANIONS

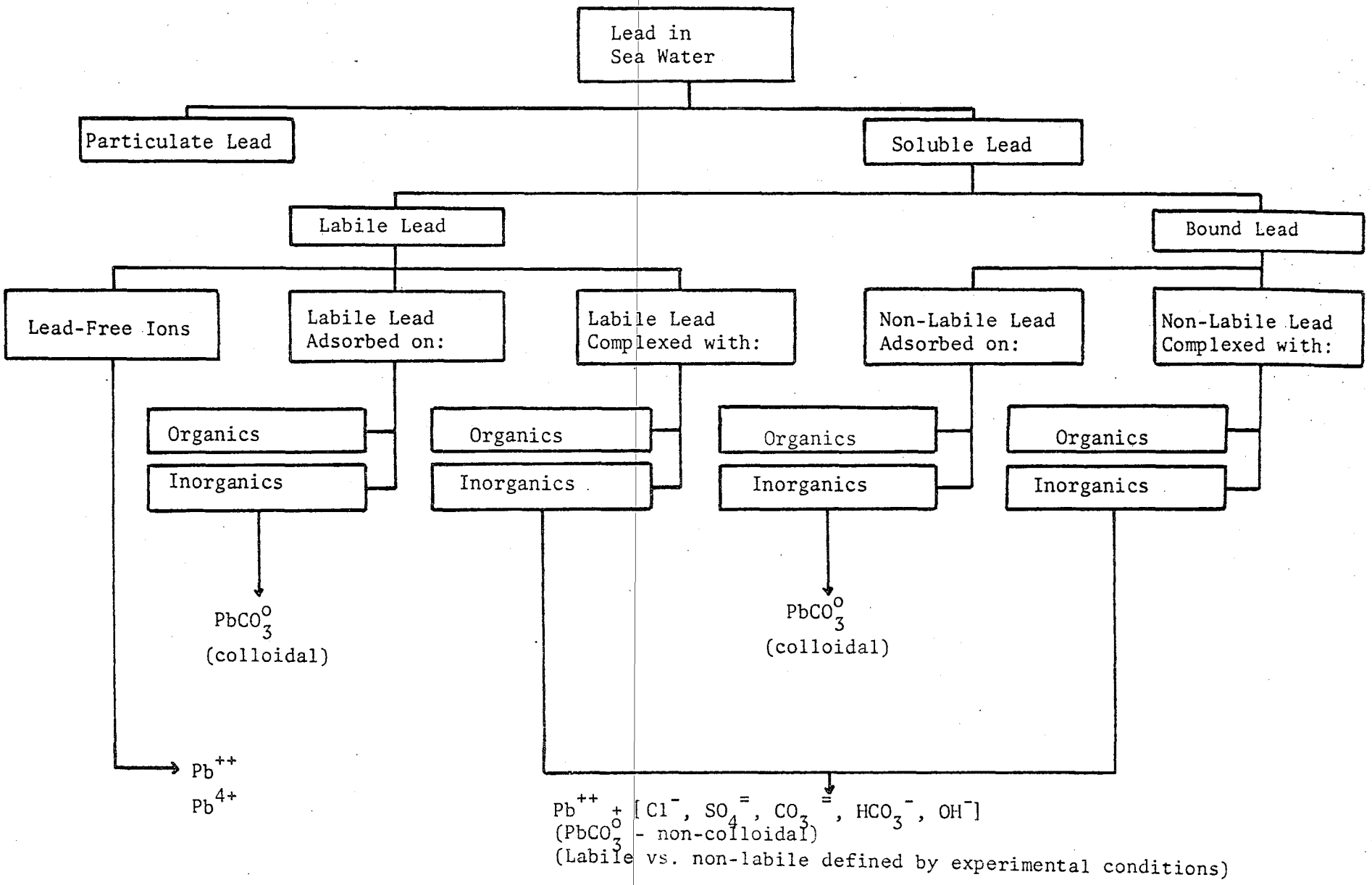

Goldberg (1965, p.163) outlines a system for determining the dominant anions which complex with transition trace metals where the d shells have between zero and ten electrons. Expression (5-14) is the general relationship for this method:

(5-14) if: $\log K_i - \log K_j > \log a_j - \log a_i$

with: K_i = stability constant for the ith ion

K_j = stability constant for the jth ion

a_j = activity of the jth ion

a_i = activity of the ith ion

then anion $L(i)_n$ is dominant over $L(j)_n$.

Expression (5-15) shows the dominant order of the major complexes from the mass balance equation. Stability constant values are from Sillén and Martell (1964), and the activity coefficient and concentration values are from Whitfield (1975, p.1549 and 1552).

(5-15) $PbCO_3^o > PbSO_4^o > PbSO_4^{++} > PbCl^+ > PbOH^+ > PbCl_2^o > PbCl_3^- > PbCl_4^= > Pb(OH)_2 > Pb(OH)_3^- > Pb(OH)_4^=$

One expects to see $PbCO_3^o$ as the most dominant of the lead species.

Electrochemical traits of Certain Lead Species

Table 5-6 lists the electrochemical traits of various forms of lead. These next paragraphs explain these traits and the ASV method and equations for measuring them.

TABLE 5-6

ELECTROCHEMICAL TRAITS OF VARIOUS CHEMICAL FORMS OF LEAD

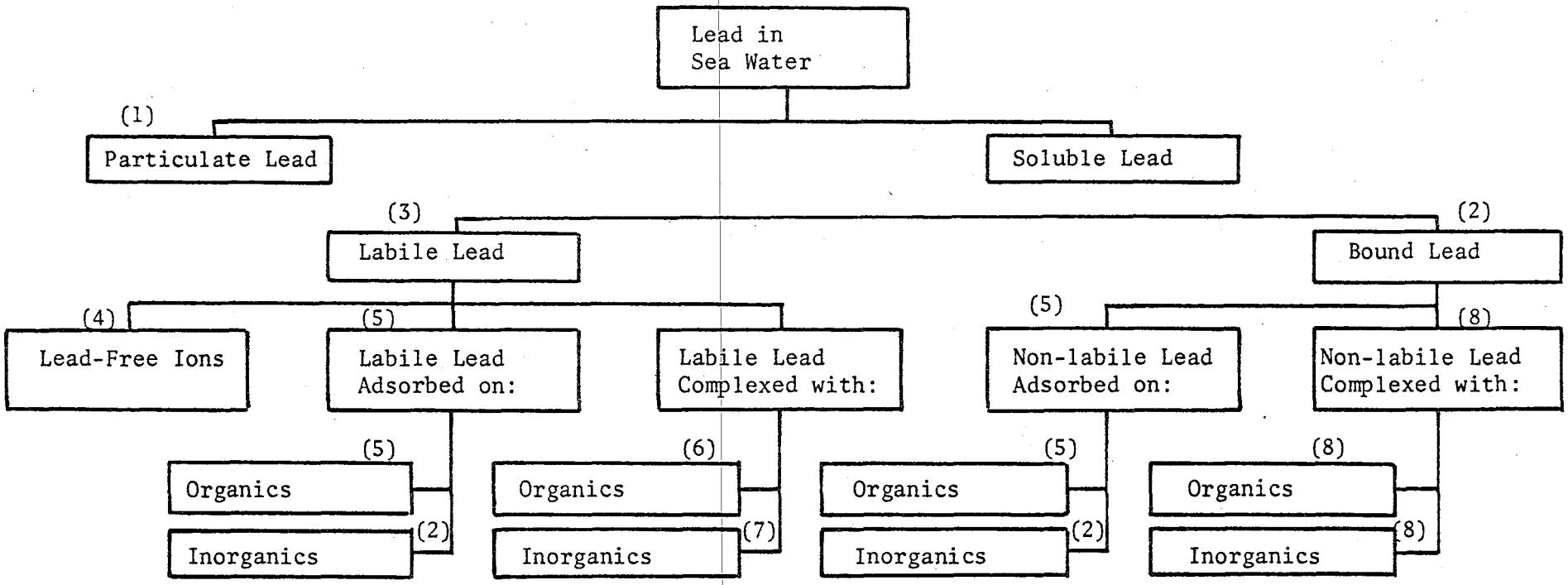

(1) Particulate lead will be separated from soluble lead by filtering the sea water samples.
(2) For bound lead, dissociation of the couples is the limiting effect resulting in repression of the current peak
(3) For labile lead, speciation dissociation is more rapid than the trace element oxidation step, resulting in a shift of the peak potential.
(4) Pb^{++} will oxidize at a potential of $E = E^{o} + \frac{RT}{NF} \ln \frac{[Pb^{++}]}{[Pb(Hg)]}$
(5) Discharged colloids of limited stability are not distinguishable with ASV.
(6) The stable organic complexes will not cause a shift in the oxidizing potential.
(7) The stable inorganic complexes will oxidize at a potential of $E = E^{o} + \frac{RT}{NF} \ln \frac{[Pb\ L(i)n]}{[Pb(Hg)][L(i)n]}$
(8) Stable organic and inorganic complex oxidation reactions will be limited by the dissociation rate, resulting in a repression of the current peaks.

1) Particulate Lead

Particulate lead is separated from soluble lead by filtering the sea water samples through a 0.45 μm membrane filter (Batley and Florence, 1976, p.353). The usual sampling practice is for suspended particulate matter to be separated from sea water as soon as possible after collection because: (a) the composition of the samples may change as trace metals are lost from the samples by adsorption on the particulate matter; and (b) the composition of the particulate material may change as trace metals are lost to the solution. The 0.45 - 0.50 μm filter is a standard size, and the material retained by this filter is considered particulate matter for other chemical and physical determinations (Dean, 1972, vol. I, p.11).

2) Labile (unstable) Lead

Labile lead includes lead as a free ion, unstable lead adsorbed on organics and inorganics, and unstable lead complexed with organics and inorganics. For ASV analysis, unstable is a relative term, defined by the experimental conditions which are explained in the following paragraphs.

a) Lead as free ions:

Lead as a free ion is reduced directly to the mercury amalgam: $Pb^{++} \xrightarrow{k_c} Pb(Hg)$. K_c is the reaction rate constant; equation (2-43) gives the plating potential; and equation (2-59) gives the oxidation potential:

$$(2\text{-}59) \qquad E_{app_{oxid}} = \{E^o + \frac{RT}{nF} \ln (K)\}_{\frac{1}{2}cell} + \{E^o + \frac{RT}{nF} \ln (K)\}_{ref.} + \frac{RT}{nF} \ln \{\frac{\delta l t_s nF}{D_o RT}\} + \{\frac{RT}{nF} (\frac{i_a}{i_o})\} \pm 5\% \ (E_{misc.})$$

The $E_{\frac{1}{2}cell}$ term is given by:

$$(5\text{-}6) \qquad E_{\frac{1}{2}cell} = E^o + \frac{RT}{nF} \ln \frac{[Pb^{++}]}{[Pb(Hg)]}$$

b) <u>Labile lead complexed with inorganics</u>

For lead complexed with inorganic ligands, the complex must undergo dissociation into Pb^{++} and the respective ligands prior to the reduction of lead as the mercury amalgam. The general reactions are these:

$$(5\text{-}16) \qquad PbL(i)_n \underset{}{\overset{K_{L(i)n}}{\rightleftharpoons}} L(i)_n + Pb^{++} \xrightarrow{K_c} Pb(Hg)$$

with: $L(i)_n$ = the ligand or anion

$K_{L(i)_n}$ = dissociation rate for the labile ligand (cm/sec)

K_c = reaction rate constant (cm/sec)

Labile lead complexes dissociate at a faster rate than the rate for plating free ions (Mancy, 1972), $K_{L(i)_n} > K_c$. If lead occurs as either free ions or labile lead complexed with inorganics, the current peak height, i_p, is the same provided the dissociation rate for the labile ligand is faster than the mercury amalgam reduction rate constant.

General equation (2-59) gives the oxidation potential, and the $E_{\frac{1}{2}cell}$ term is:

$$(5\text{-}17) \qquad E_{\frac{1}{2}cell} = E^{o} + \frac{RT}{nF} \ln \frac{[PbL(i)_n]}{[Pb(Hg)][L(i)_n]}$$

Bradford (1973) shows that in certain cases the diffusion term, D_o, for the linear sweep term of the general equation is constant and that the anodic over-potential is small and constant for alkaline media. Fried (1973, p.46) also finds a low anodic over-potential. Therefore, as $E_{misc.}$ values are small, and as the $E_{ref.}$ value is constant the only difference in the total oxidation for lead in sea water as a free ion and for labile lead in sea water complexed with inorganics is the $E_{\frac{1}{2}cell}$ term.

$$(5\text{-}18) \qquad E_{\frac{1}{2}cell} \text{ for Pb as a free ion} = E^{o} + \frac{RT}{nF} \ln \frac{[Pb^{++}]}{[Pb(Hg)]}$$

$$(5\text{-}19) \qquad E_{\frac{1}{2}cell} \text{ for Pb as labile inorganic complexes} =$$

$$E^{o} + \frac{RT}{nF} \ln \frac{[PbL(i)_n]}{[Pb(Hg)][L(i)_n]}$$

During the linear sweep for oxidation of lead, the shift of the oxidation potential for the current peak, i_p, will distinguish Pb as a free ion from Pb as a labile inorganic complex.

c) Labile lead complexed with organics

Researchers (Bradford, 1973; Ernst and others, 1975) found that shifts of the current peak potentials do not occur with labile organic complexes. No reason for this is given, but perhaps the potential does not shift because the organic ligands do not re-bind the free lead ions as they are stripped off the electrode. Equations (5-20) and (5-21) are the stripping reactions for the free ion and labile inorganic complexes:

(5-20) Lead in sea water as a free ion: $Pb(Hg) \xrightarrow{K_a} Pb^{++}$

with: K_a = oxidation reaction constant (cm/sec)

(5-21) Lead in sea water as a labile inorganic complex:

$$Pb(Hg) \xrightarrow{K_c} Pb^{++} + L(i)_n \xrightarrow{K_{L(i)_n}} PbL(i)_n$$

with: $K_{L(i)_n}$ = dissociation rate for the labile ligand (cm/sec)

The inorganic ligands re-bind the free lead ions, but this does not seem to occur for the labile organic complexes. Evidently the reaction is not electrochemically reversible (Ernst and others, 1975, p.970).

d) Labile and non-labile lead adsorbed on organics and inorganics:

Zirino and Yamamoto (1972, p.669) found that uncharged species of limited solubility behave in inert fashion at the working electrode and are the basis for colloid formation. Batley and Florence (1976, p.348)

define this chemical form as lead occluded in or adsorbed on highly dispersed colloids. Such uncharged species of limited solubility may include lead bound to clays, silicates, carbonates, and hydroxides. The inert behavior of these colloids at the working electrode suggests that the dissociation rate for these species is less than the reaction rate constant, and that these species are non-labile compared to the reduction electrode reaction. Therefore lead in this form has a repressive effect on the current peak, i_p, and this effect appears to be present for most inorganic colloids.

3) Non-Labile (unstable lead)

Non-labile lead includes stable lead adsorbed, or complexed with, organics and inorganics.

a) non-labile lead complexed with inorganics:

Equation (5-22) shows the process by which lead, as an inorganic complex, is reduced as part of a mercury amalgam:

$$\text{(5-22)} \qquad PbL(i)_n \xrightleftharpoons{K_{L(i)_n}} L(i)_n + Pb^{++} \xrightarrow{K_c} Pb(Hg)$$

For a non-labile or stable complex the dissociation constant, $K_{L(i)_n}$ is less than the reduction reaction constant, K_c. "Under these conditions the rate of dissociation of the metal complex is less than the rate limiting step, and a reduction of i_p is observed. On this basis, it is possible to differentiate between free metals and labile metal complexes on one hand and non-labile complexes on the other."

(Mancy, 1972, p.7). Lead as a free ion or labile inorganic complex causes the potential for the current peak to shift, and lead as a non-labile inorganic complex has a repressive effect on the current peak. Lead as an inorganic colloid also has this repressive effect. (Table 5-6 lists these traits.) A potential shift for the stripping peak is expected for the non-labile reactions, but this shift may be difficult to notice because of the reduced i_p.

b) Non-labile lead complexed with organics:

Zirino and Healy (1970, p.956) found in their studies that the peak currents of lead are controlled by the major inorganic complexes, not by the organic ones. No reason is given for this behavior, but it must be that the organic complexes are completely inert compared to the reduction process.

The Chemical Model

The electrochemical traits of the chemical forms along with the oxidation potential expression (2-59) are the fundamental constituents of the chemical model. The model operates in this manner.

Expression (2-59) gives the precise oxidation potential at which a particular element is stripped from the working electrode:

$$(2\text{-}59) \qquad E_{app_{oxid}} = \{E^o + \frac{RT}{nF} \ln (k)\}_{\frac{1}{2}cell} + \{E^o + \frac{RT}{nF} \ln (k)\}_{ref.} + \frac{RT}{nF} \ln \{\frac{\delta l t_s nF}{D_o RT}\} + \{\frac{RT}{nF} (\frac{i_a}{i_o})\} \pm 5\% \ (E_{meas.})$$

This expression is rewritten as:

$$(5\text{-}23) \qquad E_k = E_{app_{oxid}} - \{E^o + \frac{RT}{nF} \ln (k)\}_{\frac{1}{2}cell}$$

$$\text{with:} \qquad E_k = \{E^o + \frac{RT}{nF} \ln (k)\}_{ref.} + \{\frac{RT}{nF} \ln \{\frac{\delta l t_s nF}{D_o RT}\}\} + \{\frac{RT}{nF} (\frac{i_a}{i_o})\} \pm 5\% \ (E_{meas.})$$

The preceding section explains in detail why, by making certain reasonable assumptions, E_k is constant during ASV analysis for a particular trace element. This constant is calculated by substituting the proper values into the expression (5-23). The preceding section also explains that for certain chemical forms of lead the only terms of the oxidation potential which are affected are the ½ cell terms (5-18) and (5-19). These expressions are combined and rewritten as follows:

$$(5\text{-}24) \qquad E_{meas.} - E_k = E_{PbL(i)_n} = E^o + \frac{RT}{nF} \ln \frac{[\gamma(PbL(i)_n)]}{[Pb(Hg)][L(i)_n]}$$

with: $E_{measured}$ = the measured potential at which the current peak appears.

$E_{Pb(L(i)_n)}$ = the ½ cell potential for a particular lead complex.

γ_n = the activity coefficient for the lead complex.

Values in expression (5-24) are obtained in this manner:

$E_{measured}$	=	graph plotted by the X-Y recorder;
E_k	=	constant determined by expression (5-23);
E^o	=	variable determined from the free energies of the reactants and products;
$E_{PbL(i)_n}$	=	$E_{measured} - E_k$;
$\frac{RT}{F}$	=	constant;
n	=	number of electrons involved in the reaction;
γ	=	unknown;
$PbL(i)_n$	=	concentration of complex n obtained from the literature;
$[L(i)_n]$	=	activity of the major anion obtained from the literature;
[Pb(Hg)]	=	activity of lead in the mercury amalgam and assigned a value of unit activity (Garrels and Christ, 1965, p.48).

Tables in the next chapter show values of $E_{PbL(i)_n}$ for the various complex reactions. These values, based on 100% complexing for each particular form, give an indication of which labile form of lead is being measured; the solution to equation (5-24) gives the activity coefficient, γ_n, for the particular species; the current peak i_p, gives the concentration of the species; and the non-linearity of the calibration curve indicates the non-labile complex type and concentration. Expression (5-15) shows the expected dominant order of complexes.

CHAPTER VI

RESULTS - CHEMICAL MODELING WITH FIELD SAMPLES

"I pass with relief from the tossing sea of Cause and Theory to the firm ground of Result and Fact."

Winston Churchill, 1898, The Malakand Field Force

Calculations for Model - The Constant E_k

The preceding chapter explains the importance to the chemical model of the constant, E_k. E_k is equal to the four potential terms which remain constant during the oxidation step:

$$(6\text{-}1) \qquad E_k = \{E^o + \frac{RT}{nF} \ln (k)\}_{ref.} + \{\frac{RT}{nF} \left(\frac{i_a}{i_o}\right)\} + E_{misc.} + \{\frac{RT}{nF} \ln \left[\frac{\delta l t_s nF}{[D_o RT]}\right]\}$$

The first term, $\{E^o + \frac{RT}{nF} \ln (k)\}_{ref.}$, is the potential for the saturated calomel electrode. The value is -0.244 volts.

The second term, $\{\frac{RT}{nF}\left(\frac{i_a}{i_o}\right)\}$, represents the anodic transfer overpotential. The value, shown by expression (2-46), is -0.013 volts.

The third term, $E_{misc.}$, is the term for various additional potentials which are explained and derived in Chapter II. This term, which includes experimental error, is 5% of the $E_{measured}$ term.

By making these substitutions equation (6-1) is rewritten as:

$$(6\text{-}2) \qquad E_k = -0.244 \text{ volts } -0.013 \text{ volts} \pm 5\% \; E_{meas.} + \{\frac{RT}{nF} \ln \frac{\delta l t_s nF}{D_o RT}\}$$

These are the values for the variables in the last term:

(a) $\frac{RT}{nF} \ln (x) = 0.0592 \log (x)$

(b) n = number of electrons involved in the reaction = 2

(c) t_s = potential sweep speed = 10 mv/sec.

(d) 1 = mercury film thickness = 1×10^{-4} cm (Roe and Toni, 1965, p.1503)

(e) D_o = the diffusion coefficient for Pb^{++} = 1×10^{-5} cm^2/sec.

[According to the Handbook of Chemistry and Physics, 57th Edition, F-62, and the Encyclopedia of Chemistry, 1973, p.342, the diffusion coefficients for metals in electrolyte solutions are usually of the order of 1×10^{-5}. Equation (6-3) derives this value (Handbook of Chemistry and Physics, 57th Edition, F-62):

$$D_o = \frac{RT}{F^2} \left[\frac{(\nu_1 + \nu_2)(\lambda_1^o + \lambda_2^o)}{(\nu_1)[z_1](\lambda_1^o + \lambda_2^o)} \right] \tag{6-3}$$

with: ν_1 and ν_2 = number of cations and anions formed from one molecule of electrolyte

λ_1^o and λ_2^o = cation and anion equivalent conductiveness

z_1 = cation valancy]

Delahay (1954, p.224) estimates a general value for δ of 5×10^{-3} cm in a stirred solution. The limiting current (or current peak, i_p) during the stripping step gives the value of δ in an unstirred solution:

$$(2\text{-}49) \qquad \delta = \frac{-ZFD_oC_b}{i_l}$$

The value of δ is 4×10^{-3} cm by making these substitutions into equation (2-49): $C_b = 1.9 \times 10^{-8}$ moles/cm^3 (Whitfield, 1975, p.1549); $D_o = 1 \times 10^{-5}$ cm^2/sec; $F = 9.6 \times 10^{-4}$ coulombs/equivalent; $Z = 2$; and $i_l = 1 \times 10^{-5}$ amps/cm^2.

By making these substitutions into the last term of (6-2), $\frac{RT}{nF} \ln \left[\frac{\delta l t_s nF}{D_o RT} \right]$, the term becomes:

$$(6\text{-}4) \quad (0.0246) \log \left[\frac{(4 \times 10^{-3}\text{cm})(1 \times 10^{-4}\text{cm})(2)(1 \times 10^{-2}\text{v/sec})}{(1 \times 10^{-5}\text{cm}^2/\text{sec})(0.0257)} \right] = 0.037 \text{ volts}$$

Equation (6-2) becomes:

$$(6\text{-}5) \qquad E_k = 0.257 \text{ volts} \pm 5\% \ (E_{meas.}) + 0.037 \text{ volts}$$

and:

$$(6\text{-}6) \qquad E_k = 0.294 \text{ volts} \pm 5\% \ (E_{meas.})$$

$E_{\frac{1}{2}cell}$ for Chemical Forms of Lead

Tables 6-1A and 6-1B show the ½ cell potentials for various chemical forms of lead. The potential differences between the chemical forms differentiate between the species in the chemical model. Because only the relative potential differences between the chemical forms are important for the model, values for the potential expression, $E^o + \frac{RT}{nF} \ln \frac{[PbL(i)_n]}{[Pb(Hg)][L(i)_n]}$, are based on the following assumptions and estimates:

a) The central problem for all chemical models is to arrive at reliable values for the activities of trace elements which are in complex form. To do this one must know the concentrations, activity coefficients, and ionic interactions, but then the original purpose of the model is to arrive at this information. Because of this dichotomy and because only the relative potential difference between forms is important, expression (6-7) is in the form of the ½ cell potentials:

$$(6\text{-}7) \quad - \left\{\left(E^o - \frac{RT}{2F} \ln [Pb(Hg)][L(i)_n]\right) + \frac{RT}{2F} \ln [PbL(i)_n]\right\}$$

For example, the ½ cell potential for Pb^{++} is:

$$(6\text{-}8) \quad - \left\{\left(0.126 - \frac{RT}{2F} \ln [1]\right) + \frac{RT}{2F} \ln [(7.5 \times 10^{-2})\ (1.9 \times 10^{-8} \text{ moles})]\right.$$

$$\left. = -0.388 \text{ v}\right\}$$

with: $\gamma_{Pb^+} = 7.5 \times 10^{-2}$

$Cb_{Pb^{++}} = 1.9 \times 10\text{-}8$ (Whitfield, 1975, p.1549 and p.1552)

TABLE 6-1A

$E_{\frac{1}{2}cell}$ FOR CHEMICAL FORMS OF LEAD

	Chemical Form	Potential Expression	Activities, Activity Coefficients, Concentrations
1.	Pb^{++}	$E^o + \frac{RT}{nF} \ln \frac{[Pb^{++}]}{[Pb(Hg)]}$	$C_{b_{Pb^{++}}} = 1.9 \times 10^{-8}$ moles $\gamma_{Pb^{++}} = 7.5 \times 10^{-2}$ $a_{Pb(Hg)} = 1$
2.	$PbCl_2^o$	$E^o + \frac{RT}{nF} \ln \frac{[PbCl_2^o]}{[Pb(Hg)][Cl^-]^2}$	$\gamma_{Cl^-} = 6.91 \times 10^{-1}$ $C_{b_{Cl^-}} = 5.51 \times 10^{-1}$ moles
3.	$PbCl^+$	$E^o + \frac{RT}{nF} \ln \frac{[PbCl^+]}{[Pb(Hg)][Cl^-]}$	$\gamma_{Cl^-} = 6.91 \times 10^{-1}$ $C_{b_{Cl^-}} = 5.51 \times 10^{-}$ moles
4.	$PbCl_3^-$	$E^o + \frac{RT}{nF} \ln \frac{[PbCl_3^-]}{[Pb(Hg)][Cl^-]^3}$	$\gamma_{Cl^-} = 6.91 \times 10^{-1}$ $C_{b_{Cl^-}} = 5.51 \times 10^{-1}$ moles

TABLE 6-1A (Continued)

	Chemical Form	Potential Expression	Activities, Activity Coefficients, Concentrations
5.	$PbCl_4^{=}$	$E^o + \frac{RT}{nF} \ln \frac{[PbCl_3^-]}{[Pb(Hg)][Cl^-]^3}$	$\gamma_{Cl^-} = 6.91 \times 10^{-1}$ $C_{b_{Cl^-}} = 5.51 \times 10^{-1}$ moles
6.	$Pb(SO_4)^o$	$E^o + \frac{RT}{nF} \ln \frac{[Pb(SO_4)^o]}{[Pb(Hg)][SO_4^{=}]}$	$\gamma_{SO_4^{=}} = 2.81 \times 10^{-2}$ $C_{b_{SO_4^{=}}} = 1.25 \times 10^{-1}$ moles
7.	$Pb(SO_4)_2^{=}$	$E^o + \frac{RT}{nF} \ln \frac{[Pb(SO_4)_2^{=}]}{[Pb(Hg)][SO_4^{=}]^2}$	$\gamma_{SO_4^{=}} = 2.81 \times 10^{-2}$ $C_{b_{SO_4^{=}}} = 1.25 \times 10^{-1}$ moles
8.	$PbCO_3^o$	$E^o + \frac{RT}{nF} \ln \frac{[PbCO_3^o]}{[Pb(Hg)][CO_3^{=}]}$	$\gamma_{CO_3^{=}} = 1.15 \times 10^{-1}$ $C_{b_{CO_3^{=}}} = 3.0 \times 10^{-4}$ moles

TABLE 6-1A (Continued)

	Chemical Form	Potential Expression	Activities, Activity Coefficients, Concentrations
9.	$Pb(OH)^+$	$E^o + \frac{RT}{nF} \ln \frac{[Pb(OH)^+]}{[Pb(Hg)][OH^-]}$	pH = 7.5 $a_{OH^-} = 1 \times 10^{-6.5}$
10.	$Pb(OH)_2^o$	$E^o + \frac{RT}{nF} \ln \frac{[Pb(OH)_2^o]}{[Pb(Hg)][OH^-]^2}$	pH = 7.5 $a_{OH^-} = 1 \times 10^{-6.5}$
11.	$Pb(OH)_3^-$	$E^o + \frac{RT}{nF} \ln \frac{[Pb(OH)_3^-]}{[Pb(Hg)][OH^-]^3}$	pH = 7.5 $a_{OH^-} = 1 \times 10^{-6.5}$
12.	$Pb(OH)_4^=$	$E^o + \frac{RT}{nF} \ln \frac{[Pb(OH)_4^=]}{[Pb(Hg)][OH^-]^4}$	pH = 7.5 $a_{OH^-} = 1 \times 10^{-6.5}$

TABLE 6-1B

$E_{\frac{1}{2}cell}$ FOR CHEMICAL FORMS OF LEAD

	Chemical Form	Equation (volts)	$E_{\frac{1}{2}cell}$ (volts)
1.	Pb^{++}	$E_{\frac{1}{2}cell} = 0.126 + \frac{RT}{2F} \ln \frac{[Pb^{++}]}{[Pb(Hg)]}$ $= 0.126 + 0.296 \log \frac{[(7.5 \times 10^{-2})(1.9 \times 10^{-7})]}{[1]}$	-0.388
2.	$PbCl_2^o$	$E_{\frac{1}{2}cell} = 0.126 + \frac{RT}{2F} \ln \frac{[PbCl_2^o]}{[Pb(Hg)][Cl^-]^2}$ $= 0.126 + 0.0296 \log \frac{[PbCl_2^o]}{[1][(6.91 \times 10^{-1})(5.51 \times 10^{-1})]}$	0.151 + 0.0296 log $[PbCl_2^o]$
3.	$PbCl^+$	$E_{\frac{1}{2}cell} = 0.126 + \frac{RT}{2F} \ln \frac{[PbCl^+]}{[Pb(Hg)][Cl^-]}$ $= 0.126 + 0.0296 \log \frac{[PbCl^+]}{[1][(6.91 \times 10^{-1})(5.51 \times 10^{-1})]}$	0.138 + 0.0296 log $[PbCl^+]$
4.	$PbCl_3^-$	$E_{\frac{1}{2}cell} = 0.126 + \frac{RT}{2F} \ln \frac{[PbCl_3^-]}{[Pb(Hg)][Cl^-]^3}$ $= 0.126 \times 0.0296 \log \frac{[PbCl_3^-]}{[1][(6.91 \times 10^{-1})(5.51 \times 10^{-1})]^3}$	0.163 + 0.0296 log $[PbCl_3^-]$

TABLE 6-1B (Continued)

	Chemical Form	Equation (volts)	$E_{\frac{1}{2}cell}$ (volts)
5.	$PbCl_4^{=}$	$E_{\frac{1}{2}cell} = 0.126 + \frac{RT}{2F} \ln \frac{[PbCl_4^{=}]}{[Pb(Hg)][Cl^-]^4}$ $= 0.126 + 0.0296 \log \frac{[PbCl_4^{=}]}{[1][(6.91 \times 10^{-1})(5.51 \times 10^{-1})]^4}$	0.176 + 0.0296 log $[PbCl_4^{=}]$
6.	$Pb(SO_4)^o$	$E_{\frac{1}{2}cell} = 0.126 + \frac{RT}{2F} \ln \frac{[Pb(S)_4)^o]}{[Pb(Hg)][(SO_4)^{=}]}$ $= 0.126 + 0.0296 \log \frac{[Pb(SO_4)^o]}{[1][(2.81 \times 10^{-2})(1.25 \times 10^{-1})]}$	0.198 + 0.0296 log $[Pb(SO_4)^o]$
7.	$Pb(SO_4)_2^{=}$	$E_{\frac{1}{2}cell} = 0.126 + \frac{RT}{2F} \ln \frac{[Pb(SO_4)_2^{=}]}{[Pb(Hg)][(SO_4)^{=}]^2}$ $= 0.126 + 0.0296 \log \frac{[Pb(SO_4)_2^{=}]}{[1][(2.81 \times 10^{-2})(1.25 \times 10^{-1})]^2}$	-0.271 + 0.0296 log $[Pb(SO_4)_2^{=}]$

TABLE 6-1B (Continued)

	Chemical Form	Equation (volts)	$E_{\frac{1}{2}cell}$ (volts)
8.	$PbCO^{o}_{3}$	$E_{\frac{1}{2}cell} = 0.126 + \frac{RT}{2F} \ln \frac{[PbCO^{o}_{3}]}{[Pb(Hg)][CO^{=}_{3}]}$ $= 0.126 + 0.0296 \log \frac{[PbCO^{o}_{3}]}{[1][(1.5 \times 10^{-1})(3.0 \times 10^{-4})]}$	$-0.258 +$ $0.0296 \log [PbCO^{o}_{3}]$
9.	$Pb(OH)^{+}$	$E_{\frac{1}{2}cell} = 0.126 + \frac{RT}{2F} \ln \frac{[Pb(OH)^{+}]}{[Pb(Hg)][OH^{-}]}$ $= 0.126 + 0.0296 \log \frac{[Pb(OH)^{+}]}{[1][1 \times 10^{-6.5}]}$	$-0.318 +$ $0.0296 \log [Pb(OH)^{+}]$
10.	$Pb(OH)^{o}_{2}$	$E_{\frac{1}{2}cell} = 0.126 + \frac{RT}{2F} \ln \frac{[Pb(OH)^{o}_{2}]}{[Pb(Hg)][OH^{-}]^{2}}$ $= 0.126 + 0.0296 \log \frac{[Pb(OH)^{o}_{2}]}{[1][1 \times 10^{-6.5}]^{2}}$	$-0.518 +$ $0.0296 \log [Pb(OH)^{o}_{2}]$

TABLE 6-1B (Continued)

	Chemical Form	Equation (volts)	$E_{\frac{1}{2}cell}$ (volts)
11.	$Pb(OH)_3^-$	$E_{\frac{1}{2}cell} = 0.126 + \frac{RT}{2F} \ln \frac{[Pb(OH)_3^-]}{[Pb(Hg)][OH^-]^3}$ $= 0.126 + 0.0296 \log \frac{[Pb(OH)_3^-]}{[1][1 \times 10^{-6.5}]^3}$	$-0.703 +$ $0.0296 \log [Pb(OH)_3^-]$
12.	$Pb(OH)_4^=$	$E_{\frac{1}{2}cell} = 0.126 + \frac{RT}{2F} \ln \frac{[Pb(OH)_4^=]}{(Pb(Hg)][OH^-]^4}$ $= 0.126 + 0.0296 \log \frac{[Pb(OH)_4^=]}{[1][1 \times 10^{-6.5}]^4}$	$-0.896 +$ $0.0296 \log [Pb(OH)_4^=]$

For $PbCl_2^o$, though, the activity coefficient for the complex is unknown:

$$(6\text{-}9) \quad - \left(0.126 - \frac{RT}{2F} \ln [1][(6.91 \times 10^{-1})(5.5 \times 10^{-1})]^2\right) + \frac{RT}{2F} \ln [PbCl_2^o]$$

$$= -0.151 \text{ volts} + 0.0296 \log [PbCl_2^o]$$

with: $\gamma_{Cl^-} = 6.91 \times 10^{-1}$

$C_{b_{Cl^-}} = 5.51 \times 10^{-1}$ moles (Whitfield, 1975, p.1549 and p.1552)

2) The purpose of the model is to arrive at concentrations and complex types, but in order to arrive at one it is necessary to know the other. Therefore, concentration values from the Whitfield model (1975, p.1549) are inserted in the ½ cell formula to indicate the complex type.

3) Also for each complex type 100% of the lead is complexed with the particular anion of that complex.

Tables 6-1A and 61-B show the ½ cell potentials for the lead species, and Table 6-2 lists these potentials and the total potentials in order of increasing magnitude.

The total potentials in Table 6-2 are in this form:

$$(6\text{-}10) \quad E_{total} = E_{\frac{1}{2}cell\ PbL(i)_n} + E_k =$$

$$(E^o + E_k + 0.0296 \log [Pb(Hg)]^{-1}[L(i)\ ]^{-1} +$$

$$0.0296 \log [PbL(i)_n] \pm 5\%\ E_{meas}.$$

TABLE 6-2

E_{total} WITHOUT ACTIVITIES FOR COMPLEXES

	Chemical Form	$E_{\frac{1}{2}}$ cell (volts)	$E_{\frac{1}{2}}$ cell + E_k = E_{total} (volts)
1.	$PbCl^+$	$-0.138 + 0.0296 \log [PbCl^+]$	$-0.432 + 0.0296 \log [PbCl^+] \pm 5\% E_{misc.}$
2.	$PbCl_2^o$	$-0.151 + 0.0296 \log [PbCl_2^o]$	$-0.445 + 0.0296 \log [PbCl_2^o] \pm 5\% E_{misc.}$
3.	$PbCl_3^-$	$-0.163 + 0.0296 \log [PbCl_3^-]$	$-0.457 + 0.0296 \log [PbCl_3^-] \pm 5\% E_{misc.}$
4.	$PbCl_4^=$	$-0.176 + 0.0296 \log [PbCl_4^=]$	$-0.470 + 0.0296 \log [PbCl_4^=] \pm 5\% E_{misc.}$
5.	$PbSO_4^o$	$-0.198 + 0.0296 \log [PbSO_4^o]$	$-0.492 + 0.0296 \log [PbSO_4^o] \pm 5\% E_{misc.}$
6.	$PbCO_3^o$	$-0.258 + 0.0296 \log [PbCO_3^o]$	$-0.552 + 0.0296 \log [PbCO_3^o] \pm 5\% E_{misc.}$
7.	$Pb(SO_4)_2^=$	$-0.271 + 0.0296 \log [Pb(SO_4)_2^=]$	$-0.565 + 0.0296 \log [Pb(SO_4)_2^=] \pm 5\% E_{misc.}$
8.	$PbOH^+$	$-0.318 + 0.0296 \log [PbOH^+]$	$-0.612 + 0.0296 \log [PbOH^+] \pm 5\% E_{misc.}$
9.	Pb^{++}	-0.388	$-0.682 \pm 5\% E_{misc.}$

TABLE 6-2 (Continued)

	Chemical Form	$E_{\frac{1}{2}}$ cell (volts)	$E_{\frac{1}{2}}$ cell + E_k = E_{total} (volts)
10.	$Pb(OH)_2^o$	$-0.518 + 0.0296 \log [Pb(OH)_2^o]$	$-0.812 + 0.0296 \log [Pb(OH)_2^o] \pm 5\% E_{misc.}$
11.	$Pb(OH)_3^-$	$-0.703 + 0.0296 \log [Pb(OH)_3^-]$	$-0.997 + 0.0296 \log [Pb(OH)_3^-] \pm 5\% E_{misc.}$
12.	$Pb(OH)_4^=$	$-0.896 + 0.0296 \log [Pb(OH)_4^=]$	$-1.190 + 0.0296 \log [Pb(OH)_4^=] \pm 5\% E_{misc.}$

Goldberg (1965, p.165) uses these activity values for the ionic forms in his dominant species model: (a) monovalent ions, $a_i = 0.7$; (b) divalent ions, $a_i = 0.1$; and (c) uncharged species, $a_i = 1.0$. These values are inserted into the 0.0296 log $[PbL(i)_n]$ term in the (6-10) expression. The purpose of this is to have a basis to compare the total potential of the complex forms, where the activities are unknown, with the total potential of Pb^{++}, where the activity is known. Table 6-3 shows the results. The maximum concentration of the complex is equal to the total lead concentration, and even if this is inaccurate by an order of magnitude the difference will only be 0.0296 volts, which is not important in the relative scale.

Chemical Model of Laboratory Samples

1) KCl with Purge

Chapter IV describes the analysis of a KCl electrolyte. During this analysis increments of lead are added for the calibration curve. Figure 6-1 shows the stripping potential at which the current peaks appear plotted as a function of lead concentration. The potential appears relatively stable between -0.64 to -0.76 volts through the error bars as a constant linear function at -0.680 volts.

One sees by examining Table 6-3 that this is well within the ± 5% range of -0.682 volt potential for Pb^{++}. In the KCl electrolyte inorganic labile lead is present then as 100% Pb^{++}. Figure 6-2 shows the current repression from non-labile lead. At a lead concentration of 1.2×10^{-3} g/l there is a 12% current repression from the linear function and at a concentration of 1.8×10^{-3} g/l there is a 48% current

TABLE 6-3

E_{total} WITH ACTIVITIES FOR COMPLEXES

	γ of Pb $L(i)_n$	Revised Term	ΔE (volts)	$E_{\frac{1}{2}}$ cell (volts)	E_{total} (volts)
1.	$PbCl^+$ (0.7)	$0.0296 \log [0.7 \times 1.9 \times 10^{-8}]$	+0.182	+0.044	$-0.250 \pm 5\%\ E_{misc.}$
2.	$PbCl_3^-$ (0.7)	$0.0296 \log [0.7 \times 1.9 \times 10^{-8}]$	+0.182	+0.019	$-0.275 \pm 5\%\ E_{misc.}$
3.	$PbCl_2^o$ (1)	$0.0296 \log [1 \times 1.9 \times 10^{-8}]$	+0.149	+0.002	$-0.292 \pm 5\%\ E_{misc.}$
4.	$PbCl_4^=$ (0.1)	$0.0296 \log [0.1 \times 1.9 \times 10^{-8}]$	+0.171	-0.005	$-0.299 \pm 5\%\ E_{misc.}$
5.	$PbSO_4^o$ (1)	$0.0296 \log [1 \times 1.9 \times 10^{-8}]$	+0.149	-0.049	$-0.343 \pm 5\%\ E_{misc.}$
6.	$Pb(SO_4)_2^=$ (0.1)	$0.0296 \log [0.1 \times 1.9 \times 10^{-8}]$	+0.171	-0.100	$-0.394 \pm 5\%\ E_{misc.}$
7.	$PbCO_3^o$ (1)	$0.0296 \log [1 \times 1.9 \times 10^{-8}]$	+0.149	-0.109	$-0.403 \pm 5\%\ E_{misc.}$
8.	$Pb(OH)^+$ (0.7)	$0.0296 \log [0.7 \times 1.9 \times 10^{-8}]$	+0.182	-0.136	$-0.430 \pm 5\%\ E_{misc.}$
9.	$Pb(OH)_2^o$ (1)	$0.0296 \log [1 \times 1.9 \times 10^{-8}]$	+0.147	-0.371	$-0.665 \pm 5\%\ E_{misc.}$

TABLE 6-3 (Continued)

	γ of Pb $L(i)_n$	Revised Term	ΔE (volts)	$E_{\frac{1}{2}}$ cell (volts)	E_{total} (volts)
10.	Pb^{++}			-0.388	-0.682 ± 5% $E_{misc.}$
11.	$Pb(OH)_3^-$ (0.7)	0.0296 log [0.7 x 1.9 x 10^{-8}]	+0.182	-0.521	-0.815 ± 5% $E_{misc.}$
12.	$Pb(OH)_4^=$ (0.1)	0.0296 log [0.1 x 1.9 x 10^{-8}]	+0.171	-0.725	-1.019 ± 5% $E_{misc.}$

(For the calculations, the concentrations are changed from moles to g/l)

FIGURE 6-1

MEASURED POTENTIAL DURING STRIPPING OF LEAD IN KCl (WITH PURGE)

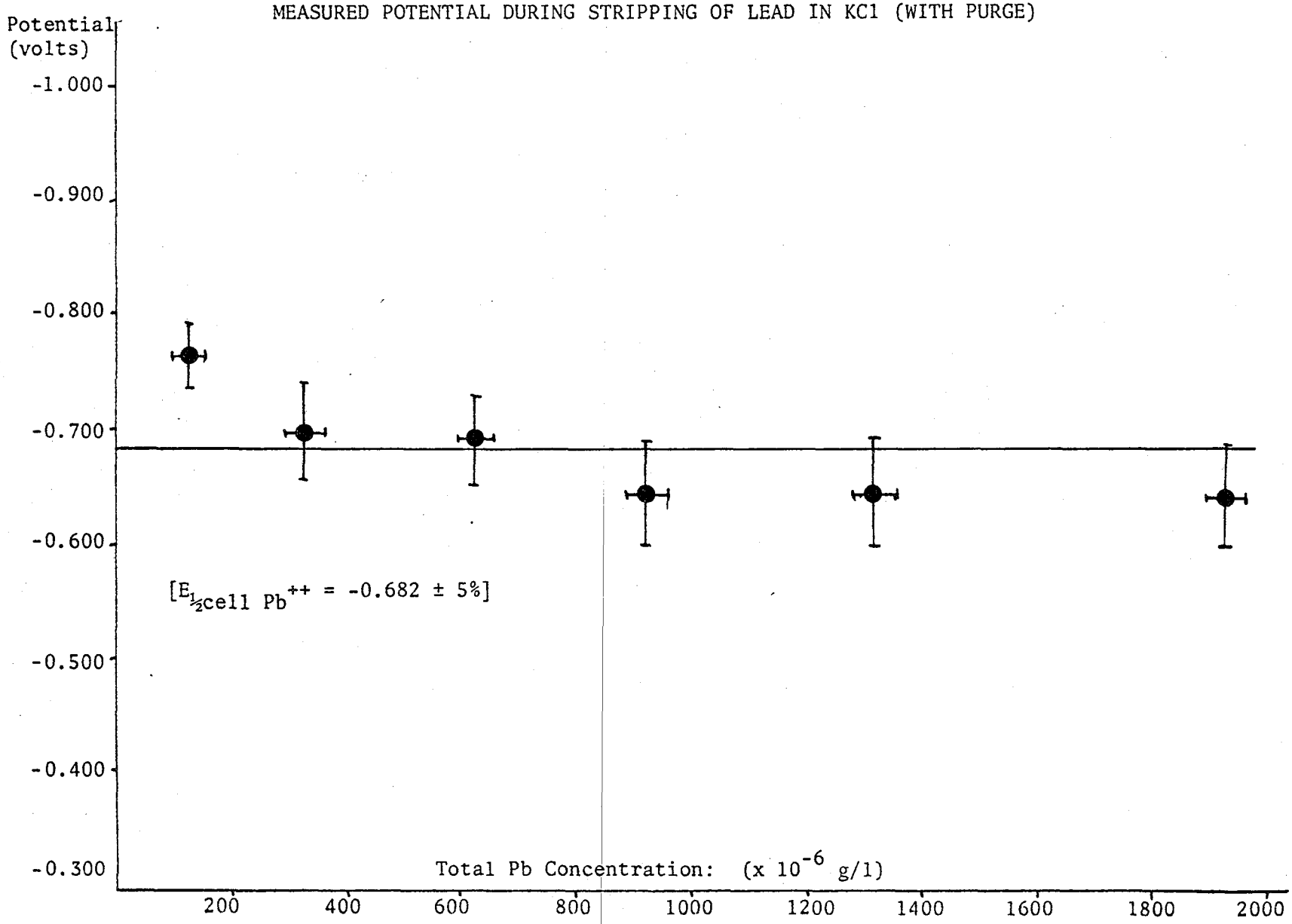

FIGURE 6-2

CURRENT REPRESSION OF NON-LABILE LEAD -KCl ELECTROLYTE (PURGE)

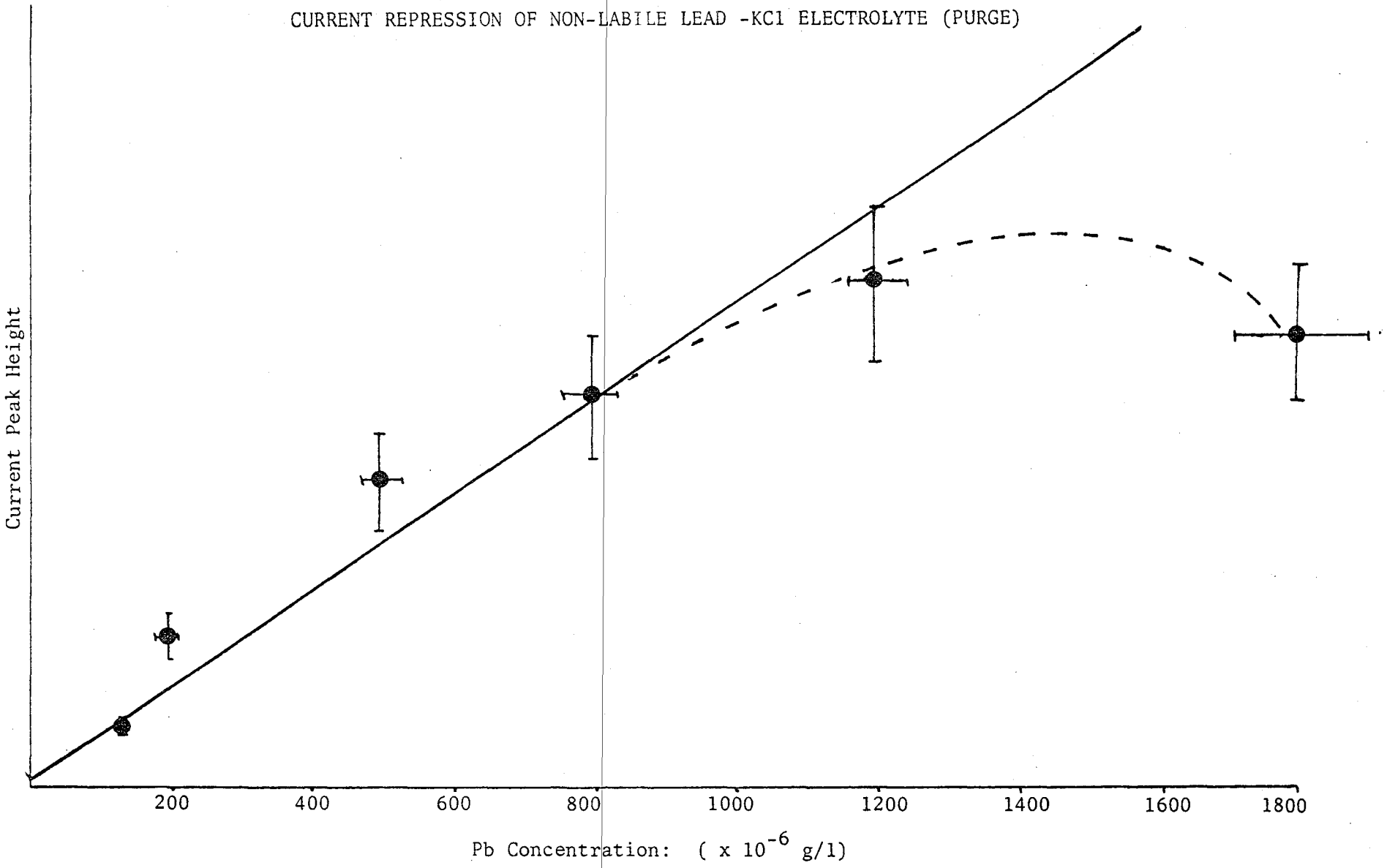

reduction. At the original electrolyte concentration of lead the curve is linear, and so it seems at this level lead is in the non-labile form. With the lead additions, lead becomes present increasingly in the non-labile form. This non-labile complex is almost certainly $Pb(NO_3)_2$, the chemical form of lead in the additions solution. Another possibility is that the additional lead complexes with CO_3^- as a stable colloid. A stable colloid such as this also represses the current. At higher concentrations and at higher pH one expects to see the carbonate species, but in the relatively labile form, not as a colloid (Zirino and Yamamoto, 1972, p.668; Ernst and others, 1975, p.973; and Long and Angino, 1977, p.1188). $PbCO_3^o$ is the dominant form of lead in expression (5-15), but the solution is purged of CO_2, and there should be a low concentration of carbonate ions to complex with lead.

Table 6-4 summarizes the forms of lead in the KCl electrolyte. The mass balance equations for lead are:

(6-11) (Ambient concentration of 1.0 - 1.6 x 10^{-4} g/l)

$$[Pb]_{total} \cong 100\% \ [Pb^{++}]$$

(6-12) (Additions concentration of 1.2 x 10^{-3} g/l)

$$[Pb]_{total} \cong 90\% \ [Pb^{++}] + 10\% \ [Pb(NO_3)_2] + [PbCO_3^o]$$

(6-13) (Additions concentration of 1.8 x 10^{-3} g/l)

$$[Pb]_{total} \cong 50\% \ [Pb^{++}] + 50\% \ [Pb(NO_3)_2] + [PbCO_3^o]$$

TABLE 6-4 - CHEMICAL FORMS OF LEAD IN KCl ELECTROLYTE (PURGE)

Soluble Lead					Particulate Lead
Labile Lead			Non-Labile Lead		
Lead: Free Ions - Pb^{++}	Lead: Adsorbed On:	Lead: Complexed With:	Lead: Adsorbed On:	Lead: Complexed With:	
Species of lead at ambient concentration of 1.0_4- 1.6 x 10^{-4} g/l ≅ 100% Pb^{++} (stripping potential is -0.680v, within ± 5% of -0.682v for Pb^{++})	Non-stable, uncharged organic colloids cannot be distinguished with this method. Inorganic colloids repress the current peak, but as there is no peak repression at the ambient concentration, no lead is present in the inorganic colloid form. Some $PbCO_3°$ may be present as a colloid at higher Pb concentrations.	The stripping peak is sharp and well distinguished at -0.680v, and there are no peak broadenings or multiple peaks from labile complex forms. This situation is the same for additional concentrations of lead up to 1.8 x 10^{-3} g/l. Lead does not appear as labile complex forms in this solution.	(Same as labile lead: Adsorbed On: section.)	The correct repression curve shows that there are no non-labile complexes at ambient concentration. At a concentration of 1.2 x 10^{-3} g/l 12% of the lead is complexed as $Pb(NO_3)_2$ and at 1.8 x 10^{-3} g/l 48% of the lead is present as $Pb(NO_3)_2$.	There is no measurable particulate matter in this solution.

2) KCl Without Purge

Figure 6-3 shows the stripping potential at which the current peaks appear for the KCl analysis without a purge. These peaks are plotted as a function of lead concentration. Chapter V describes this analysis. There is a linear trend for a decreasing stripping potential as the lead concentration increases. At the ambient concentration of 6.0 - 8.0 x 10^{-5} g/l the stripping potential is -0.78 volts and at 2.95 x 10^{-3} g/l the potential is -0.64 volts. This seems to indicate that at low concentrations a slight shift of the peak is caused by the presence of lead complexed with hydroxyl ions. $Pb(OH_3)^-$ has a stripping potential of -0.815 ± 5%. Bradford (1973) and Long and Angino (1977, p.1188) point out that this particular hydroxyl complex is expected in solutions only with high pH (> 10), and it does not seem reasonable to expect such a complex in this situation. By attributing the first few potential shifts to experimental error, a constant line can be drawn at -0.70 volts. This value is within 5% of the 0.682 volts for Pb^{++}. The downward potential trend could also be caused by lead complexed with the dominant labile carbonate anion. Bradford (1973) found that in the case of zinc the carbonate complex occurs in a relatively unstable form and causes the potential to shift. This same behavior should occur for lead, particularly in the case of a solution not purged of CO_2.

Figure 6-4 shows the current repression from non-labile lead. Only the first two data points deviate from the linear function. It is difficult to say whether this deviation is from experimental error, or, if with increasing lead additions, a small percentage, perhaps

FIGURE 6-3

MEASURED POTENTIAL DURING STRIPPING OF LEAD IN KCl (WITHOUT PURGE)

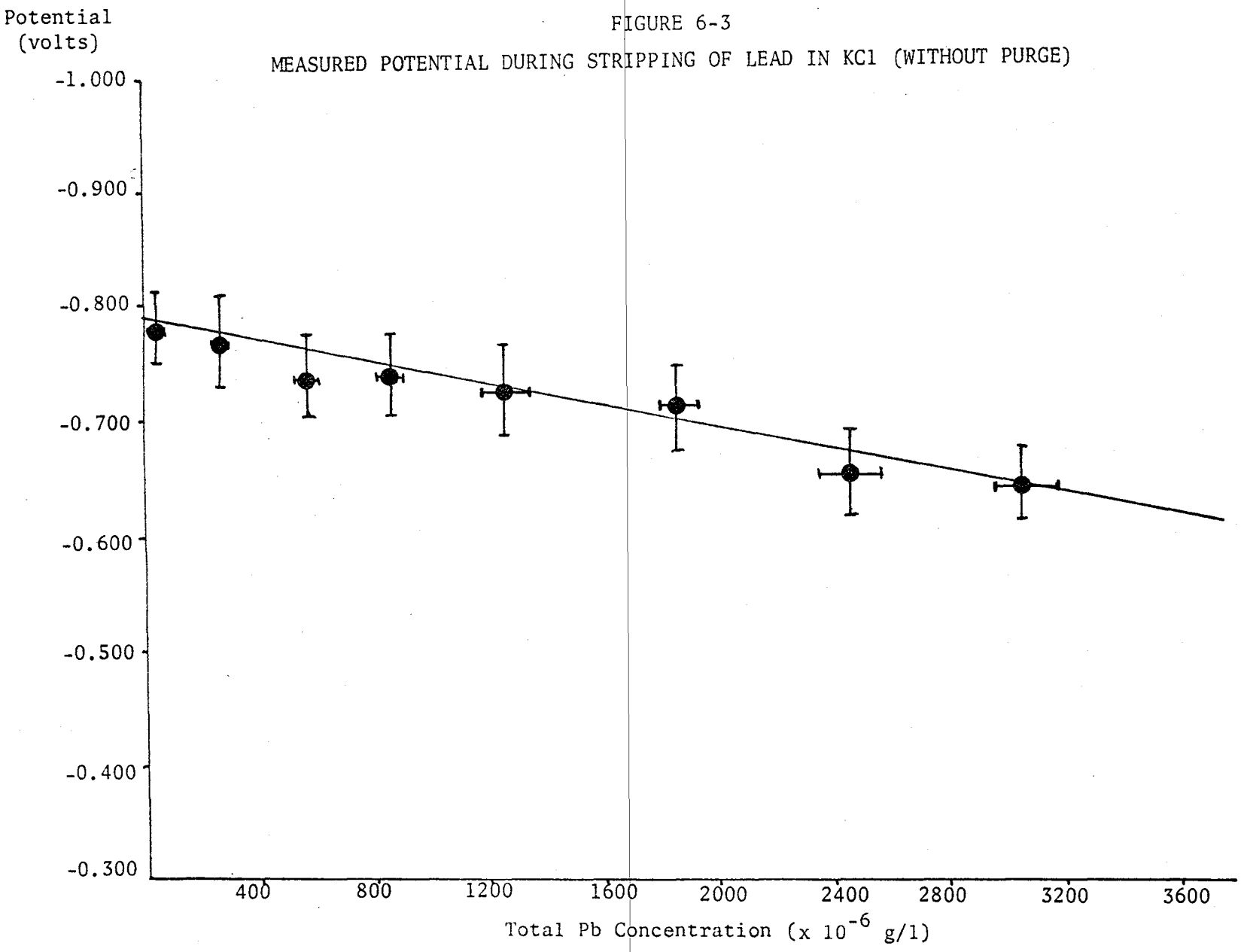

FIGURE 6-4

CURRENT REPRESSION OF NON-LABILE LEAD -KCl ELECTROLYTE (NO PURGE)

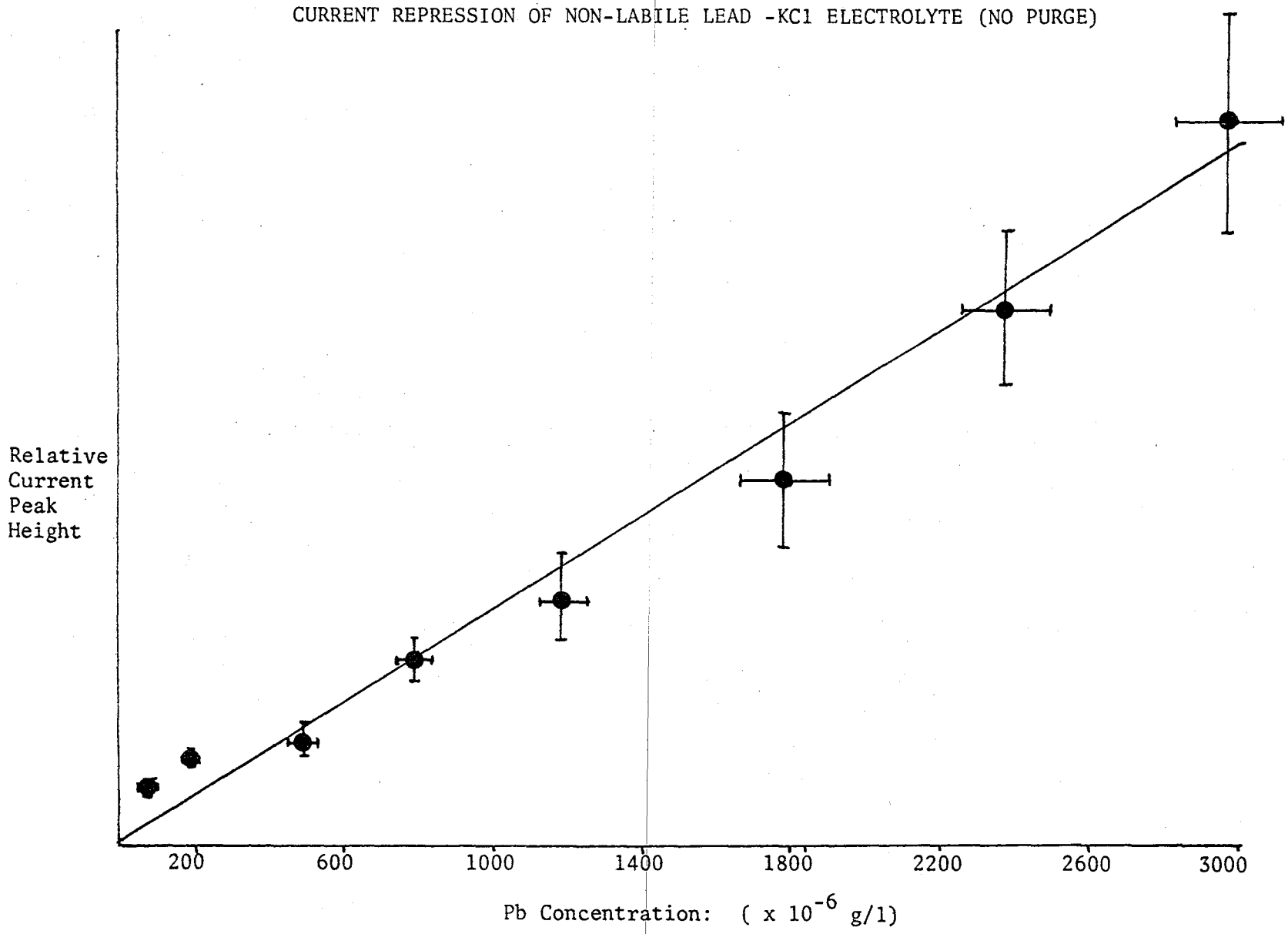

10-15%, of the lead occurs as $Pb(NO_3)_2$. The deviation occurs at approximately 5.0×10^{-4} g/l, the same concentration magnitude where the deviation occurs in the previous experiment.

Table 6-5 summarizes the chemical forms of lead in a KCl electrolyte without a purge. The mass balance equations for lead are:

(6-13) (Ambient concentration of $6.0 - 8.0 \times 10^{-5}$ g/l)

$$[Pb]_{total} \cong 100\% \ [Pb^{++}]$$

(6-14) (With successive lead additions)

$$[Pb]_{total} \cong [Pb^{++}] + [PbCO_3^o] + [PbOH^+] + [Pb(NO_3)_2]$$

3) Sea Water With Purge

Figure 6-5 shows the stripping potentials for the current peaks for a lead analysis in sea water with a purge. Chapter V describes this analysis. There is a definite constant linear relationship between the stripping potential and the increasing lead concentrations. The stripping potential remains constant at -0.445 volts as the lead concentration increases from 5.0×10^{-5} g/l to 1.75×10^{-3} g/l. This potential is well below the $-0.682 \pm 5\%$ $E_{meas.}$ volts range for Pb^{++}. These potential shift values are relative, not absolute, because in certain cases the concentration of a complex or ligand may affect the potential value, and in this case there is a significant relative shift from the stripping potentials in the KCl electrolyte. The ambient total lead concentration of 5.0×10^{-5} g/l does not differ significantly from the 1.0×10^{-4} g/l in the KCl analysis under similar conditions.

TABLE 6-5 - CHEMICAL FORMS OF LEAD IN KCl ELECTROLYTE (NO PURGE)

Soluble Lead					Particulate Lead
Labile Lead			Non-Labile Lead		
Lead: Free Ions - Pb^{++}	Lead: Adsorbed On:	Lead: Complexed With:	Lead: Adsorbed On:	Lead: Complexed With:	
Species of lead at ambient concentration of 8.0×10^{-5} g/l is mostly as Pb^{++} but there is an increasing trend towards $PbCO_3°$	Non-stable uncharged organic colloids cannot be distinguished with this method. Inorganic colloids repress the current peak, but as there is no peak repression at the ambient concentration, no lead is present in the inorganic colloid form.	There is a decreasing trend for the stripping potential which suggests that at the high potential (-0.78v) and low concentration there may be some complexing with OH^-, perhaps as $Pb(OH)^-_3$. The solution pH does not support this contention. At higher concentrations there is a shift towards the $PbCO_3°$ complex, with perhaps some complexing as $PbOH^+$.	(Same as Labile Lead: Adsorbed On: section)	At non-ambient concentrations there may be current repression although this may be due to experimental error. A small percentage, 10-15%, of the lead may be present as $Pb(NO_3)_2$.	There is no measurable particulate matter in this solution.

FIGURE 6-5

MEASURED POTENTIAL OF LEAD DURING STRIPPING IN SEA WATER (WITH PURGE)

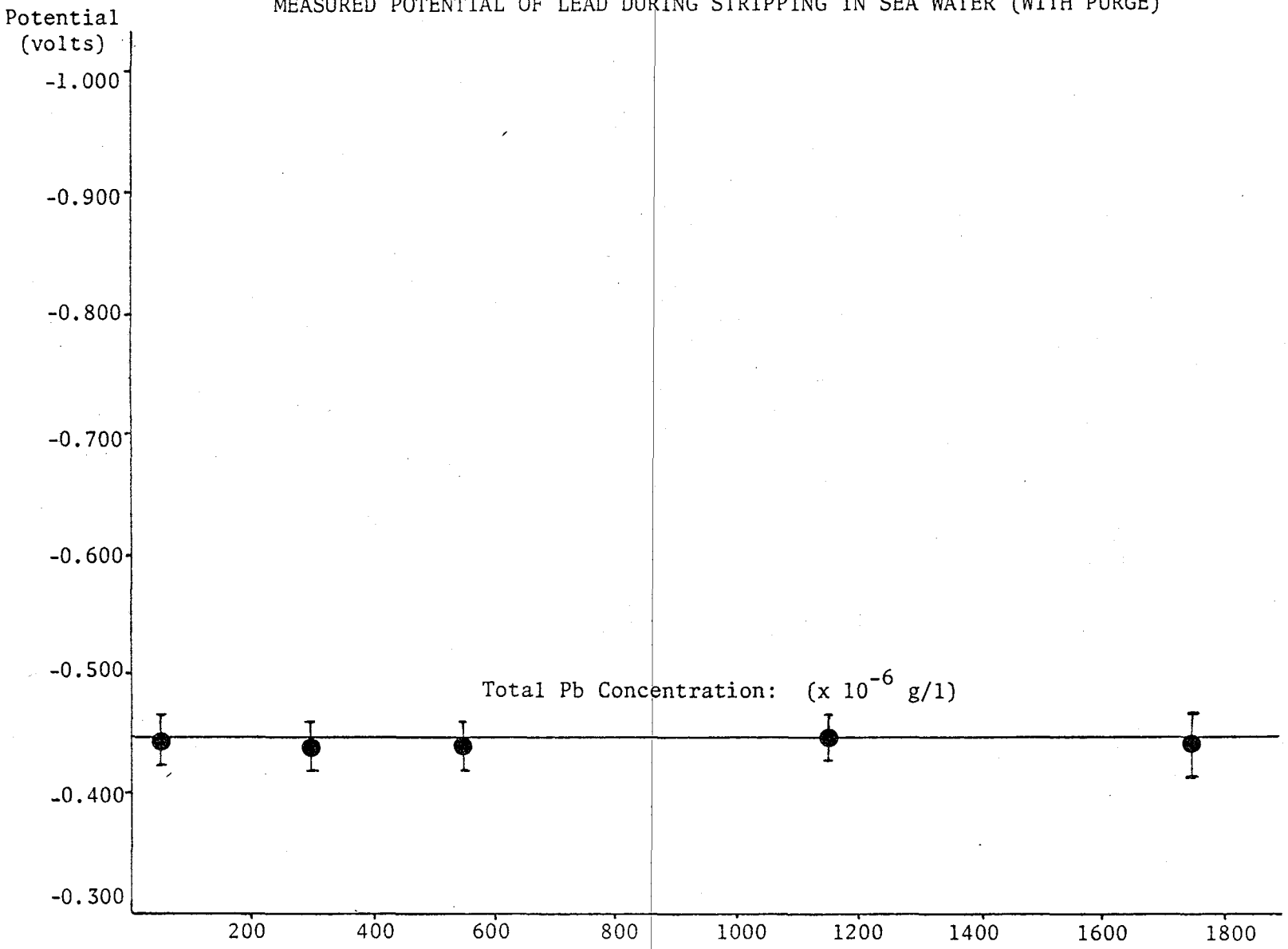

The stripping peaks are distinct, and therefore it seems reasonable to attribute this change in potential from the previous experiments to a labile complex of lead. The constant potential of -0.445 volts is considerably below the value for Pb^{++} and is closest to -0.403 volts ± 5% $E_{measured}$ for $PbCO_3^o$. The dominant form of lead at a pH of 8.1 appears to be $PbCO_3^o$. This conclusion is in agreement with the models of Zirino and Yamamoto (1972, p.669), Ernst and others (1975, p.973), and Long and Angino (1977, p.1188).

Figure 6-6 shows the repression of the current peaks caused by non-labile complexing from increasing lead concentrations. There is an abrupt change of slope at 2.0×10^{-4} g/l, almost certainly caused by the stable $Pb(NO_3)_2$ complex in the additions solution.

Table 6-6 lists the chemical forms of lead in this sea water sample with purge. The mass balance equations are:

(6-15) (Ambient concentration of 5.0×10^{-5} g/l)

$$[Pb]_{total} \cong 100\% \ [PbCO_3]$$

(Undoubtedly other forms are present but these are masked by the strong dominance of $PbCO_3^o$.)

(6-16) (With successive lead additions)

$$[Pb]_{total} \cong 50\% \ [PbCO_3^o] + 50\% \ [Pb(NO_3)_2]$$

(This patitioning is a bit arbitrary but seems reasonable from the significant change in slope of the non-labile relationship.)

FIGURE 6-6

CURRENT REPRESSION OF NON-LABILE LEAD - SEA WATER (PURGE)

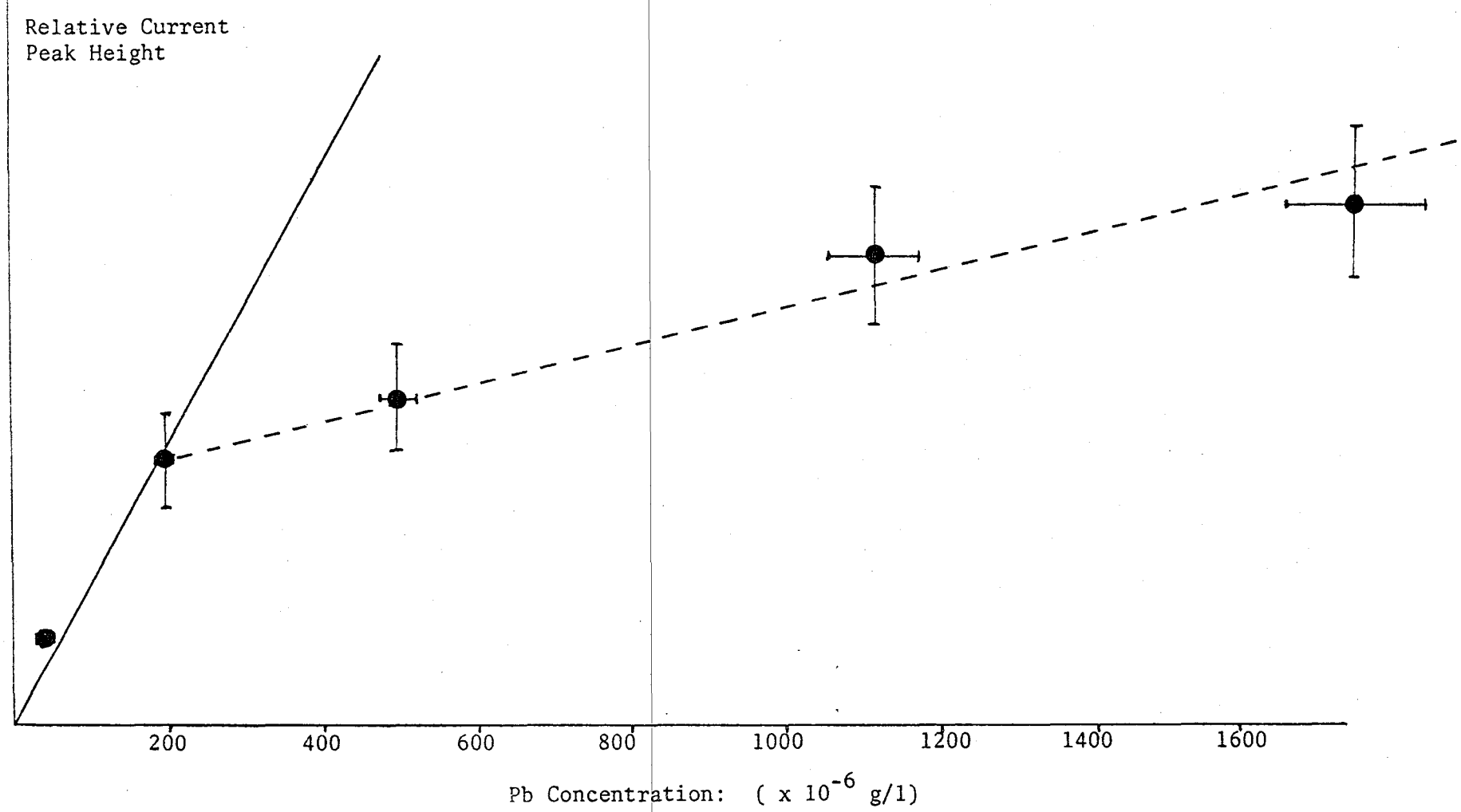

TABLE 6-6 - CHEMICAL FORMS OF LEAD IN SEA WATER (PURGE)

Soluble Lead					Particulate Lead
Labile Lead			Non-Labile Lead		
Lead: Free Ions - Pb^{++}	Lead: Adsorbed On:	Lead: Complexed With:	Lead: Adsorbed On:	Lead: Complexed With:	
Species of lead at ambient concentration of 5.0×10^{-5} g/l $\cong PbCO_3°$. (Stripping potential is -0.445, within the $PbCO_3°$ stripping potential range.)	Non-stable, uncharged organic colloids cannot be distinguished with this method. Inorganic colloids repress the current peak, but as there is no peak repression at the ambient concentration, no lead is present in the inorganic colloid form.	The stripping peak is sharp and well distinguished and constant at -0.445v, and there are no peak broadenings or multiple peaks. This is the same for all lead additions. The predominant form of lead, to the exclusion of all other labile forms, appears to be $PbCO_3°$. This may be in part caused by the purge and change in pH.	(Same as Labile Lead: Adsorbed On: section.)	There is a considerable change in slope of the current repression line at non-ambient concentrations. About 50% of the soluble lead seems to be in the form $Pb(NO_3)_2$ and the other 50% as $PbCO_3°$.	There is no measurable particulate matter in this solution.

One conclusion from (6-15) is that the change in pH from the purge causes the predominance of $PbCO_3^o$. Conclusions from calculated models, including those of Zirino and Yamamoto (1972, p.668) and Garrels and Christ (1965, p.233) support this idea: The complexing of lead with $PbCO_3^o$ increases with increasing pH.

4) Sea Water Without Purge

Figure 6-7 shows the stripping potentials for lead in sea water with no purge. Chapter V describes this analysis. Figure 5-6 shows the multiple peaks which occur during the lead additions. At the ambient concentration of 2.5×10^{-5} g/l only one peak occurs at -0.640 volts. This value corresponds to the relative stripping potential for Pb^{++}, -0.682 volts ± 5% $E_{meas.}$. Therefore, the ambient species of lead is Pb^{++}. Two stripping peaks appear at the additions concentration of 2.25×10^{-4} g/l. One peak is at the same value as the one for ambient conditions, -0.640 volts. (Peaks at this value appear at all additions levels.) A second peak appears at -0.445 volts, the $PbCO_3^o$ value. By comparing the relative height of the current peaks it seems that the labile species is split about evenly between Pb^{++} and $PbCO_3^o$.

Three peaks occur at a concentration of 5.25×10^{-4} g/l. One peak occurs at -0.625, another at -0.445, and a third at -0.320 volts. The first two peaks represent Pb^{++} and $PbCO_3^o$, and the third is most likely from either a species of Cl^- of $SO_4^=$. All four of the Cl^- species have stripping potentials between -0.250 volts and -0.299 volts ± 5% $E_{meas.}$, and the $PbSO_4^o$ potential is -0.343 volts. Most likely, all of these

FIGURE 6-7

MEASURED POTENTIAL DURING STRIPPING OF LEAD IN SEA WATER (WITHOUT PURGE)

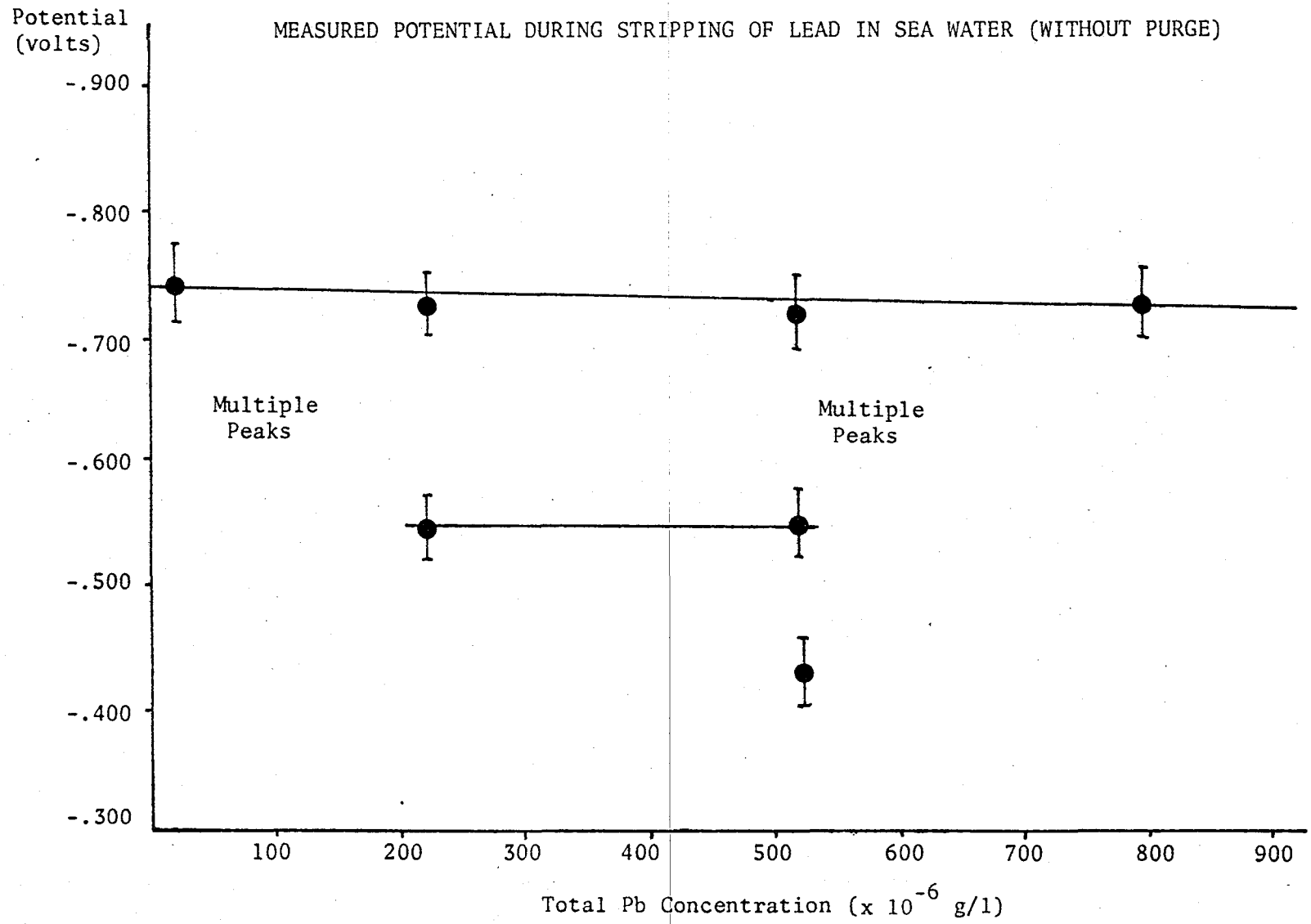

complexes are present to a certain extent, although the peak potential most nearly matches that of $PbSO_4^o$.

Only one peak occurs at a concentration of 8.0×10^{-4} g/l, and this peak is at the relatively constant potential of -0.625 volts. Other complexes are undoubtedly still present, but at this concentration the Pb^{++} peak is masking them. These multiple peaks from various species of a single element are an interesting experimental result, and the experimental conditions must be just right for them to occur. Usually a series of complexes with similar potentials manifest themselves by the broadening of a single peak. It is interesting to note that the multiple peaks occur only when the solution is not purged. Either the purge masks the multiple peaks or changes the species. The latter interpretation seems correct. The multiple peaks indicates species which are the logical ones for this solution, follow the dominant complex order (5-8), and are in agreement with other models (Zirino and Yamamoto, 1972; Ernst and others, 1975; Garrels and Christ, 1965).

The mapping of repressive current from multiple peaks is difficult, and a somewhat arbitrary approach is taken by plotting the height for Pb^{++}, as this is the only species present at all concentrations. Figure 6-8 shows this plot. This plot is almost identical to the linear current plot for KCl without the purge. There appears to be no current repression along the plot, except for a slight one at 5.0×10^{-4} g/l which almost falls within experimental error. Either the stable complex $Pb(NO_3)_2$ is not present, which seems unlikely, or the entire plot after the ambient determination is repressed, the amount of which is difficult to determine.

FIGURE 6-8

CURRENT REPRESSION FOR NON-LABILE LEAD - SEA WATER (NO PURGE)

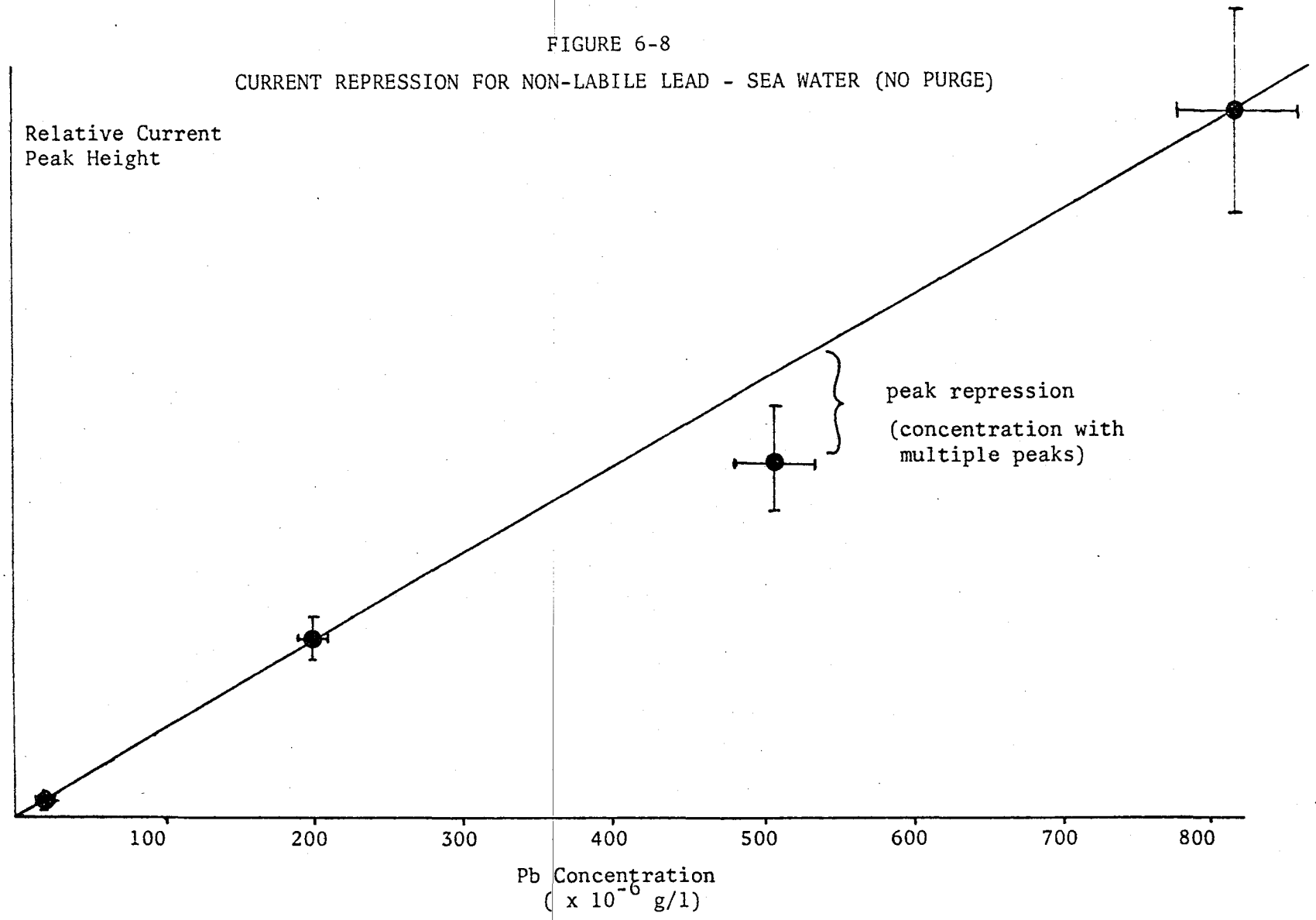

Table 6-7 summarizes the chemical forms of lead in sea water without a purge. The mass balance equations are:

(6-17) (Ambient concentration of 2.5×10^{-5} g/l)

$$[Pb]_{total} \cong 100\% \ [Pb^{++}]$$

(6-18) (Additions concentration of 2.25×10^{-4} g/l)

$$[Pb]_{total} \cong 50\% \ [Pb^{++}] + 50\% \ [PbCO_3^o] + [Pb(NO_3)_2]$$

(6-19) (Additions concentration of 5.25×10^{-4} g/l)

$$[Pb]_{total} \cong 30\% \ [Pb^{++}] + 30\% \ [PbCO_3^o] + 30\% \ [PbSO_4^o] + [PbCl^+] + [Pb(NO_3)_2]$$

Conclusions on Analysis of Laboratory Samples

The following are a few of the conclusions from this analyses work.

(a) The purpose of these laboratory experiments is to see if this ASV method and chemical model can be used to detect labile and non-labile inorganic lead complexes in saline solutions. With a few restrictions mentioned in these next paragraphs, this system does provide these data For certain dominant labile and non-labile complexes there are either measurable potential shifts or current repressions.

TABLE 6-7 - CHEMICAL FORMS OF LEAD IN SEA WATER (NO PURGE)

Soluble Lead					Particulate Lead
Labile Lead			Non-Labile Lead		
Lead: Free Ions - Pb^{++}	Lead: Adsorbed On:	Lead: Complexed With:	Lead: Adsorbed On:	Lead: Complexed With:	
At ambient concentration of 2.5×10^{-5} g/l $\cong$ 100% Pb^{++}. At higher concentrations from lead additions other labile complexes cause multiple peaks.	Non-stable, uncharged organic colloids cannot be distinguished with this method. Inorganic colloids repress the current peak, but as there is no peak repression at the ambient concentration, no lead is present in the inorganic colloid form.	At ambient concentrations there is no potential shift from -0.645v for Pb^{++}. At higher concentrations multiple peaks show the presence of $PbCO_3°$, $PbSO_4°$ and various complexes with Cl^-.	(Same as Labile Lead: Adsorbed On: section.)	The entire current plot, except the data point from the ambient concentration is repressed, probably from the stable $Pb(NO_3)_2$ complex. The percentage concentration is difficult to determine.	There is no measurable particulate matter in this solution.

(b) The potential shifts for the complexes correspond in most cases, within experimental error, to the values predicted by the relative potential stripping scale. Also, in most cases, the relative scale is absolute as the concentrations and activities do not vary significantly from the estimated values.

(c) The method does not use a purge, highly developed working electrodes, and other controls which are impractical during extended field use. A price is paid for this - at times the system exhibits erratic behavior caused by working electrode impurities, short electrode life, marred electrode surfaces, occasional inter-metallic oxides on the electrode surfaces, and spurious dissolved oxygen effects. Despite this occasional noise, all the laboratory results are reproducible, but the erratic behavior does seem to raise the lower threshold of detection from parts per trillion to parts per billion. The section on field samples from the Gulf of Mexico discusses this threshold problem.

(d) The measured stripping potentials indicate the complexes but should not be used to develop activity coefficient data. A discrepancy of -0.0296 volts means an order of magnitude for an activity value.

(e) In most cases it is not necessary to use the purge for either KCl, NaCl, or sea water analyses. The purge does affect the species, either by altering the pH or altering the solubility of certain anions. When the purge is used, there is a definite current repression effect from $Pb(NO_3)_2$. Without the purge, the current peaks are linear during lead additions.

(f) The $Pb(NO_3)_2$ solution for additions is a dominant non-labile complex and hinders the modeling of species with increasing lead concentrations. Despite the repression effect, the additions method is an accurate, reproducible system for measuring concentrations and determining non-labile complexes.

(g) Under certain conditions multiple peaks appear for various complexes. Without multiple peaks it is still possible to identify and measure major complexes. The potential stripping scale is the key to identifying these species. It is difficult to identify specific complexes other than the most dominant such as $PbCO_3^o$, $PbSO_4^o$, and $PbCl^+$.

(h) In the examples cited, concentration affects the chemical forms. Figure 6-9 and 6-10 show which chemical forms exist for various concentrations. Most results agree with the literature as mentioned, but a few do not, either because other methods depend on the purge or because of the dominance of $Pb(NO_3)_2$. These disagreements with the literature are also cited. I do not include pH profiles because of the narrow pH range of the samples, 7.5 to 8.5, and because in cases when pH affects the complexing, the results are shown.

Field Samples - Quatsino Sound, British Columbia

Anoxic basins, located in a number of places in British Columbia, include Saanich Inlet, British Columbia (Gucluer and Gross, 1964; Herlinveaux, 1962; Nissenbaum and others, 1972; Presley and others, 1972; and Brown and others, 1972), Lake Nitinat, British Columbia (Richards and others, 1965), and various British Columbian mainland fjords (Tully and Dodimead, 1957). These zones are a function of the

FIGURE 6-9

CHEMICAL FORMS VS. CONCENTRATIONS - ELECTROLYTE

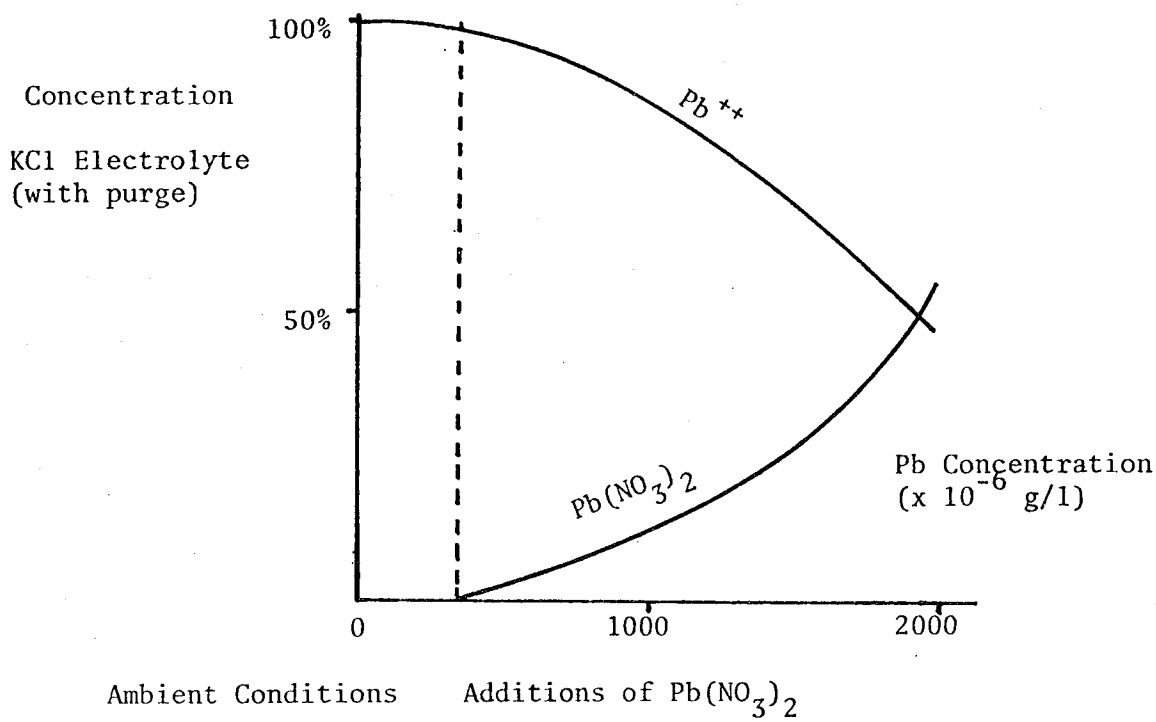

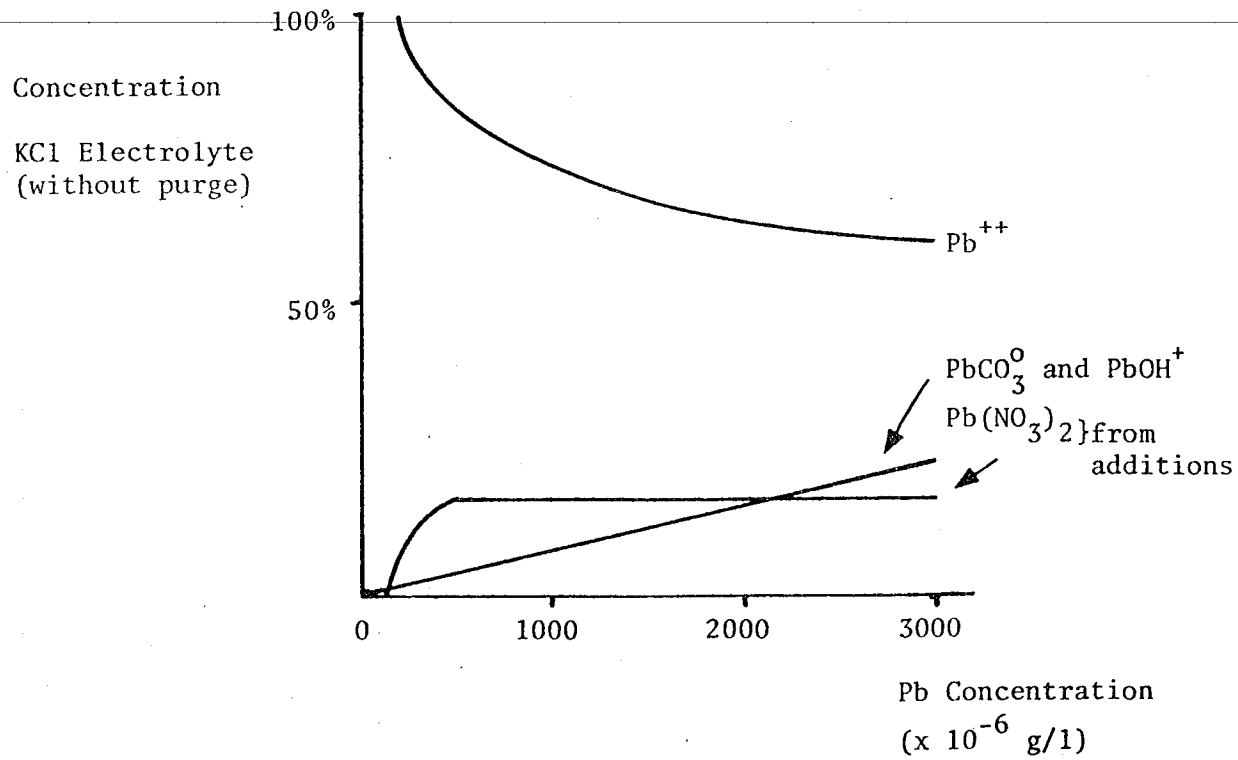

FIGURE 6-10

CHEMICAL FORMS VS. CONCENTRATIONS - SEA WATER

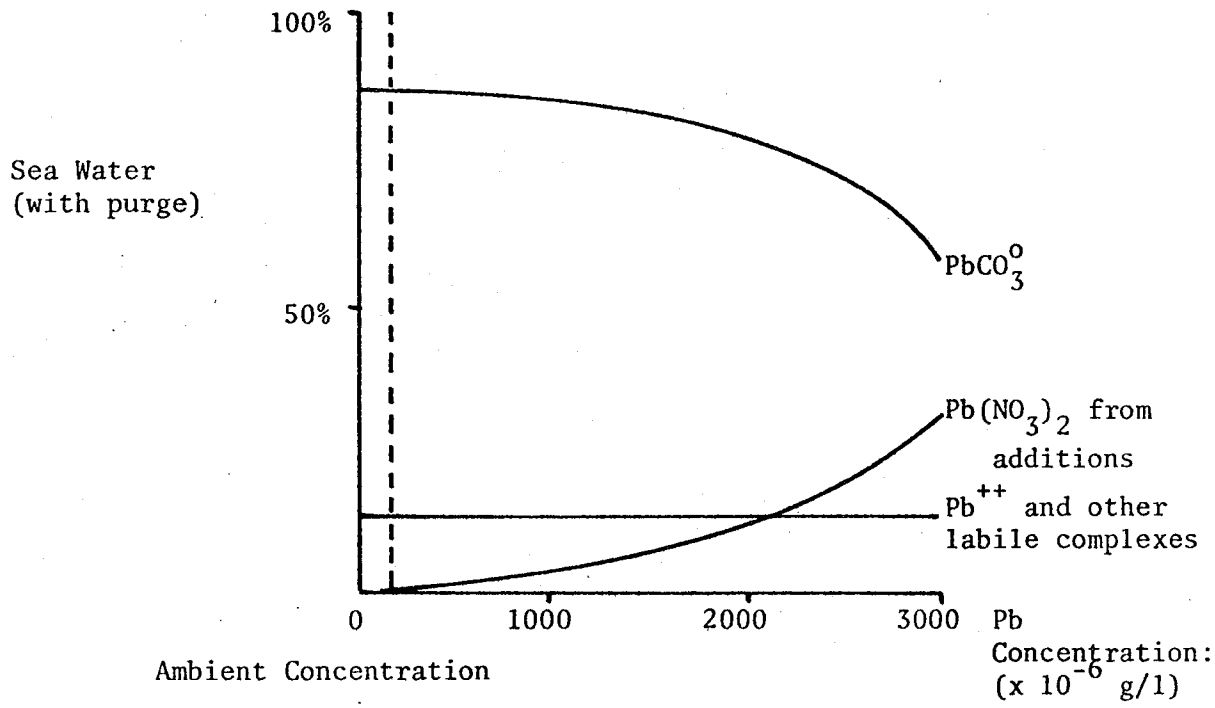

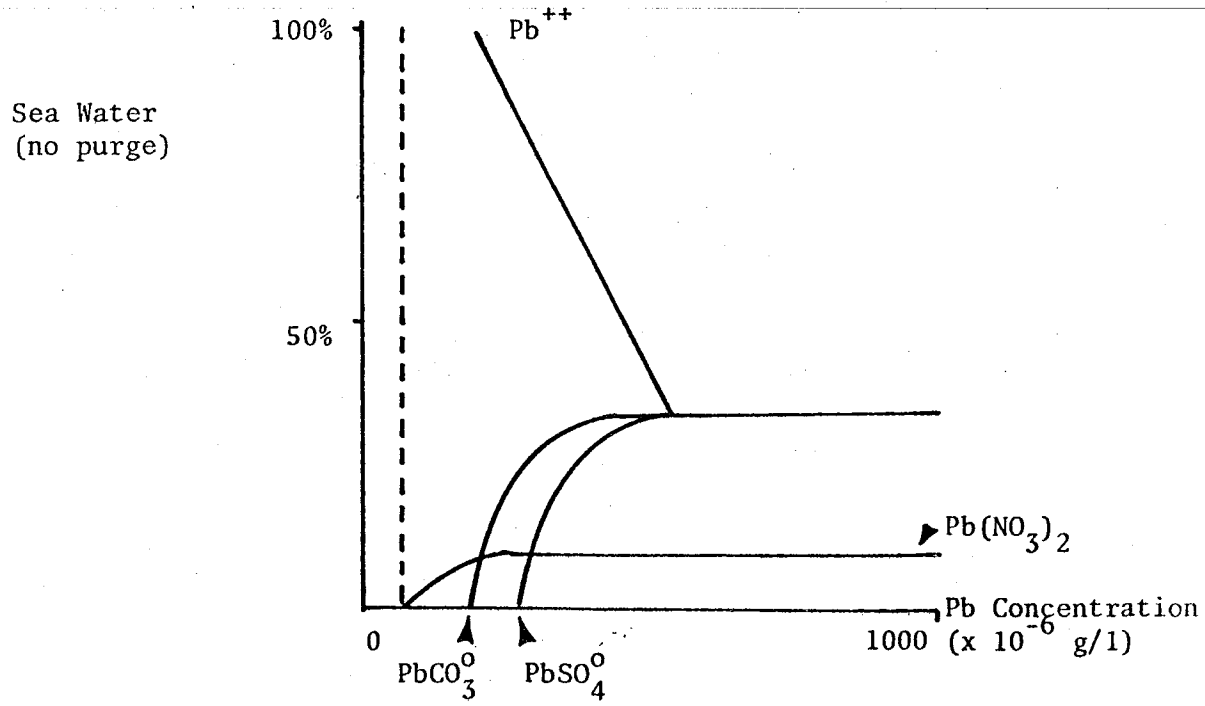

basin bathymetry and for partially anoxic basins are situated at a depth below the influx of oxygenated water (Glucluer and Gross, 1964). Presley and others (1972) and Gross (1967) show that the reducing conditions affect minor trace element concentrations and species in interstitial and in sea-bottom interface waters. The lead species should include $PbCO_3^o$ and $PbSO_4^o$ because of the high concentration of $CO_3^=$ and $SO_4^=$ ions. The reducing conditions and low redox potential of this partially anoxic basin also affects the complexing (Richards, 1965, p.623), particularly in the case of partial sulphate reduction during organic decomposition according to this equation (Richards, 1965, p.625):

$$(6\text{-}20) \qquad (CH_2O)_{106}\ (NH_3)_{16}\ H_3PO_4 + 53SO_4^= = 106\ CO_2 + 53S^= + 16\ NH_3 + 106\ H_2O + H_3\ PO_4$$

I took my samples at a number of depths and locations in a partially anoxic basin at the mouth of Rupert Inlet, Quatsino Sound, on the northern tip of Vancouver Island in British Columbia. Figure 6-11 shows the location, and Table 6-8 lists the locations with depths. Because of adverse weather conditions, the inaccessibility of Quatsino Sound, equipment problems, and a seven knot current, I was unable to collect water samples from the bottom, but instead from the relatively well oxygenated waters above the Inlet sill. (I used Winkler titration methods on dissolved oxygen samples, but because of contamination problems, the results were inconclusive.)

FIGURE 6-11

QUATSINO SOUND, BRITISH COLUMBIA

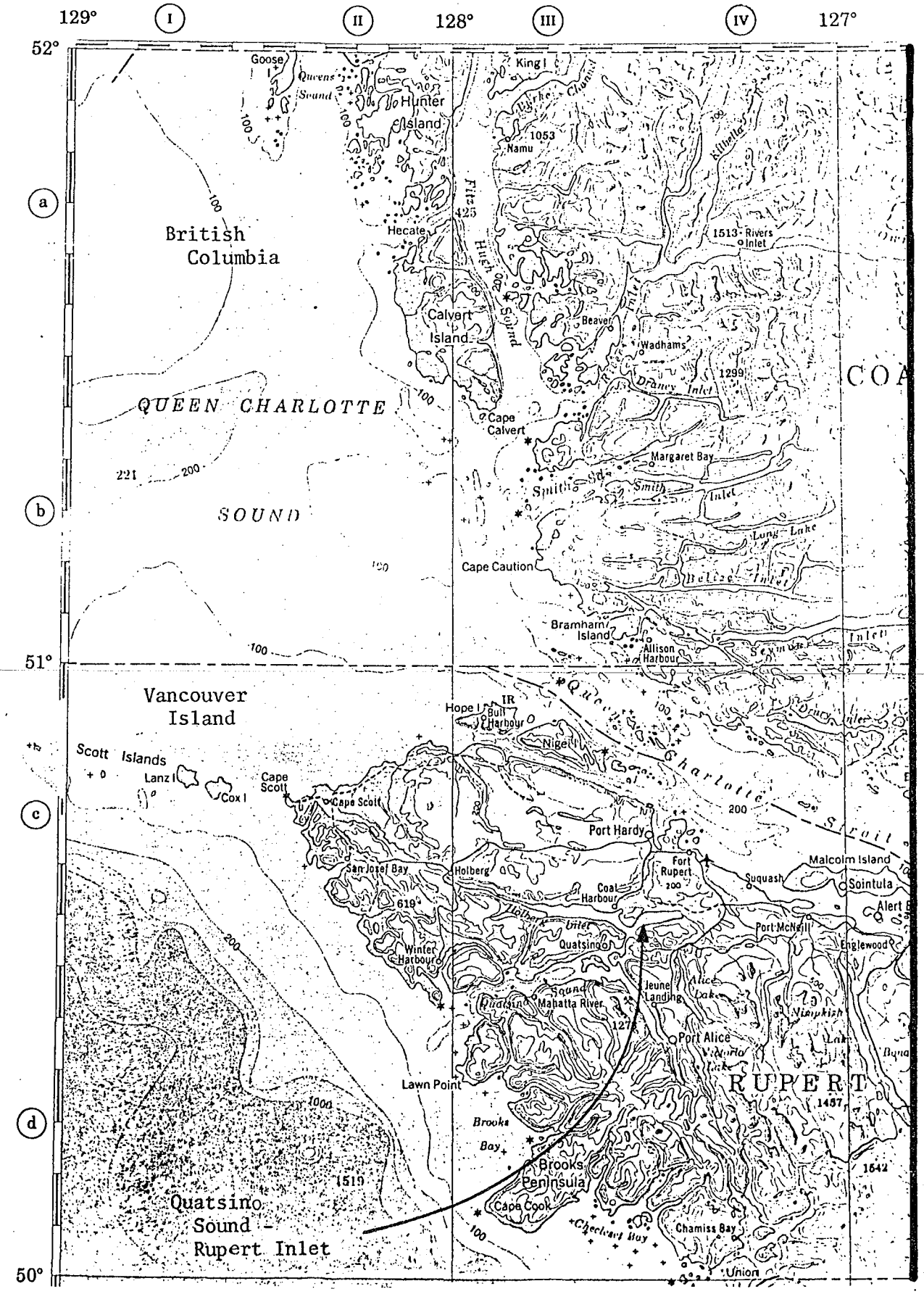

TABLE 6-8

SAMPLES FROM RUPART INLET, QUATSINO SOUND, BRITISH COLUMBIA

Sample Number	Location	Depth (meters)
7	Station #1: about 500 m in front of the Utah Mine.	2
8		15
9		25
10	Station #2: Mouth of Rupart Inlet	25
11		15
12		2
13	Station #3: 100 m east of mine tailings	45
14	Station #4: 20 m in front of mine tailings	2
15		2

The trace element samples became contaminated though during the long six month storage period, and the results of the analyses were unsatisfactory. Either the trace elements were scavenged by the containers to a level below the ASV sensitivity threshold, or the ambient concentration itself is below this threshold. There are a number of procedures in the collection process which also can cause contamination. Hume (1975) describes these pitfalls, and with advice and help from the personnel from the Lawrence Berkeley Laboratory, which are cited in the acknowledgments, I did not have these problems with the other samples.

Figure 6-12 shows the analysis of two samples taken 500 meters offshore from a tailings deposit of the Utah Mines copper processing plant. (This is the only industry and about the only sign of civilization on Quatsino Sound.) Samples (A) and (D) are from a depth of 25 meters, and samples (B) and (C) are from near surface. Only sample (D) shows a current peak and the presence of lead. It is difficult to tell the concentration or form of lead based on just this one peak. I measured the current, which was to the order of 1×10^{-5} amps, compared it to the measured current from calibration curves, and estimated that for this one sample lead was present in the low parts per million range.

The stripping potential occurs at -0.630 volts which may mean that the dominant forms of lead are Pb^{++} or $Pb(OH)_2^o$.

Table 6-9 shows the results of the one successful analysis. The slight potential shift to -0.630 indicates that lead is in the form of Pb^{++}, with some $Pb(OH)_2^o$, $PbCO_3^o$, and $PbSO_4^o$. This is expected under these somewhat normal dissolved oxygen conditions.

FIGURE 6-12

ANALYSIS OF SAMPLES FROM QUATSINO SOUND, BRITISH COLUMBIA

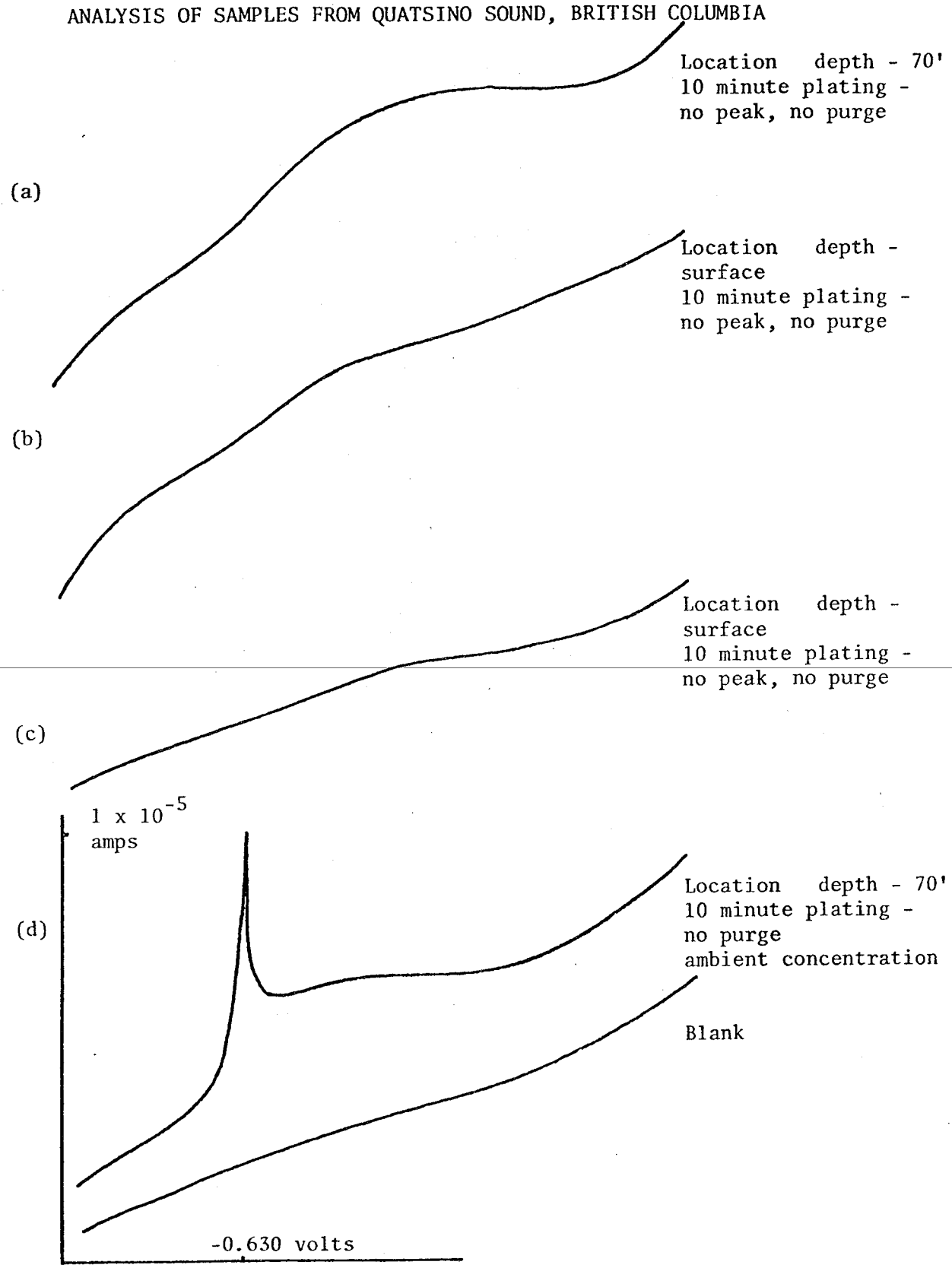

TABLE 6-9 - CHEMICAL FORMS OF LEAD IN SEA WATER - RUPART INLET, QUATSINO SOUND, BRITISH COLUMBIA

Soluble Lead					Particulate Lead
Labile Lead			Non-Labile Lead		
Lead: Free Ions - Pb^{++}	Lead: Adsorbed On:	Lead: Complexed With:	Lead: Adsorbed On:	Lead: Complexed With:	
At ambient concentrations of low parts per million the dominant form of lead appears to be Pb^{++}.	Non-stable uncharged organic colloids cannot be distinguished with this method. Inorganic colloids repress the current peak, but as there is no peak repression at ambient concentration, no lead is present in the inorganic colloid form.	The potential shift to -0.630 suggests that complexes such as $Pb(OH)_2^o$, $PbCO_3^o$, and $PbCO_4^o$ are present. Data are insufficient to reach a definite conclusion.	(Same as Labile Lead: Adsorbed On: section.)	Data insufficient to reach conclusions on current repression.	These samples were not filtered, so data are not available.

Field Samples - San Francisco Bay

For the last few years scientists at the Lawrence Berkeley Laboratory have been studying the seasonal and spatial variations in solute and particulate concentrations of certain trace elements in San Francisco Bay (Girvin and others, 1976). I helped collect sea water samples on one of their cruises with their equipment and advice, cited in the acknowledgments. Appendix D describes the sophisticated trace element sampling techniques which Girvin and others (1976) have developed for their studies.

Figure 6-13 shows the various sampling locations in central and southern San Francisco Bay. On this particular excursion surface samples were taken at location #27, Coyote Point, and at Foster City. I planned to use these samples only for additional testing and calibrating of the ASV system, and did not plan to construct depth or other physical and chemical trace element profiles. Therefore I collected 2000 ml of sea water at location #27 only. Appendix D discusses how these samples were filtered with a 0.4 μm filter. 1000 ml were acidified immediately with National Bureau of Standards twice distilled nitric acid (HNO_3) in order to prevent loss of dissolved trace elements on the walls of the common polyethelene (CP) storage bottles. I left the other 1000 ml as collected, except for refrigerating, because I did not wish to add chemicals to part of the sea water. I analyzed the samples within twenty-four hours and hoped to keep part of the samples as close to ambient conditions as possible. Within that time span, the untreated CP bottles should have little if any effect on the lead concentration.

FIGURE 6-13 - SAMPLING LOCATIONS IN SAN FRANCISCO BAY

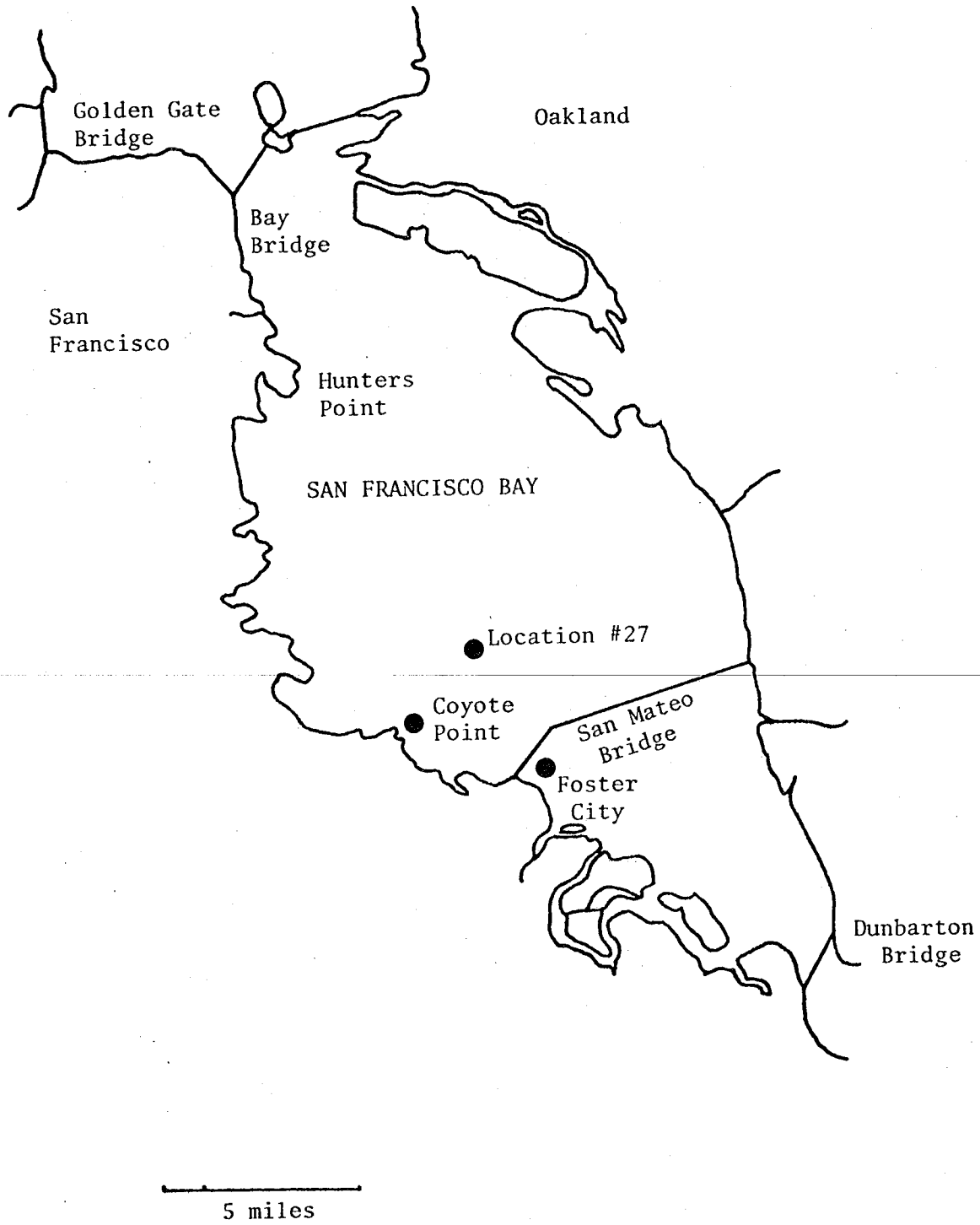

Chemical Models of San Francisco Bay Samples

1) San Francisco Bay Water With Purge (A):

A series of three analyses were run with the unacidified Bay water with a purge. The results of each analysis are described separately. Figure 6-14 shows the raw data from the X-Y recorder, and Figure 6-15 shows the calibration curve from successive lead additions. This analysis determines that the sample has a concentration of 1.2 - 1.3 x 10^{-4} g/l of sea water. Figure 6-16 plots the stripping potentials for the current peaks, and Figure 6-17 shows the current repression curve.

The current peaks are sharp, well defined, and occur at a constant potential of -0.610 volts. This potential indicates that either Pb^{++} or $Pb(OH)_2^o$ are the predominant labile chemical forms. As mentioned earlier, this hydroxyl form occurs only with a pH > 10.0, and in this case the pH is 8.03. Therefore it seems logical that the predominant chemical form is Pb^{++}, and minor contributions of $PbCO_3^o$, $PbSO_4^o$, and $PbOH^+$ cause the potential to shift slightly from -0.682 volts.

The current curve is repressed from the linear shape for concentrations higher than 2.0 x 10^{-4} g/l. This repression seems to occur for all analyses with the purge. Non-labile $Pb(NO_3)_2$ probably causes this deviation from the linear model.

Table 6-9 combines the data from the three analyses and summarizes the chemical forms of lead.

FIGURE 6-14

ANALYSIS OF SAN FRANCISCO BAY WATER - SAMPLE (A)

Sweep: 1 sec/min., normal X and Y, 2 sweeps, first sweep recorded - 1 minute rest; V = -.95

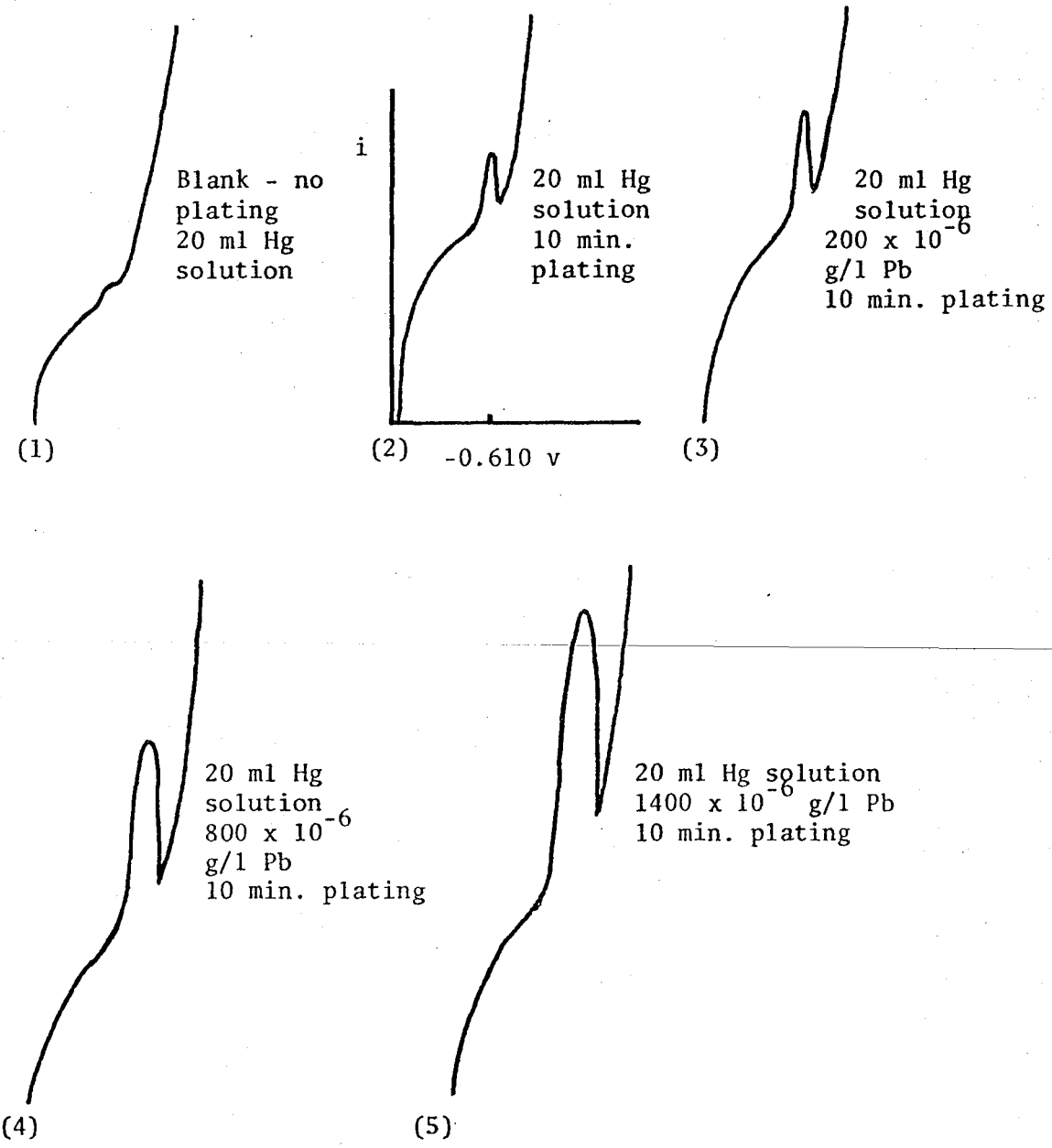

FIGURE 6-15

CALIBRATION CURVE - CONCENTRATION OF LEAD IN BAY SAMPLE: ANALYSIS (A)

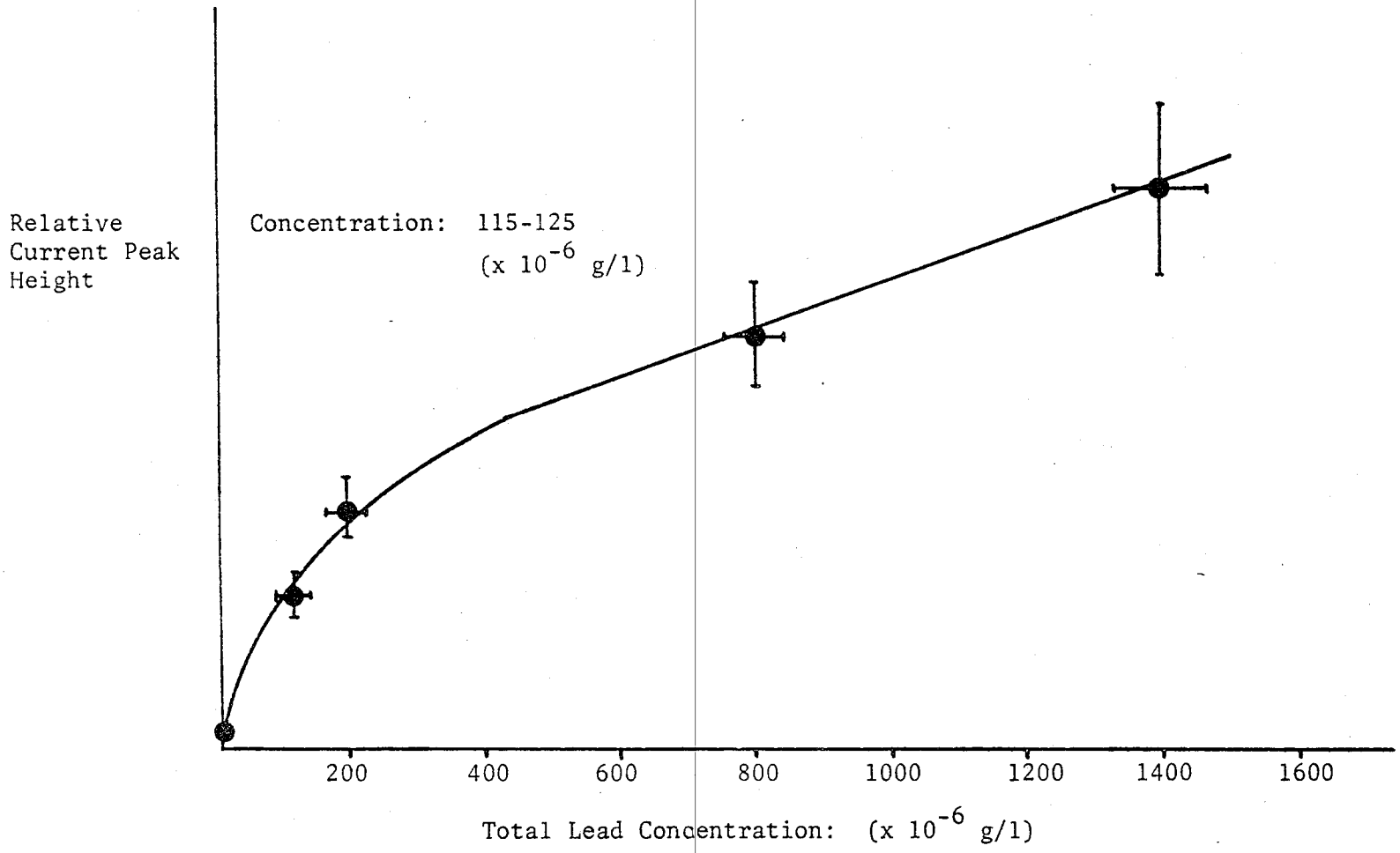

FIGURE 6-16

MEASURED POTENTIAL OF LEAD DURING STRIPPING - SAN FRANCISCO BAY WATER (WITH PURGE)

SAMPLE (A)

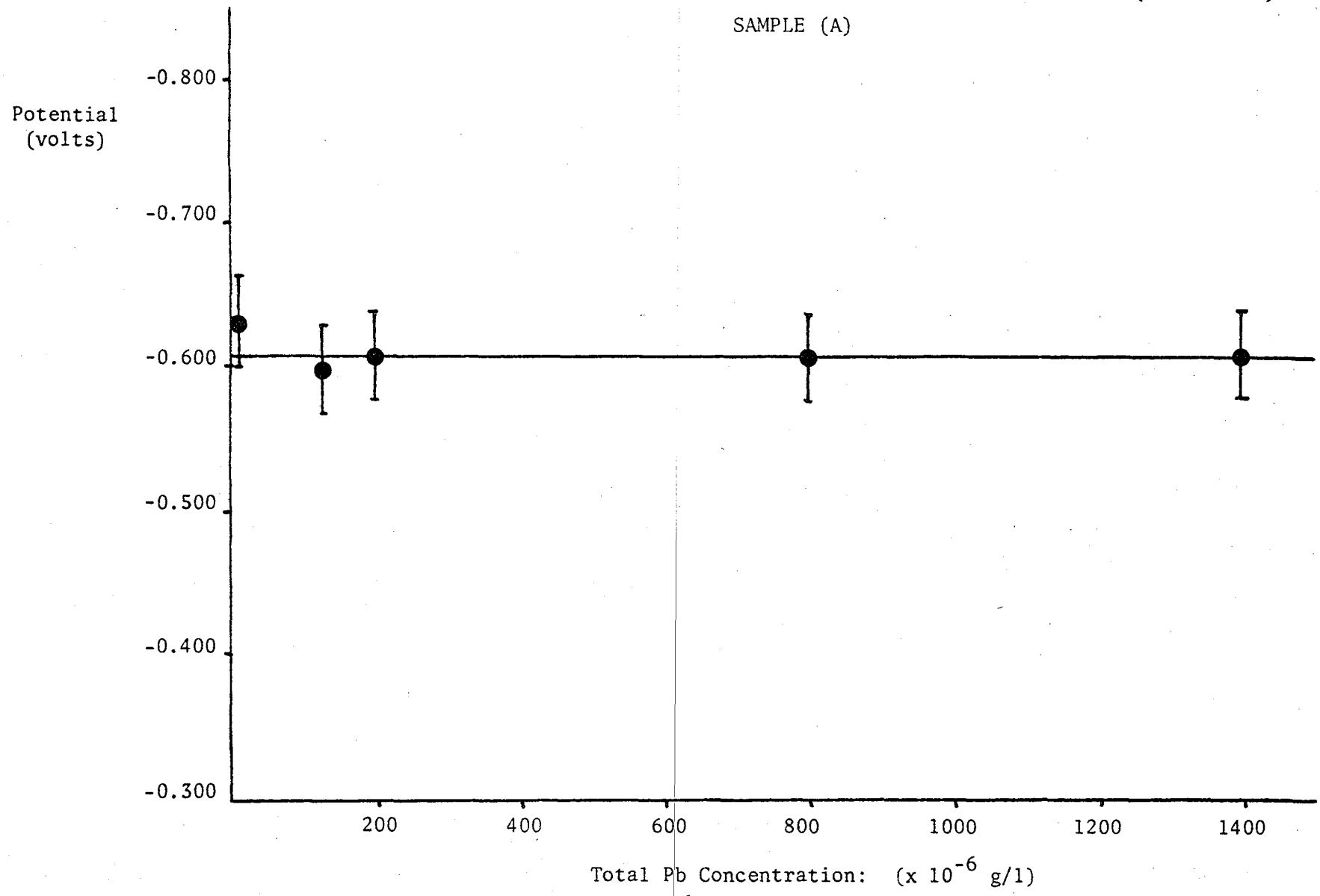

FIGURE 6-17

CURRENT REPRESSION OF NON-LABILE LEAD - SAN FRANCISCO BAY WATER (PURGE)

SAMPLE (A)

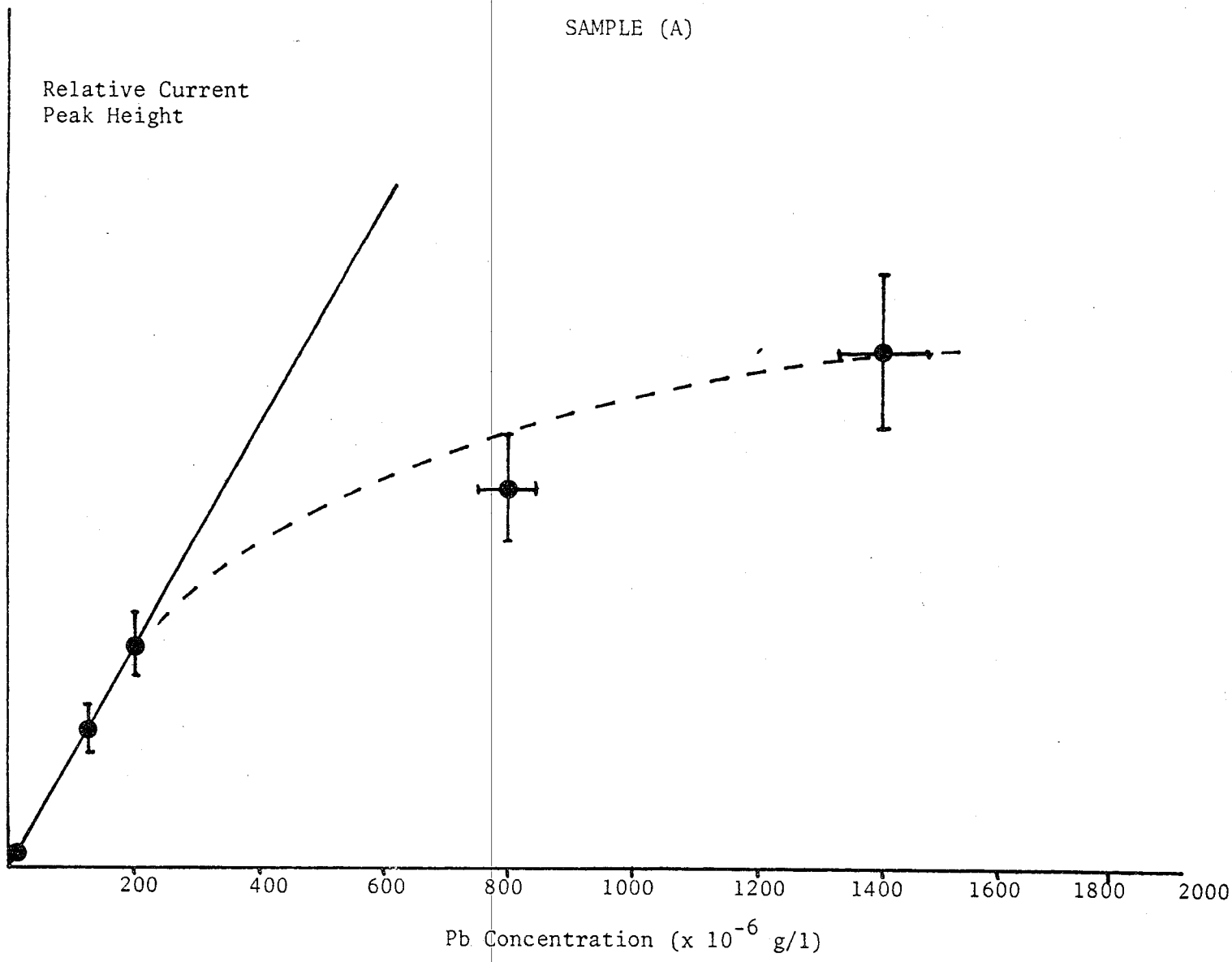

TABLE 6-10 - CHEMICAL FORMS OF LEAD IN SEA WATER - SAN FRANCISCO BAY (WITH PURGE)

Soluble Lead					Particulate Lead
Labile Lead			Non-Labile Lead		
Lead: Free Ions - Pb^{++}	Lead: Adsorbed On:	Lead: Complexed With:	Lead: Adsorbed On:	Lead: Complexed With:	
At ambient concentration of 1.0-1.2 x 10^{-4} g/l the dominant form of lead is Pb^{++}. Other species of lead are also present. These species include $PbCO_3^o$, $PbSO_4^o$, $PbOH^+$, and $PbCl^+$. At conditions above ambient $Pb(NO_3)_2$ becomes dominant.	Non-stable uncharged organic colloids cannot be distinguished with this method. Inorganic colloids repress the current peak, but as there is no peak repression at ambient concentration, no lead is present in the inorganic colloid form.	The potential shift to -0.610 indicates that labile complexes of $PbCO_3^o$, $PbOH^+$, $PbSO_4^o$, and $PbCl^+$ are present at ambient conditions. At higher concentrations $Pb(NO_3)_2$ begins to dominate.	(Same as Labile Lead: Adsorbed On: section.)	At concentrations greater than ambient the current peaks are repressed showing the presence of non-labile $Pb(NO_3)_2$.	The results of the particulate analysis are not available yet.

2) San Francisco Bay Water With Purge (B):

Figure 6-18 shows the current peaks for the analysis of sample (B). Figure 6-19 shows the calibration curve. Note that the analysis does not detect any ambient lead. This is probably due to erratic electrode behavior as mentioned in an earlier section. Figure 6-20 and 6-21 plot the stripping potentials and the repressive curve for the additions. The results are the same as those for sample (A).

3) San Francisco Bay Water With Purge (C):

Figures 6-22 through 6-25 show the current peaks, calibration curve, potential as a function of concentration, and current repression curve. This analysis determines a concentration of 1.0 - 1.2 x 10^{-4} g/l, in close agreement with analysis (A). The peak is difficult to see though, and this peak may have been masked in analysis (B). The potential curve is constant for ambient and addition concentrations at -0.610 volts, showing that the lead is predominantly Pb^{++} with some $PbCO_3^o$, $PbSO_4^o$, and $PbCl^+$.

There are two data points at the concentration of 5.0 x 10^{-4} g/l, but the lower one is most likely spurious as the upper point follows the trend of earlier experiments with the purge. Once again $Pb(NO_3)_2$ represses the current as the concentration increases above 5.0 x 10^{-4} g/l.

These are the mass balance equations, based on these three analyses:

(6-21) (Ambient concentration of 1.0 - 1.2 x 10^{-4} g/l)

$$[Pb]_{total} = [Pb^{++}] + [PbCO_3^o] + [PbSO_4^o] + [PbCl^+] + [PbOH^+]$$

FIGURE 6-18

ANALYSIS OF SAN FRANCISCO BAY WATER - SAMPLE (B) (Unacidified Bay Water, N_2 Purge, 150 ml, sweep: 1 sec/in, normal x and y, 2 sweeps - first sweep recorded, 1 min. rest)

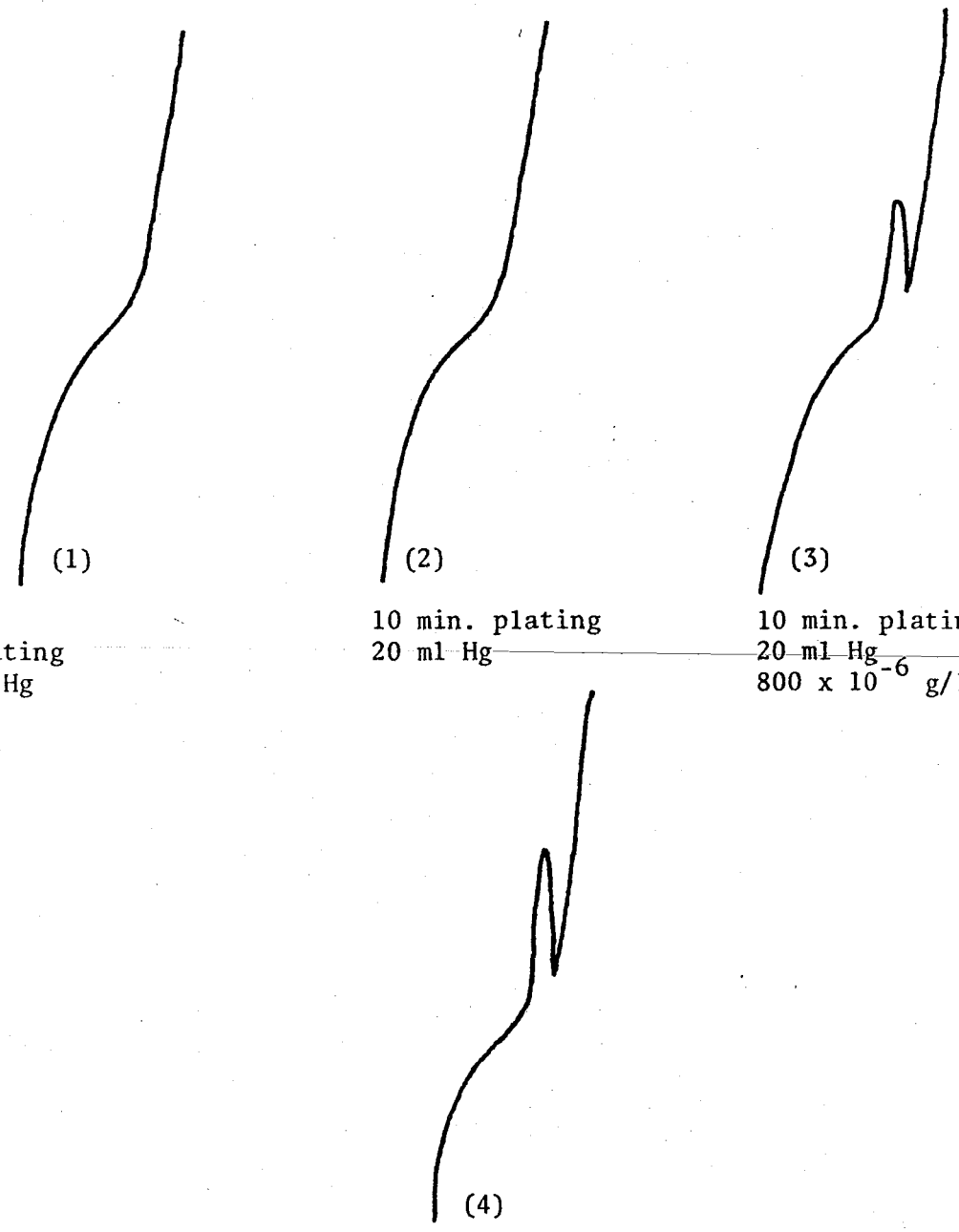

(1) Blank
no plating
20 ml Hg

(2) 10 min. plating
20 ml Hg

(3) 10 min. plating
20 ml Hg
800 x 10^{-6} g/l Pb

(4) 10 min. plating
20 ml Hg
1500 x 10^{-6} g/l Pb

FIGURE 6-19

CALIBRATION CURVE - CONCENTRATION OF LEAD IN BAY SAMPLE: ANALYSIS (B)

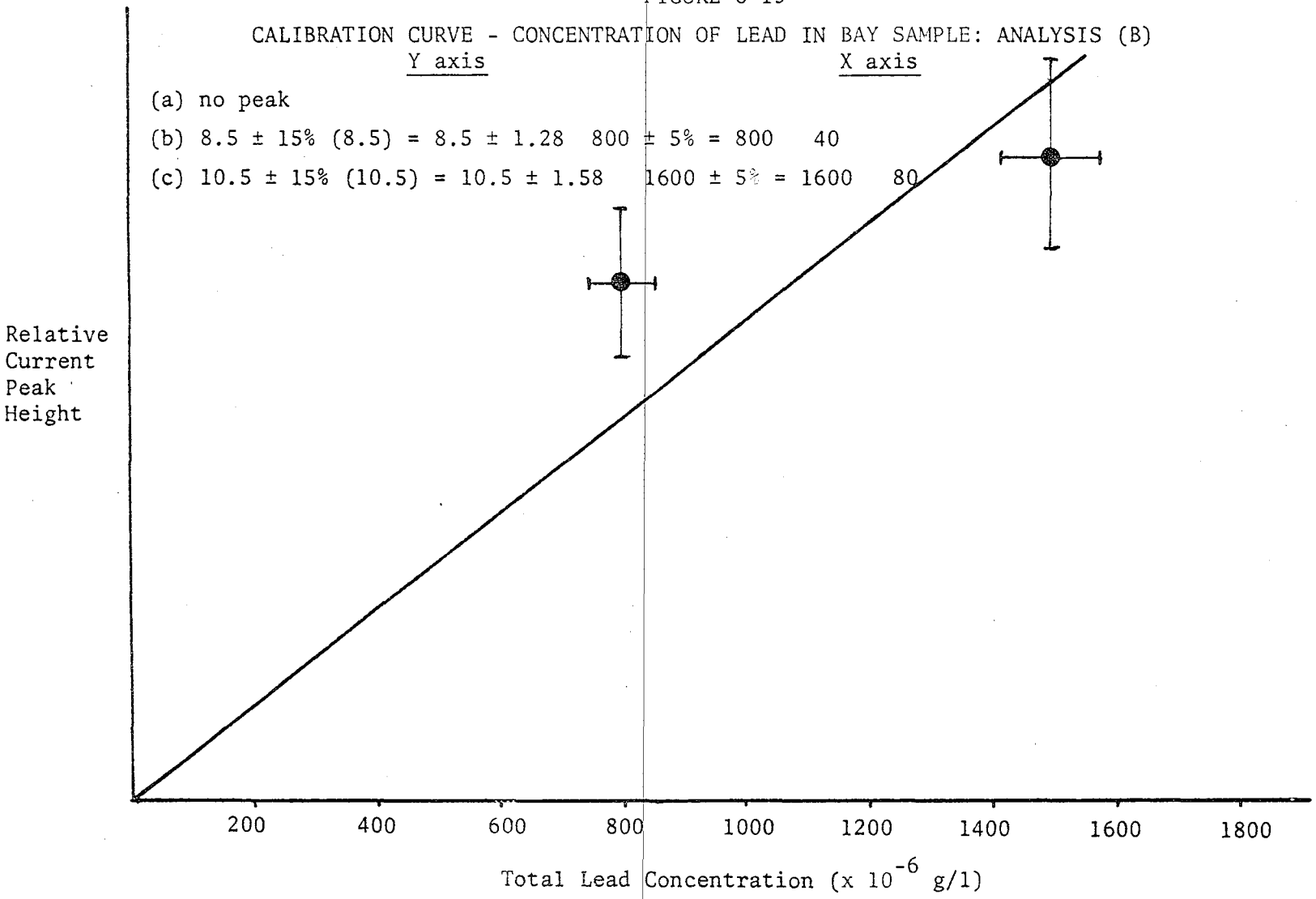

FIGURE 6-20

MEASURED POTENTIAL OF LEAD DURING STRIPPING - SAN FRANCISCO BAY WATER (WITH PURGE)

SAMPLE (B)

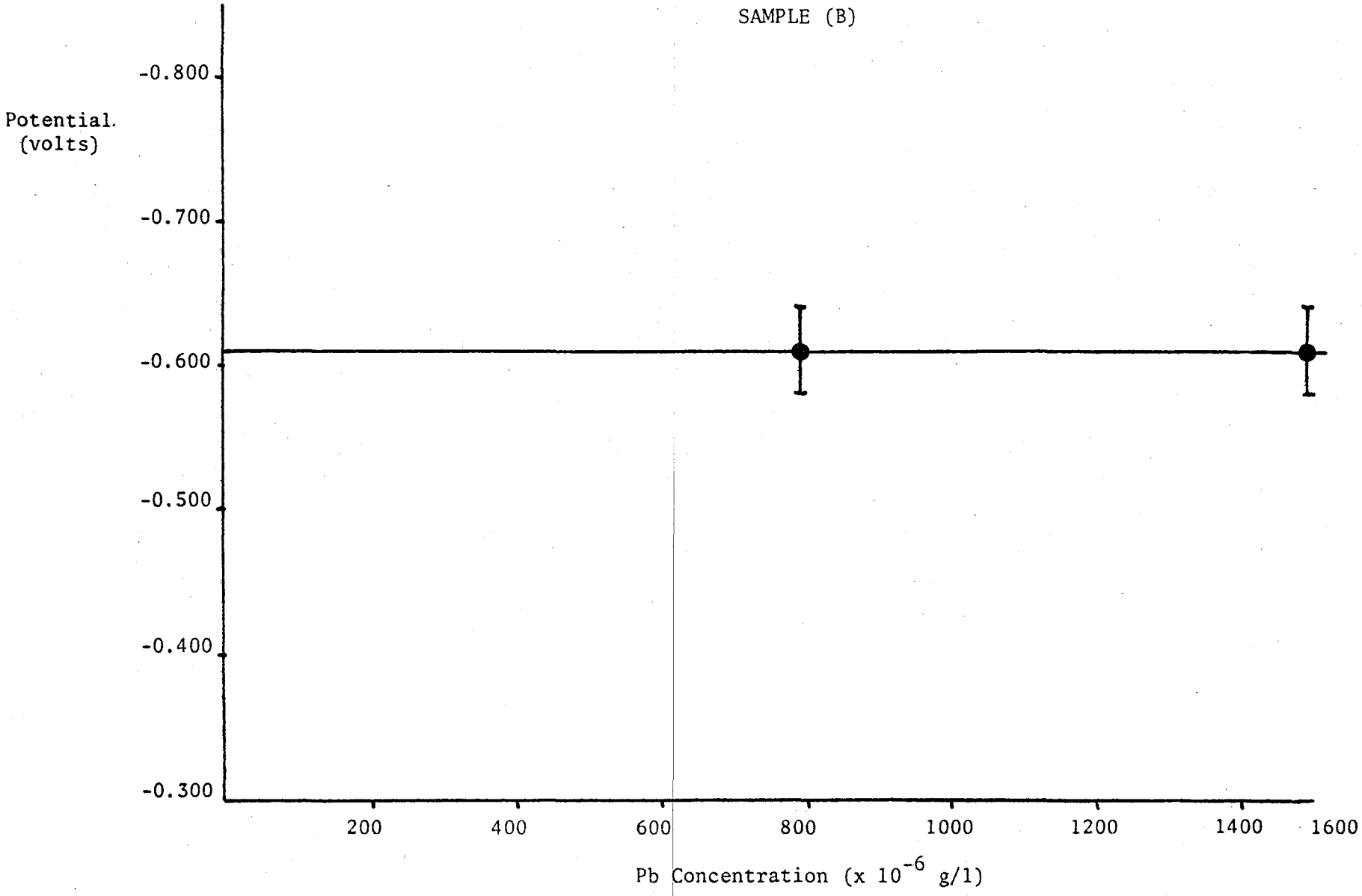

FIGURE 6-21

CURRENT REPRESSION OF NON-LABILE LEAD - SAN FRANCISCO BAY (PURGE) SAMPLE (B)

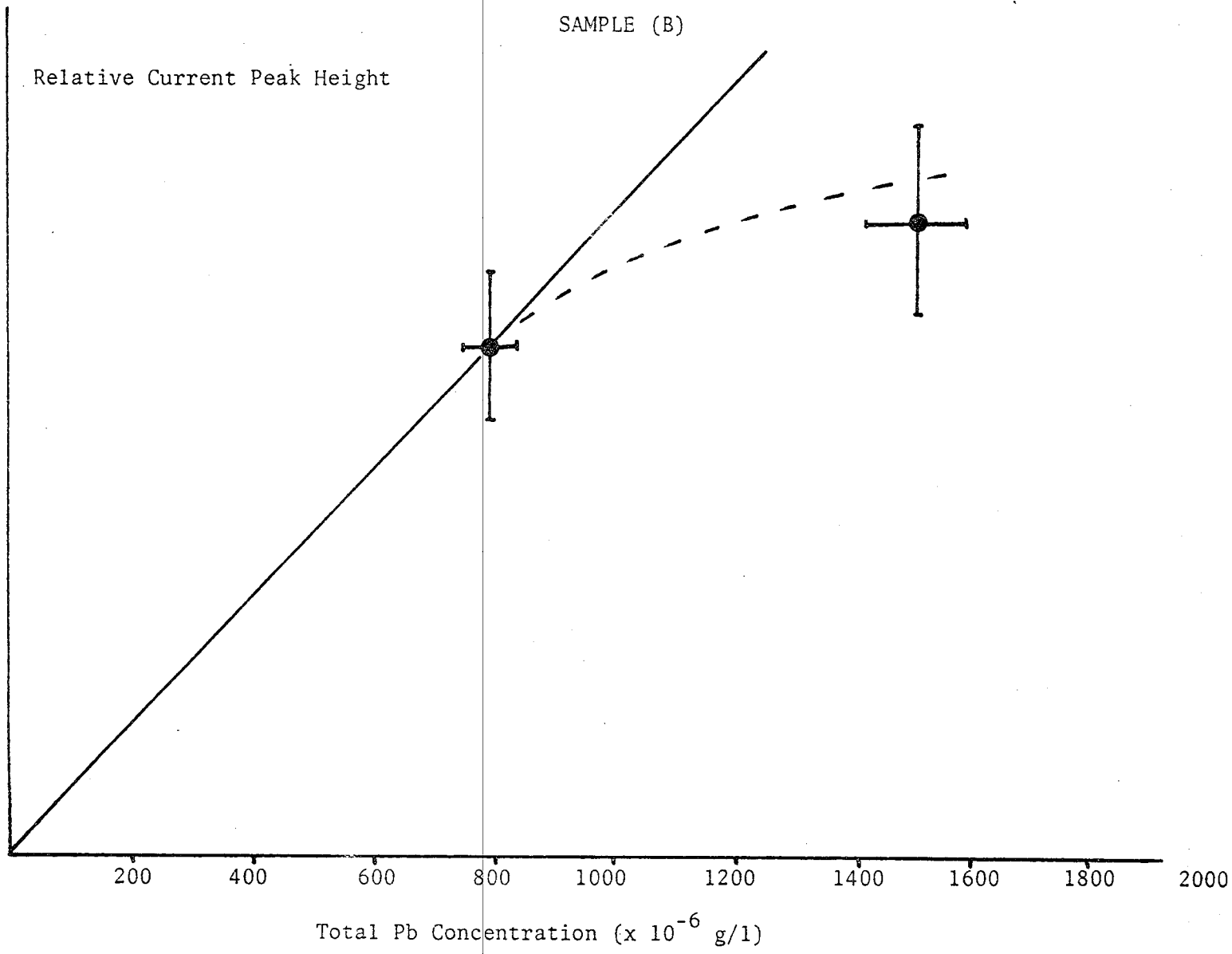

FIGURE 6-22

ANALYSIS OF SAN FRANCISCO BAY WATER - SAMPLE (C)

(Unacidified Bay Water, N_2 Purge, 150 ml, sweep: 1 sec/in, normal x and y, 2 sweeps - first sweep recorded 1 min. rest)

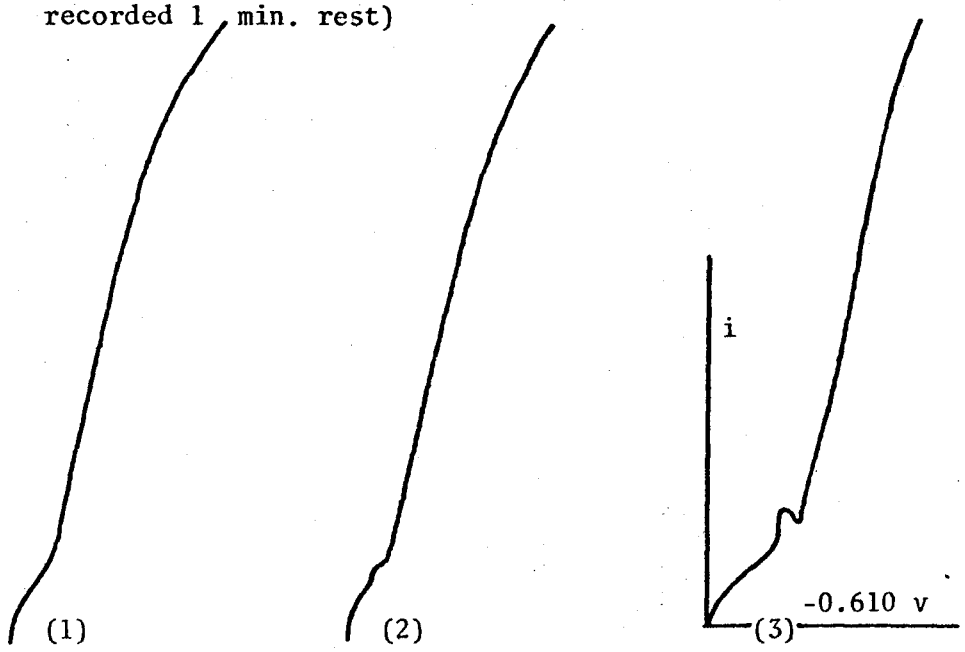

(1) Blank
no plating
20 ml Hg sol.

(2) 10 min. plating
20 ml Hg sol.

(3) 10 min. plating
200 x 10^{-6} g/l Pb
20 ml Hg sol.

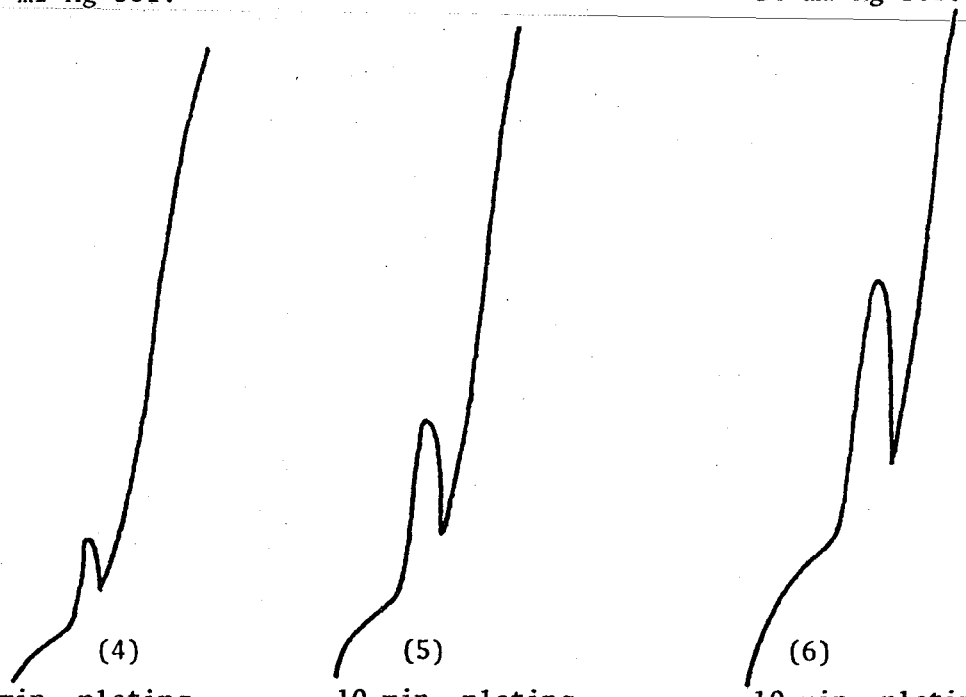

(4) 10 min. plating
500 x 10^{-6} g/l Pb
20 ml Hg sol.

(5) 10 min. plating
500 x 10^{-6} g/l Pb
20 ml Hg sol.

(6) 10 min. plating
1000 x 10^{-6} g/l Pb
20 ml Hg sol.

FIGURE 6-23

CALIBRATION CURVE - CONCENTRATION OF LEAD IN BAY SAMPLE: ANALYSIS (C)

Y axis	X axis
(a) .75 ± 15% (.75) = .75 ± .11	
(b) 1.75 ± 15% (1.75) = 1.75 ± .26	200 ± 5% = 200 ± 10
(c) 4.0 ± 15% (4.0) = 4.0 ± .60	500 ± 5% = 500 ± 25
(d) 9.75 ± 15% (9.75) = 9.75 ± 1.46	500 ± 5% = 500 ± 25
(e) 14.25 ± 15% (14.25) = 14.25 ± 2.14	1000 ± 5% = 1000 ± 50

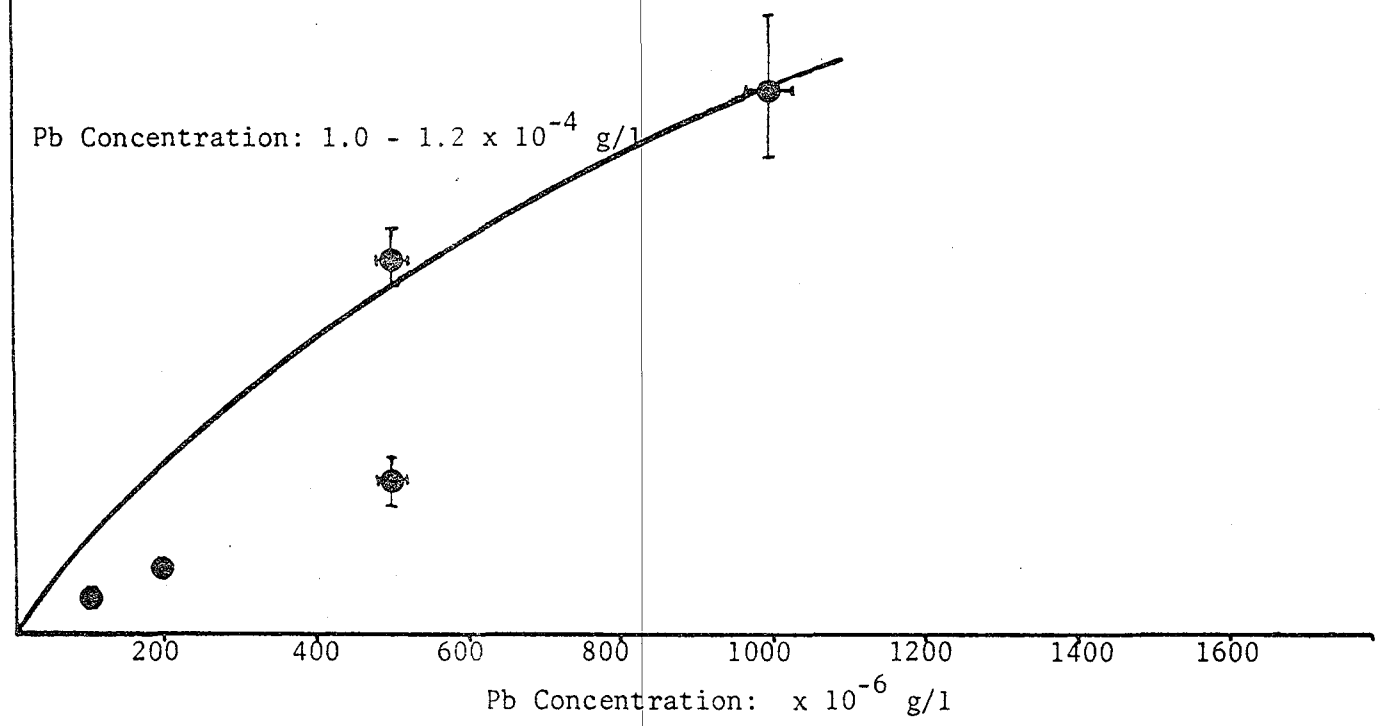

FIGURE 6-24

MEASURED POTENTIAL OF LEAD DURING STRIPPING - SAN FRANCISCO BAY WATER (PURGE) SAMPLE (C)

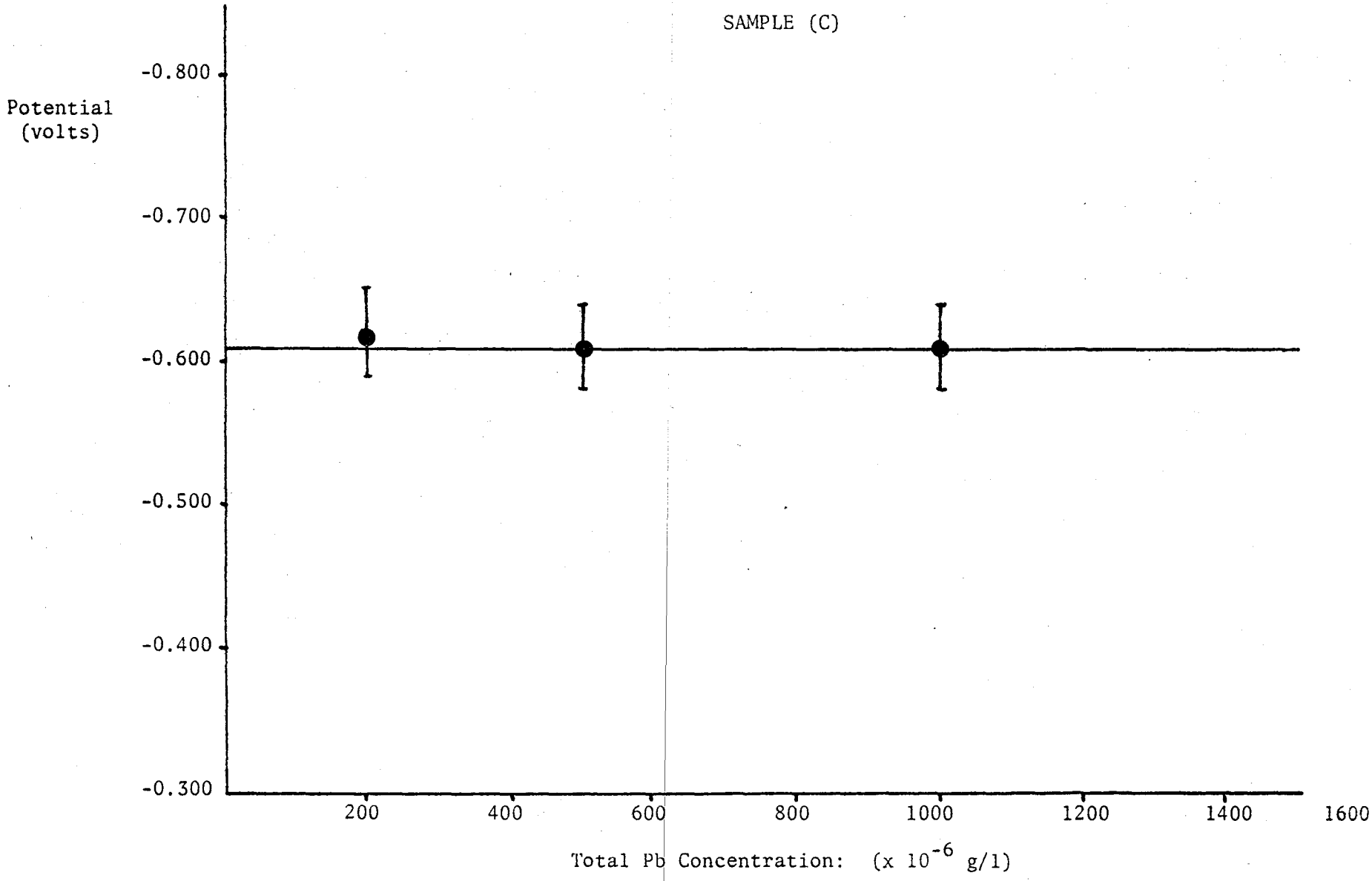

FIGURE 6-25

CURRENT REPRESSION OF NON-LABILE LEAD - SAN FRANCISCO BAY WATER (PURGE) SAMPLE (C)

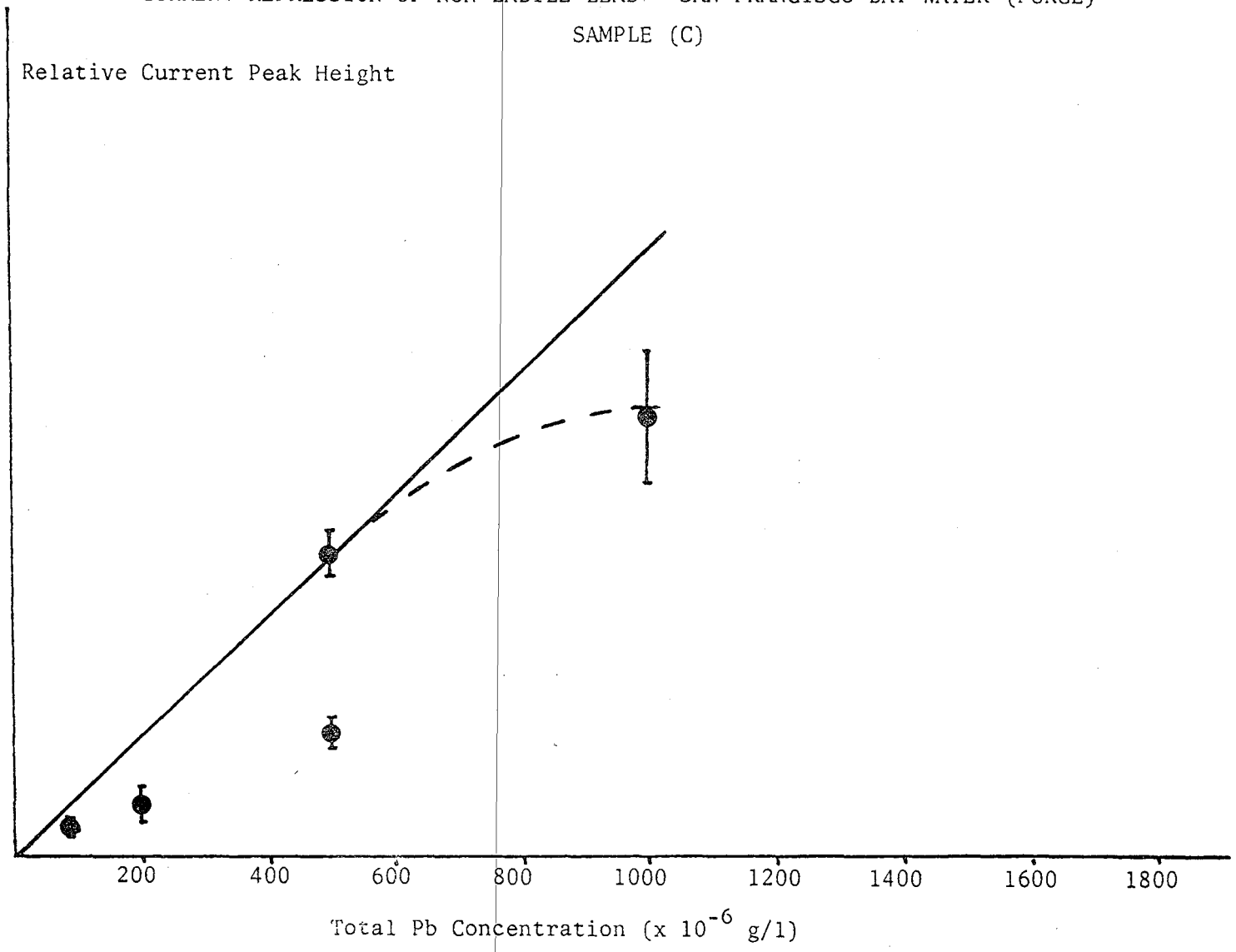

(6-22) (With additions)

$$[Pb]_{total} = [Pb^{++}] + [Pb(NO_3)_2] + [PbCO_3^o] + [PbSO_4^o] + [PbCl^+] + [PbOH^+]$$

Table 6-10 combines these three analyses and shows that the results for ambient concentrations are in partial agreement with the models of Long and Angino (1977, p.1188) for various combinations of sea water and fresh water. With a comparable pH of 8.03 Long and Angino show dominant anions of Cl^-, OH^-, and CO_3 for both 100% sea water, and 50% sea water and 50% fresh water. In both cases Pb^{++} is also a dominant form, but $PbSO_4^o$ is present to a lesser degree.

4) San Francisco Bay Water Without Purge (A, B, and C)

A series of three analyses were run with the unacidified Bay water without a purge. The results of all three analyses are similar and therefore are described together in this section. Figure 6-26 shows the current peaks from the X-Y recorder; curve (1) is the blank and curves (2), (3), and (4) are the analyses for samples (A), (B), and (C). The successive addition method is ineffective for establishing the calibration curve, either because of a complete repression of the peaks by $Pb(NO_3)_2$ or because of erratic electrode behavior. Complete repression seems to be the cause as this effect happened for all three samples - a highly unlikely occurrence for erratic electrodes. This total supression of the peaks occurs when $Pb(NO_3)_2$ totally dominates Pb^{++} and the labile complexes. The peaks for the three samples are distinct, and by measuring the current during the stripping reaction, the analyses

TABLE 6-10 - CHEMICAL FORMS OF LEAD IN SEA WATER - SAN FRANCISCO BAY (WITH PURGE)

Soluble Lead					Particulate Lead
Labile Lead			Non-Labile Lead		
Lead: Free Ions - Pb^{++}	Lead: Adsorbed On:	Lead: Complexed With:	Lead: Adsorbed On:	Lead: Complexed With:	
At ambient concentration of 1.0 - 1.2 x 10^{-4} g/l the dominant form of lead is Pb^{++}. Other species of lead are also present. These species include $PbCO_3^o$, $PbSO_4^o$, $PbOH^+$, and $PbCl^{++}$. At conditions above ambient $Pb(NO_3)_2$ becomes dominant.	Non-stable, uncharged organic colloids cannot be distinguished with this method. Inorganic colloids repress the current peak, but as there is no peak repression at the ambient concentration, no lead is present in the inorganic colloid form.	The potential shift to -0.610 indicates that labile complexes of $PbCO_3^o$, $PbOH^+$, $PbSO_4^o$, and $PbCl^+$ are present at ambient conditions. At higher concentrations $Pb(NO_3)_2$ begins to dominate.	[Same as the Labile Lead: Adsorbed On: section.]	At concentrations greater than ambient the current peaks are repressed showing the presence of non-labile $Pb(NO_3)_2$.	The results of the particulate analysis are not available yet.

FIGURE 6-26

ANALYSES OF SAN FRANCISCO BAY WATER (WITHOUT PURGE)

(150 ml unacidified San Francisco Bay Water - No purge - sweep: 1 sec/in, normal X and Y, two sweeps, second recorded)

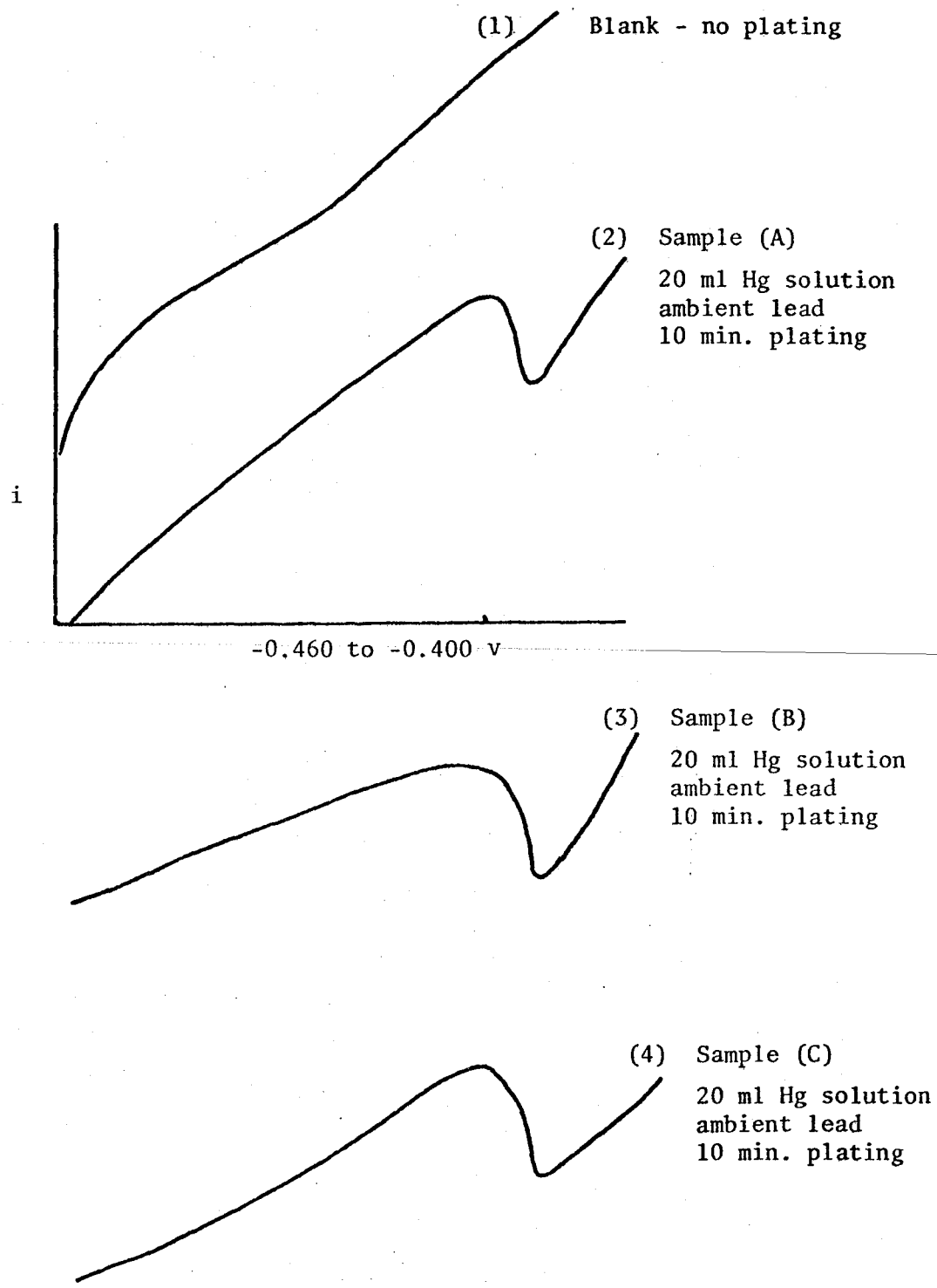

show the lead concentration to be at 1-10 x 10^{-4} g/l. Although these figures represent a wide range, they agree in magnitude with the Bay with purge analyses.

Stripping for all three samples occurs between -0.460 and -0.400, indicating that $PbCO_3^o$ is decidedly the dominant species. A mass balance equation showing $PbCO_3^o$ as the dominant species then agrees with the Long and Angino model (1977, p.1188) and the dominant anion relationship (Goldberg, 1965, p.163). Table 6-11 shows the chemical forms of lead in the Bay Water without a purge.

Below the Threshold of Detection - Field Samples - Gulf of Mexico

The results of the analyses of samples from the Gulf of Mexico are simple to present - the lead concentrations are below the threshold of detection by this ASV method. Lawrence Berkeley Laboratory scientists took a Department of Energy sponsored Ocean Thermal Energy Conversion (OTEC) oceanographic cruise in the Gulf of Mexico. In preparation for these samples, I cleaned 48 conventional polyethelene Nalgene® 500 ml narrow mouth bottles by the standard plasticware procedures described in Chapter IV. Scientists, using the only available collection of bottles, Niskin bottles, took a number of sea water samples for a variety of oceanographic purposes at two prospective OTEC prototype platform sites in the Gulf of Mexico. These samples are from various zones of the water column, including the surface waters, the base of the thoroughly mixed zone, and the base of the thermocline. These samples were filtered, acidified, and refrigerated, and were analyzed within a month after collection.

TABLE 6-11 - CHEMICAL FORMS OF LEAD IN SEA WATER - SAN FRANCISCO BAY (WITHOUT PURGE)

Soluble Lead					Particulate Lead
Labile Lead			Non-Labile Lead		
Lead: Free Ions Pb^{++}	Lead: Adsorbed On:	Lead: Complexed With:	Lead: Adsorbed On:	Lead: Complexed With:	
At ambient concentrations of $1\text{-}10 \times 10^{-4}$ g/l some Pb^{++} is present but the dominant form is $PbCO_3^o$.	Labile uncharged organic complexes cannot be distinguished with this method. The ambient peak is sharp and shows no sign of being repressed from inorganic colloids.	The ambient shift to (-0.460) - (-0.400) shows that $PbCO_3^o$ is the dominant species.	[Same as the Labile Lead: Adsorbed On: section.]	$Pb(NO_3)_2$ completely dominates the successive additions curve.	The results of the particulate analysis are not available yet.

Trace element analyses by highly-developed methods using an atomic adsorption spectrophotometer with a graphite furnace (Girvin and others, 1976, p.10) show the lead concentrations to be in the low parts per trillion range. This level is well below the detection threshold for many analytic techniques and mine proved not to be an exception. I obtained curves similar to blank curves for all samples despite using a plating time of up to an hour, varying the sweep speed, replacing the working electrode, varying the length of the purge, and varying the mercury concentration. This result is not unexpected though, and the advantages and disadvantages of this ASV technique are listed in detail earlier in this chapter. For most sea water analyses, particularly in bottom waters of anoxic basins, lead concentrations will be above this lower boundary of detection (Gross, 1967 and Presley and others, 1972).

APPENDICES

TABLE A-1

LEAD DATA

	Lead Species	State	$\Delta H_F°$ (kCal)	S° (Cal/Deg)	$\Delta F_F°$ (kCal)
1.	Pb (metal)	C	0	15.51	0
2.	Pb^{++}	aq.	0.39	5.1	-5.81
3.	Pb^{4+}	aq.			72.3
4.	PbO (red)	C, II	-52.40	16.2	-45.25
5.	PbO (yellow)	C, I	-52.07	16.6	-45.05
6.	$HPbO_2^-$	aq.			-81.0
7.	$PbO_3^=$	aq.			-66.34
8.	PbO_4^{4-}	aq.			-67.42
9.	$Pb(OH)_2$	C	-123.0	21.0	-100.6
10.	PbO_2	C	-66.12	18.3	-52.34
11.	Pb_3O_4	C	-175.6	50.5	-147.6
12.	PbF_2	C	-158.5	29.0	-148.1
13.	$PbCl_2$	C	85.85	32.6	-75.04
14.	PbS	C	-22.54	21.8	-22.15
15.	PbS_2O_3	C	-150.1	35.4	-134.0

TABLE A-1

LEAD DATA (Continued)

	Lead Species	State	$\Delta H_F°$ (kCal)	S° (Cal/Deg)	$\Delta F_F°$ (kCal)
16.	$PbSO_4$	C, II	-219.50	35.2	-193.89
17.	$PbSO_4$-PbO	C	-282.5	48.7	-258.9
18.	$Pb_3(PO_4)_2$	C	-620.3	84.45	-581.4
19.	$PbHPO_3$	C	-234.5	31.9	-208.3
20.	$PbCO_3$	C	-167.3	31.3	-149.7
21.	PbO-$PbCO_3$	C	-220.0	48.5	-195.6
22.	2PbO-$PbCO_3$	C	-273.0	65.0	-242.0
23.	$Pb_3(OH)_2(CO_3)_2$	C			-406.0
24.	$PbCrO_4$	C	-225.2	36.5	-203.6
25.	$PbMoO_4$	C	-265.8	38.5	-231.7
26.	$PbSiO_3$	C	-258.8	27.0	-239.0
27.	Pb_2SiO_4	C	-312.7	43.0	-285.7
28.	Pb_2O_3	C			-98.42
29.	$PbBr_2$	C	-66.21	38.6	-62.24
30.	PbI_2	C	-41.85	42.3	-41.53
31.	PbH_2	S			69.5

(From Garrels and Christ, 1965, p.414)

TABLE A-1

LEAD DATA (Continued)

Explanation of Terms in Tables:

1) $\Delta H_F{}^\circ$ (kCal) - The heat of formation is the heat absorbed in the reaction involved in the formation of the compound from its elements in their standard states of any specified temperature (Garrels and Christ, 1965, p.308).

2) $\Delta F_F{}^\circ$ (kCal) - The free energy of formation is the free energy of the reaction to form one mole of the substances in their standard states from the stable elements under standard conditions. If $\Delta F_F{}^\circ$ is negative, then the product is stable relative to the reactants (Garrels and Christ, 1965, p.7).

3) S° (Cal/Deg) - When a substance absorbs heat from its surroundings, in any reversible process, at constant temperature T, its increase in entropy is given by the amount of heat absorbed divided by the absolute temperature ($dS = \frac{(C_p dT)}{T}$ (P constant) (Garrels and Christ, 1965, p. 313)

Appendix B - Activity Coefficient Methods

Debye-Hückel Method:

A number of authors, including MacInnes (1967, p.147), Newman (1973, p.83), and Pitzer and Brewer (1961, p.332) explain the Debye-Hückel relationship for determining activity coefficients in a dilute solution. This is the Debye-Hückel method for a single component relationship:

(B-1) $$\ln \gamma_j = \frac{-A z_j^2 \sqrt{I}}{1 + a_j^o B \sqrt{I}}$$

with: I_s = ionic strength = $\frac{1}{2} \sum m_j z_j^2$ (mole/kg)

$A = \frac{F^2 e \sqrt{2}}{8\pi (\varepsilon RT)^{3/2}} (\rho_o)$ $(\text{kg/mole})^{1/2}$

$B = \frac{F(\rho_o)}{(\varepsilon RT/2)^{1/2}}$ $\frac{(\text{kg/mole})^{1/2}}{A^o}$

γ_j = activity of the jth ion

a_j^o = experimental value dependent on the effective diameter of the central ion in solution (cm)

z_j = charge of the jth ion in solution

m_j = molality of the jth ion

ε = permittivity (farads/cm)

e = electronic charge (coulombs)

ρ_o = density of the pure solvent

Debye-Hückel used an electrostatic model, based on a "central ion" concept, to develop their expression, but this concept leads to a number of shortcomings which are mentioned by Newman (1973, p.85). "The expression of Debye and Hückel for the activity coefficients of ionic solutions is valid only in dilute solution. This restricted range of validity can be discussed in terms of neglected factors which would be important even in solutions of non-electrolytes, in terms of the mathematical approximation (author's insert: $\exp\left(\frac{-Z_j F\phi}{RT}\right) \cong 1 - \frac{Z_j F\phi}{RT}$), and from the point of view of sound application of the principles of statistical mechanics.

"The theory of Debye and Huckel gives specific consideration of only the long-range electrical interactions between ions. Even here, physical properties, such as the dielectric constant, are given values appropriate to the pure solvent. At higher concentrations, ion-solvent interactions and short-range interactions between ions become important. Solvation and association should not be ignored. These effects give contributions to the logarithm of the activity coefficient which are proportional to the solute concentrations even in solutions of non-electrolytes. Consequently, at concentrations where such terms are comparable to the square-root term, the Debye-Hückel theory can no longer adequately describe the thermodynamic properties. Refinement of the electrical contributions is not very useful unless these non-coulombic interactions are also accounted for." Newman adds though, "'Disappointly enough, it must be admitted that the rigorous justification of the D-H theory is the most important progress that has been made by the recent developments in the field of electrolyte theory.'"

Debye-Hückel Parameters for Aqueous Solutions

T, ^{o}C	0	25	50	75
α $(kg/mole)^{\frac{1}{2}}$	1.1324	1.1762	1.2300	1.2949
β $(kg/mole)^{\frac{1}{2}}$ A^{o}	0.3248	0.3287	0.3326	0.3368

For binary electrolyte solutions, additional terms are added for effects neglected in the single component Debye-Hückel expression (Newman, 1973, p.89):

$$\text{(B-2)} \quad \ln \gamma_{+-} = \frac{z_+ z_- A \sqrt{I_s}}{1 + B a_j^o \sqrt{I_s}} + A_2 m + A_3 m^{3/2} + A_4 m^2 + \cdots A_n m^{n/2}$$

with: m = molality of a single electrolyte (mole/kg)

For many purposes, it is sufficient to drop the terms beyond $A_2 m$ and write this term in the form:

$$\text{(B-3)} \quad A_2 = \frac{4 \nu_+ \nu_-}{\nu_+ + \nu_-} \beta$$

with: ν_+, ν_- = number of cations and anions into which a molecule of electrolyte dissociates

β = coefficient for ion-ion specific interactions

For multi-component electrolytes, Newman (1973, p.92) presents this equation:

$$\text{(B-4)} \quad \frac{G}{RT} = \frac{n_a \mu_a^o}{RT} + \sum_{j \neq o} \left[\ln (m_j \lambda_j^o) - 1 \right] - \frac{2}{3} A \sqrt{I_s}\, \Upsilon (B a \sqrt{I_s}) \sum_j z_j^2 n + \sum_{i \neq o} \sum_{j \neq o} \beta_{i,j} n_j m_j$$

with: $\tau(x) = \frac{3}{x^3}\left[\ln(1+x) - x + \frac{1}{2}x^2\right]$ (integration factor)

G = Gibbs free energy (joules)

a = mean diameter of ions (cm)

λ_j^o = property expressing secondary reference state (kg/mole)

μ_o^o = chemical potential of the pure solvent at the same temperature and pressure (joules/mole)

The first two terms on the right are the "ideal" contribution to the free energy, the third term represents the electrical contribution, and the fourth term is a first approximation of specific interactions between pairs of ions.

Differentiation of equation (B-4) will give the chemical potential of the solute species: $\mu_a = \left(\frac{\partial G}{\partial n_a}\right)_{T,p,n_B,\, B \neq A}$ with p = pressure:

(B-5) $$\frac{\mu_k}{RT} = \ln(m_k \lambda_k^o) - \frac{z_k^2 A \sqrt{I_s}}{1 + B_a \sqrt{I_s}} + 2 \sum_{j \neq o} \beta_{k,j}\, m_j$$

and for the chemical potential of the solvent:

(B-6) $$\frac{\mu_o}{RT} = \frac{\mu_o^o}{RT} - M_o \sum_{j \neq o} m_j + \frac{2}{3} A M_o I_s^{3/2}\, \sigma(B_a \sqrt{I_s}) - M_o \sum_{i \neq o} \sum_{j \neq o} \beta_{i,j}\, m_j\, m_j$$

with: M_o = molecular weight of species (g/mole)

$\sigma(x) = \frac{3}{x^3}\left[x - 2\ln(1+x) - \frac{1}{1+x} + 1\right]$ (integration factor)

The solute activity coefficients, then, are:

(B-7) $$\ln \gamma_k = \frac{z_k^2 A \sqrt{I_s}}{1 + B_a \sqrt{I_s}} + 2 \sum_{j \neq o} \beta_{k,j}\, m_j$$

Appendix C - Electrode Over-Potential

A number of books and articles including Delahay (1954 and 1965), Fried (1973), Mohiliner (1966), and Uhlig (1971) discuss over-potential in detail. Only facets which apply directly to ASV are mentioned here. This section is divided into three parts to facilitate the discussion: (1) inert electrodes; (2) the double layer at the electrode-solution interface; and (3) faradic and non-faradic current.

1) Inert Electrodes:

An inert electrode is an electrode made of material, such as graphite or platinum, which is chemically inactive in solution and does not react with the electrolyte over as wide a potential range as possible. The ideal working electrode includes properties of the ideal polarized electrode (in contrast to the reference or ideal non-polarized electrode). "The ideal polarized electrode has the unique capability of being in thermodynamic equilibrium at any potential whatever (within a certain range) although the temperature, pressure, and composition of its phases remain fixed," Mohiliner (1966, p.250).

As a further distinction between these two types of electrodes, a non-polarized electrode is a charge-transfer electrode because a conduction current (faradic) flows across the interface. Only displacement current (non-faradic) flows across the interface of an ideal polarized electrode. (This refers to reactions only between the solution and the electrode itself; i.e., there is not a faradic current flow because of the non-reactivity of the platinum working electrode and the solution.) Figure C-1 shows the current and potential

relationship for ideal polarizable and non-polarizable electrodes.

2) Double Layer at Electrode-Solution Interface:

In the simplest concept, when the electrode is in the electrolyte, an electric double layer forms (Figure C-2). This figure shows a positive charge on the electrode surface which is balanced by an equivalent negative charge boundary of ions or electrons in solution. Thus an excess of positive charge in the electrode side of the interface balances a negative charge of identical magnitude in the solution, forming the diffuse part of the double layer. If ions are adsorbed onto the electrode, a plane through the centers of the adsorbed ion layer defines the inner Helmholtz plane, while a plane through the ions in solution at the interface form the outer Helmholtz plane. The entire double layer configuration acts as a capacitor.

If two inert electrodes are placed in an electrolyte solution, and a potential is gradually applied between them, the double layer at each electrode is charged in a fashion similar to the charging capacitors. With each step increase of potential, a small current flows for a short period of time (milli-seconds or less) until there is equilibrium at the capacitor. This flow of current during the capacitor charging process is non-faradic because there are no chemical transformations at the interface. Figure C-3 shows schematic circuit diagrams of the electrode-solution interface.

The potential is increased gradually and eventually reaches a value which corresponds to the $E_{app.}$ value. A chemical reaction including either the oxidation or reduction of ions at the electrode surface

occurs. For a cathodic reaction, with the application of a negative potential the electrode acts as an electron source, attracting positive ions which are reduced at the electrode surface.

During this reaction a faradic, or charge-transfer, current flows (MacInnes, 1961, p.24):

(C-1) $q = nF$

with: q = electricity passed (coulombs)

n = number of chemical equivalents

F = Faraday's constant

3) Faradic and Non-Faradic Current:

The total current is the sum of the non-faradic capacity current and the faradic charge-transfer current. For the capacity current:

(C-2) $E_{app.} = q/C$

with: C = capacitance of the double layer (farads)

Taking the time derivative:

(C-3) $dq_c/dt = CdE_{app}/dt\ dC/dt$

with: q_c = electricity passed - capacitor (coulombs)

If the area of the electrode is constant:

(C-4) $i_c = CdE_{app}/dt$

with: i_c = capacitor current (amps/cm^2)

The only current flow from the capacitor is current from a changing potential (plus perhaps a small amount from capacitor leak).

For the charge-transfer current the time derivative of Faraday's Law is:

(C-5) $i_f = dq_f/dt = nFdM/dt$

with: q_f = electricity passed - faradic (coulombs)

i_f = faradic current (amps/cm^2)

The faradic current then is proportional to either the reduction or oxidation rate of reaction.

The total current is:

(C-6) $i_t = i_f + i_c = nFdM/dt + CdE_{app}/dt$

with: i_t = total current (amps/cm^2)

The first term is proportional to the rate of reaction and the second term to the rate of change of potential (Fried, 1973, p.14).

FIGURE C-1

CURRENT VS. POTENTIAL CURVES FOR IDEAL POLARIZABLE AND NON-POLARIZABLE ELECTRODES

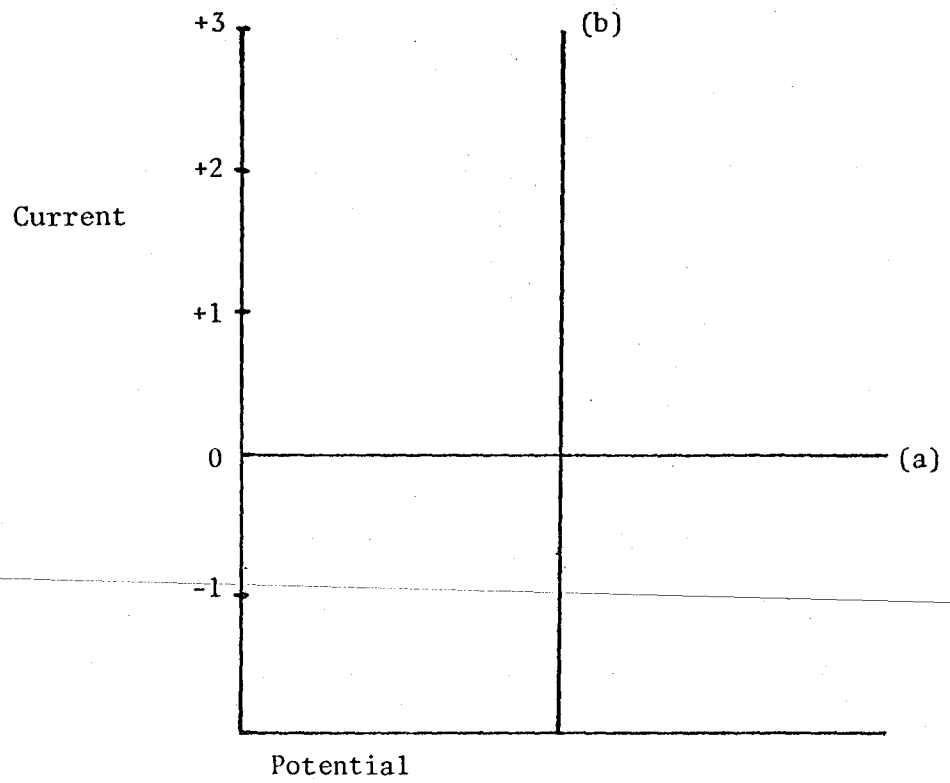

(a) = polarizable electrode

(b) = non-polarizable electrode

(Fried, 1973, p.21)

FIGURE C-2

SCHEMATIC DIAGRAM OF THE ELECTRICAL DOUBLE LAYER

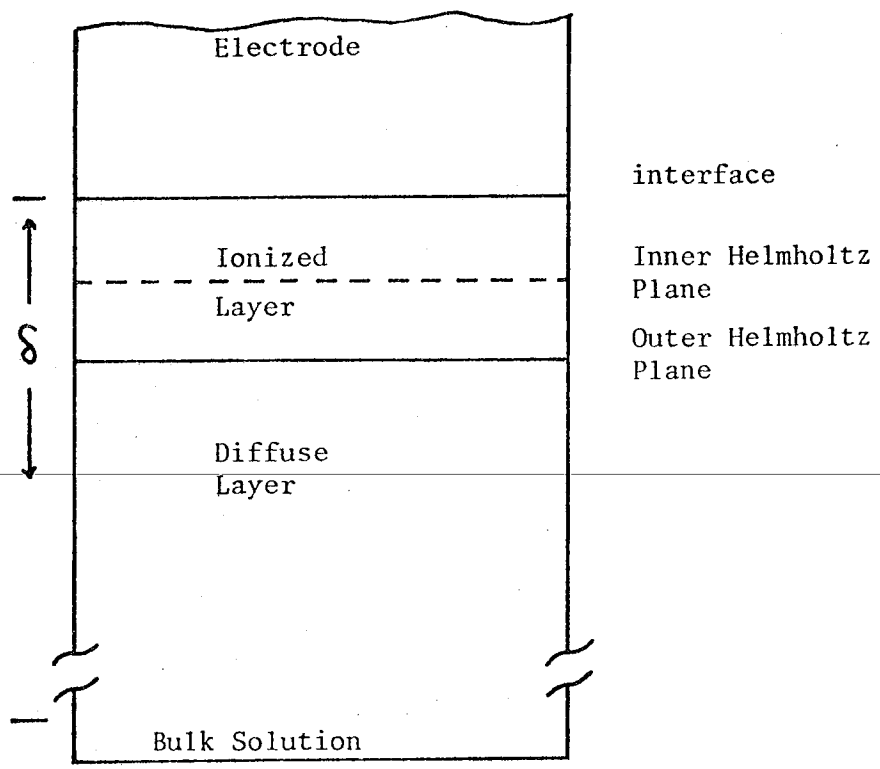

Double layer is approximately 10-100 Å in thickness (Mohilner, 1966, p.243)

FIGURE C-3

SCHEMATIC CIRCUIT DIAGRAM OF ELECTRODE - SOLUTION INTERFACE

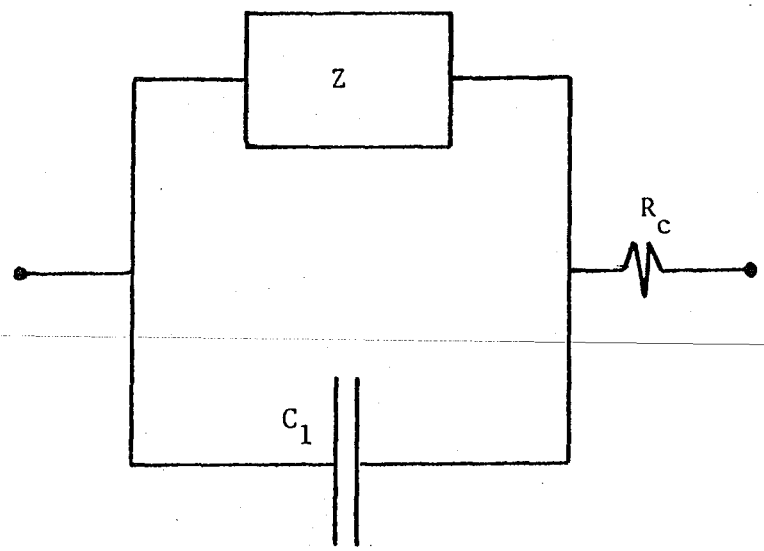

C_1 = double layer capacity

R_c = resistance of cell

Z = impedance

In summary, the double layer behaves like a capacitor in parallel to the oxidation or reduction electrode reaction. Current passing from the electrode to the solution, or from solution to electrode, is either a part of the charge-transfer reaction or contributes to the capacitor charge.

$E_{\frac{1}{2}}$ is the equilibrium ½ cell potential developed by an oxidation or a reduction reaction at a working electrode as predicted by the Nernst equation. The over-potential is the difference between the actual or polarization potential of the working electrode necessary for a faradic current to flow because of a charge-transfer reaction and the equilibrium potential of that electrode, $E_{\frac{1}{2}}$.

Appendix D - Sampling Techniques in San Francisco Bay

The following is a description of the techniques used to collect samples during the study by Girvin and others (1976, p.2) of trace elements in San Francisco Bay.

"All south bay ship channel and central bay reference samples were taken aboard the U.S. Geological Survey vessel RV Polaris. At all of these stations, except reference station 19, the ship was anchored before sampling began.

"The water and suspended particulate samples for trace element analyses were collected with a specially constructed pumping system. This system consisted of a high volume, Little Giant®, peristaltic pump; a 3/4 hp Dayton, reversible, variable speed, DC motor; a 20 m length of Dow Corning, 0.95 cm ID, silastic, medical grade tubing connected to 7 m of 0.95 cm ID polyethylene tubing; and a weighted collection device ("fish") which held the intake end of the silastic tubing.

"The 'fish' was constructed of a 1 m length of 2.3 cm ID, PVC pipe with four large, polyurethane coated, PVC fins welded to the tail. The intake tubing protruded 5 cm beyond the nose of the 'fish'. In operation, the 'fish' was balanced in a horizontal position with a stainless steel weight and faced into the prevailing current due to the stabilizing effect of the fins. The 'fish' was suspended at the deep water sampling depth of 2 m from nylon line which was attached to the end of a boom extending 8 m out from the side of the ship. A 14 kg, epoxy and polyurethane coated, weight was attached 2 m below the 'fish' with nylon line. All fittings were stainless steel.

"The deep water sample collection procedures were as follows: (1) the tubing was reverse flushed with deionized-distilled water while the 'fish' was being lowered through the surface of the water to the 2 m sampling depth; (2) 8 ℓ of bay water were pumped through the tubing and discarded; (3) 2-4 ℓ of bay water were pumped into an 8 ℓ polyethylene carboy; (4) the carboy was shaken and the water was discarded; (5) 8 ℓ of sample were pumped into the carboy; (6) incoming bay water was filtered to collect the suspended particulate sample; and (7) the tubing was reverse flushed with deionized-distilled water while the 'fish' was being removed from the water.

"The water samples collected in the 8 ℓ polyethylene carboy were filtered through a 142 mm diameter, 0.2 μm pore size, Nucleopore membrane filter. Positive pressure for filtration was supplied by a Masterflex peristaltic pump. The suspended particulate samples were filtered directly through a 293 mm diameter, 0.4 μm (July) or 0.2 μm (September-October) pore size, Nucleopore membrane filter using positive pressure supplied by the sample collection pump. Both filters were supported in lucite plastic holders equipped with silicone O-rings. Silastic tubing (0.48 cm ID and 0.95 cm ID) with polypropylene fittings was used in the construction of the filtration apparatus. (Note from Case: this work was done in a positive pressure "clean" air box.)

"For each station, 3 ℓ of filtrate from the 142 mm filter collected in 1 ℓ and 2 ℓ, Bel-Art, common polyethylene bottles after allowing an initial 1.5 ℓ of filtrate to pass through the filter. The 142 mm and 293 mm filter membranes, with the filtered suspended particulates intact, were composited and stored in a polyethylene freezer container at $4^{o}C$.

"To prevent the loss of dissolved trace elements to the walls of the polyethelene bottles, the water samples were acidified immediately with twice distilled nitric acid (HNO_3) prepared by the National Bureau of Standards (NBS). The 1 ℓ samples for the determination of cadmium (Cd), copper (Cu), lead (Pb), and zinc (Zn) were made to pH 2 with 0.62 ml of concentrated HNO_3. The 2 ℓ samples for the determination of silver (Ag) were made to pH 1 with 10 ml of concentrated HNO_3. (Note from Case: One half of my samples were not acidified.)

"The two shallow water trace element samples were collected at high tide in approximately 2.0 - 2.5 m of water from a 16 ft. Boston Whaler equipped with an outboard motor. During sampling the boat was headed into the prevailing current at low speed.

"The samples were obtained with a scaled down version of the shipboard pumping system. This smaller system consisted of a Masterflex peristaltic pump, and a 7 m length of Dow Corning, 0.48 cm ID, silastic, medical grade tubing. The intake end of the tubing was suspended at the shallow water sampling depth of 1 m from a nylon line held 3 m out from the side of the boat with an aluminum pole. A 2 kg plastic coated weight was attached to the line 1 m below the intake.

"The water sample collection procedures from the small boat were as follows: (1) the tubing was reverse flushed with deionized-distilled water while the intake was being lowered through the surface of the water to the 1 m sampling depth; (2) 4 ℓ of bay water were pumped through the tubing and discarded; (3) 8 ℓ of sample were pumped into an 8 ℓ polyethylene carboy; and (4) the tubing was reverse flushed with deionized-distilled water while the intake was being removed from the water. The

sample was then returned to the ship and immediately processed in the same manner as the shipboard collected water samples.

"All shipboard and small boat sampling apparatus which came into contact with water and suspended particulate samples was thoroughly cleaned in order to eliminate possible trace element contamination. In the laboratory, the silastic and polyethylene tubing was filled with 1:10 HNO_3 for 12 hours and then rinsed with deionized-distilled water for 30 minutes. After assembly of the shipboard sampling apparatus, the 'fish' with the tubing in place was partially lowered into a reservoir of 1:10 HNO_3, and the acid was pumped through the entire system for 20 minutes. The system was then flushed with deionized-distilled water for 20 minutes. The 8 ℓ, polyethylene, water sample reservoirs and the Bel-Art, polyethylene, sample containers were washed with soap and water, rinsed with deionized-distilled water, filled with 1:10 HNO_3 for 48 hours, and rinsed thoroughly with deionized-distilled water. The lucite filter holders were similarly cleaned, except that the acid contact time was 24 hours."

REFERENCES

Adams, R.N., 1963, Voltammetry at Electrodes with Fixed Surfaces; Chap. 47 in Treatise on Analytic Chemistry, Kolthoff & Elvring (ed.), John Wiley & Sons, New York, N.Y., p.2380 - 2408.

Arrhenius, S., 1887, Uber die Dissociation der in Wasser gelosten Stoffe; in Zeitschrift Fur Physikalische Chemie, vol. 1, p.631 - 648.

Ballinger, D.G., 1972, Instruments for Water Quality Monitoring; in Environmental Science and Technology, vol. 6, no. 2, p.130 - 133.

Ballinger, D.G., 1972, Monitoring for Trace Metals - Water Environment; Cycling and Control of Metals; Proceedings of an Environmental Resources Conference, National Environmental Research Center, Cincinnati, Ohio, p.145 - 148.

Barendrecht, E., 1967, Stripping Voltammetry; in Electroanalytical Chemistry, Bard, A.J. (ed.), Marcel Dekker, Inc., New York, N.Y., p.53 - 109.

Batley, G.E., and Florence, T.M., 1974, An Evaluation and Comparison of Some Techniques of Anodic Stripping Voltammetry; in Journal of Electroanalytical Chemistry, vol. 55, p.23 - 43.

Batley, G.E., and Florence, T.M., 1976, Determination of the Chemical Forms of Dissolved Cadmium, Lead and Copper in Sea Water; in Marine Chemistry, vol. 4, p.347 - 363.

Bond, A.M., 1973, Polarographic Procedures Without Removal of Oxygen, and Other Approaches to Making the Determinations More Rapidly; in Talanta, vol. 20, p.1139 - 1152.

Bradford, W.L., 1973, The Determination of a Stability Constant for Aqueous Complex $Zn(OH)_2^o$ Using Anodic Stripping Voltammetry; in Limnology and Oceanography, vol. 18, p.757 - 762.

Brainina, Kh.Z., 1971, Film Stripping Voltammetry; in Talanta, vol. 18, p.513 - 539.

Branham, D.W. and Coste, J.W., 1971, The State-Of-The-Art of Oceanographic Sensors; in Marine Technology Society Journal, vol. 5, no. 3, p.27 - 30.

Breck, W.G., 1974, Redox Levels in the Sea; Chap. 4 in The Sea, Goldberg, E.D. (ed.), vol. 5, part I, John Wiley & Sons, New York, N.Y., p.153 - 179.

Brown, F.S., Baedecker, M.J., Nissenbaum, A., Kaplan, I.R., 1972, Early Diagenesis in a Reducing Fjord, Saanich Inlet, British Columbia - III. Changes in Organic Constituents of Sediment; in Geochemica et Cosmochimica Acta, vol. 36, p.1185 - 1203.

Cantwell, E.N.; Jacobs, E.S.; Kunz, Jr., W.G.; and Liberi, V.E., 1972, Control of Particulate Lead Emissions from Automobiles; from Cycling and Control of Metals, Proceedings of an Environmental Resources Conference, National Environmental Research Center, Cincinnati, Ohio, p.95 - 107.

Carritt, D.E., 1963, Chemical Instrumentation; Chap. 5 in The Sea, Hill, M.N. (ed.), vol. 2, part I, John Wiley & Sons, New York, N.Y., p.109 - 127.

Case, C.W., Wilde, P., and Jenkins, D., 1975, Trace Metal Analyses by Anodic Stripping Voltammetry in Marine Environments, Part I - Adaptation for Field Measurements; Univ. Calif. Comm. Ocean Eng., Rept. COOE 1-11, 30p.

Chow, T.J., Bruland, K.W., Bertine, K., Soutar, A., Koide, M., and Goldberg, E.D., 1973, Lead Pollution: Records in Southern California Coastal Sediments; in Science, vol. 181, p.551 - 552.

Chow, T.J. and Patterson, C.C., 1962, The Occurrence and Significance of Lead Isotopes in Pelagic Sediments; in Geochemica et Cosmochimica Acta, vol. 26, p.263 - 298.

Clem, R.G., 1973, Rapid Anodic Stripping Analysis; in McKee - Pedersen Instruments Applications Notes, vol. 8, no. 1, p.1 - 8.

Clem, R.G., Litton, G., and Ornelas, L.D., 1973, New Cell for Rapid Anodic Stripping Voltammetry Analysis; in Analytical Chemistry, vol. 45, no. 8, p.1306 - 1316.

Clem, R.G., 1975, Cause of Loss of Hydrogen-Overvoltage on Graphite Electrodes Used for Anodic Stripping Voltammetry; in Analytical Chemistry, vol. 47, p.1778 - 1784.

Clem, R.G. and Sciamanna, A.F., 1975, Styrene Impregnated, Cobalt - 60 Irradiated, Graphite Electrode for Anodic Stripping Analysis; in Analytical Chemistry, vol. 47, p.276 - 280.

Corwin, R.F., 1973, Offshore Application of Self Potential Prospecting, PhD Thesis, Univ. Calif. Comm. Ocean Eng. Rept. COOE 1-7, 303p.

CRC, 1966, Handbook of Chemistry and Physics, 57th Ed., Chemical Rubber Co., Cleveland, Ohio, I - 18p.

Day, R.A. Jr. and Underwood, A.L., 1967, Quantitative Analysis; 2nd Ed., Prentice - Hall, Inc., Englewood Cliffs, N.J., 482p.

Delahay, P., 1954, New Instrumental Methods in Electrochemistry; Interscience Publishers, Inc., New York, N.Y., 437p.

Delahay, P., 1957, Instrumental Analysis; MacMillan Company, New York, N.Y., 384p.

Delahay, P., 1965, Double Layer and Electrode Kinetics; John Wiley & Sons, Inc., New York, N.Y., 321p.

Desoer, C.A. and Kuh, E.S., 1969, Basic Circuit Theory; McGraw-Hill Book Company, San Francisco, Calif., 876p.

Dittmar, W., 1884, Report on Researches into the Composition of Ocean Water, Collected by H.M.S. Challenger; Challenger Reports, Physics and Chemistry, vol. 1, p.1 - 251.

Ellis, W.D., 1973, Anodic Stripping Voltammetry; in Chemical Instrumentation, vol. 50, p.131 - 147.

Enke, C.G. and Baxter, R.A., 1964, A Versatile and Inexpensive Controlled Potential Polarographic Analyzer; in Journal of Chemical Ed., vol. 41, p.202 - 209.

Ernst, R., Allen, H.E., and Mancy, K.H., 1974, Characteristics of Trace Metal Species and Measurement of Trace Metal Stability Constants by Electroanalytical Techniques, in Water Resources, vol. 9, p.969 - 979.

Ewing, G.W., 1960, Instrumental Methods of Chemical Analysis; 2nd Ed., McGraw-Hill Book Company, Inc., New York, N.Y., 454p.

Faraday, M., 1834, Experimental Researches in Electricity; Everyman's Library.

Fick, A., 1855, Annalen der Physik, vol. 94, p.59.

Fleischer, M., 1972, Natural Sources of Some Trace Elements in the Environment; from Cycling and Control of Metals, Proceedings of an Environmental Resources Conference, National Environmental Research Center, Cincinnati, Ohio, p.3 - 10.

Florence, T.M., 1970, Determination of Iron by Anodic Stripping Voltammetry; in Journal of Electroanalytical Chemistry, vol. 26, p.293 - 298.

Florence, T.M., 1970, Anodic Stripping Voltammetry with a Glassy Carbon Electrode Mercury Plated In Situ; in Journal of Electroanalytical Chemistry, vol. 27, p.273 - 281.

Florence, T.M., 1972, Determination of Trace Metals in Marine Samples by Anodic Stripping Voltammetry; in Journal of Electroanalytical Chemistry, vol. 35, p.237 - 245.

Florence, T.M. and Batley, G.E., 1976, Trace Metals Species in Sea Water - I; in Talanta, vol. 23, p.179 - 186.

Forchhammer, G., 1865, Philosophical Transactions of the Royal Society; no. 155, p.203 - 262.

Fried, I., 1973, The Chemistry of Electrode Processes; Academic Press, London, England, 225p.

Garrels, R.M. and Christ, C.L. 1965, Solutions, Minerals, and Equilibria; Harper & Row, New York, N.Y., 450p.

Garrels, R.M. and Thompson, M.E., 1962, A Chemical Model for Sea Water at 25°C and One Atmosphere Total Pressure; in American Journal of Science, vol. 260, p.57 - 66.

Gibbs, J.W., 1948, On the Equilibrium on Heterogeneous Substances; from The Collected Works of J. Willard Gibbs, vol. 1, Yale University Press (1948).

Gibb, T.R.P. Jr., 1975, Analytic Methods in Oceanography; Advances in Chemistry Series #141, American Chemical Society, Washington, DC, 238p.

Gilbert, T.R. and Hume, D.N., 1973, Direct Determination of Bismuth and Antimony in Sea Water by Anodic Stripping Voltammetry; in Analytica Chemica Acta, no. 65, p.451 - 459.

Girvin, D.C., Hodgson, A.T., Tatro, M., and Anaclerio, R., 1976, Seasonal and Spatial Variations in Solute and Particulate Associated Concentrations of Trace Elements in South San Francisco Bay; First Quarterly Report to the Regional Water Quality Control Board San Francisco Bay Region, by Energy & Environment Division, Lawrence Berkeley Laboratory, Berkeley, Calif. 23p.

Goldberg, E.D., 1965, Minor Elements in Sea Water; Chap. 5 in Chemical Oceanography, Riley, J.P. and Skirrow, G. (ed.) vol. I, Academic Press, New York, N.Y., P.163 - 196.

Goldberg, E.D., 1972, Baseline Studies of Heavy Metal Halogenated Hydrocarbon, and Petroleum Hydrocarbon Pollutants in the Marine Environment and Research Recommendations; Deliberations of the International Decade of Ocean Exploration Baseline Conference, 54p.

Gross, M.G., 1967, Concentrations of Minor Elements in Diatomaceous Sediments of a Stagnant Fjord; in Estuaries, American Association for the Advancement of Science Symposium No. 83, p.273 - 282.

Gucluer, S.M. and Gross, M.G., 1964, Recent Marine Sediments in Saanich Inlet, A Stagnant Marine Basin; in Limnology and Oceanography, vol. 9, p.359 - 376.

Guillaumin, J.C., 1974, Determination of Trace Metals in Power Plant Effluents; in Atomic Absorption Newsletter, vol. 13, no. 6, p.135 - 139.

Gurney, R.W., 1953, Ionic Processes in Solution; Dover, New York, N.Y., 275p.

Hampel, C.A. and Hawley, G.G., 1973, The Encyclopedia of Chemistry, 3rd. Ed., Van Norstrand Reinhold Company, New York, N.Y., 1198p.

Handbook of Geochemistry, 1974, Wedepohl, K.H. (ed.), vol. II-4, Springer - Verlag, New York, N.Y.

Harned, H.S. and Owen, B.B., 1958, Physical Chemistry of Electrolytic Solutions; Reinhold Publishing Co., New York, N.Y., 803p.

Hawks, H.E. and Webb, J.S., 1962, Geochemistry in Mineral Exploration; Harper & Row, New York, N.Y., 415p.

Herlinveaux, R.H., 1962, Oceanography of Saanich Inlet in Vancouver Island, British Columbia; Journal of Fisheries Resource Board Canada, vol. 19, p.1 - 37.

Heyrovsky, J., 1922, Elektrolysa se Rtutovou Kapkovou Kathodou; Chem. Listy, no. 16, p.256.

Hoare, J.P., 1968, The Electrochemistry of Oxygen; Interscience Publishers, New York, N.Y., 423p.

Holland, H.D., 1972, The Geologic History of Sea Water - An Attempt to Solve the Problem; in Geochemica et Cosmochimica Acta, vol. 36, no. 6, p.637 - 652.

Hume, D., 1973, Pitfalls in the Determination of Environmental Trace Metals; in Chemical Analysis of the Environment and Other Modern Techniques, vol. 5, Plenum Press, New York, N.Y., p.3 - 17.

Hume, D.N., 1975, Fundamental Problems in Oceanographic Analysis: Analytic Methods in Oceanography; in Advances in Chemistry #147, American Chemical Society, Washington, DC, p.1 - 9.

Ilkovic, D., 1934, Polarographic Studies with the Dropping Mercury Cathode Part XLIV. The Dependence of Limiting Currents on the Diffusion Constant, on the Rate of Dropping, and on the Size of Drops; Collection Czechoslov. Chem. Communus, vol. 6, p.498.

Ives, D.J.G. and Janz, G.J., 1961, Reference Electrodes Theory and Practice; Academic Press, New York, N.Y., 651p.

Klein, J.H. and Diamond, S., 1974, Simultaneous Determination of Zinc, Lead, and Cadmium Ion Concentrations in Contaminated Sea Water Using Direct Current Polarography; in Interim Rept. for Environmental Protection Res. & Dev. Team, USNA-EPRD, 14p.

Klotz, I.M., 1950, Chemical Thermodynamics; Prentice-Hall, Inc. Englewood Cliffs, N.J., 369p.

Kramer, J.R., 1965, History of Sea Water; in Geochimica et Cosmochimica Acta, vol. 29, p.921 - 945.

Krauskopf, K.B., 1967, Introduction to Geochemistry; McGraw-Hill Book Company, San Francisco, Calif., 721p.

Latimer, W.M., 1952, Oxidation Potentials; Prentice-Hall, Inc., New York, N.Y., 392p.

Leyendekkers, J.V., 1973, The Chemical Potentials of Seawater Components; in Marine Chemistry, vol. 1, no. 2, p.75 - 88.

Livingstone, D.A., 1963, Data of Geochemistry; 6th Edition, Chap. G, Chemical Composition of Rivers and Lakes; Geological Survey Professional Paper 440-G, U.S. Gov. Printing Office, Washington, DC, 64p.

Long, D.T. and Angino, E.E., 1977, Chemical Speciation of Cd, Cu, Pb and Zn in Mixed Freshwater, Seawater, and Brine Solution; in Geochimica et Cosmochimica Acta, vol. 41, p.1183 - 1191.

Losev, L.L., 1972, Mechanisms of Stepwise Electrode Processes on Amalgams; Chap. 5 in Modern Aspects of Electrochemistry, Plenum Press, New York, N.Y., vol. 7, p.314 - 398.

MacInnes, D.A., 1961, The Principles of Electrochemistry; Dover, New York, N.Y., 478p.

Mancy, K.H., 1972, Trace Metal Characterization by Anodic Stripping Voltammetry; in Water Pollution Research, Pergamon Press, Ltd., New York, N.Y., p.1 - 10.

Manheim, F., 1961, In Situ Measurements of pH and Eh in Natural Waters and Sediments; in Stockholm Contributions in Geology, vol. VIII, no. 3, p.26 - 36.

Martin, D.F., 1972, Marine Chemistry, vols. I and II, Marcel Dekker, Inc., New York, N.Y., 389p. and 451p.

Matson, W.R., Roe, D.K., and Carritt, D.E., 1965, A Composite Mercury Graphite Electrode for Anodic Stripping Voltammetry; in Analytic Chemistry, vol. 37, no.12, p.1594 - 1595.

Maxwell, J.C., 1891, A Treatise on Electricity and Magnetism; Dover edition, 1954, vol. I and II, New York, N.Y., 506p. and 500p.

Meites, L., 1963, Voltammetry at the Dropping Mercury Electrode (Polarography); Chap. 46 in Treatise on Analytic Chemistry, Kolthoff and Elving (ed.), vol. 4, part I, John Wiley & Sons, New York, N.Y., p.2303 - 2379.

Moelwyn - Hughes, E.A., 1947, The Kinetics of Reactions in Solutions; Claredon Press, Oxford, England, 424p.

Mohilner, D.M., 1966, The Electrical Double Layer, Part I; Elements of Double Layer Theory; in Electroanalytical Chemistry, Bard, A.J. (ed.), vol. 1, Marcel Dekker, Inc., New York, N.Y., p.241 - 409.

National Academy of Sciences, 1971, Marine Environmental Quality; Ocean Science Committee of the NAS-NRC Ocean Affairs Board, August 9-13, 1971, National Academy of Sciences, Washington, DC, 107p.

National Academy of Sciences, 1975, Assessing Potential Ocean Pollutants; National Academy of Sciences, Washington, DC, 438p.

National Academy of Sciences, 1975, Petroleum in the Marine Environment; May 21-23, Airlie House, Airlie Virginia, National Academy of Sciences, Washington, DC, 107p.

National Academy of Sciences, 1976, Disposal in the Marine Environment: An Oceanographic Assessment; National Academy of Sciences, Washington, DC, 76p.

Nernst, W.Z., 1889, Uber Freie Jonen; in Zeitschrift Fur Physikalische Chemie, vol. 3, p.120 - 144.

Newman, J.S., 1973, Electrochemical Systems; Prentice-Hall, Inc., Englewood Cliffs, N.J., 432p.

Newman, J.S., 1967, Transport Processes in Electrolytic Solutions; in Advances in Electrochemistry and Electrochemical Engineering, Tobias, C.W. and Delahay, P. (ed.), vol. 5, John Wiley & Sons, New York, N.Y., 325p.

Nissenbaum, A., Presley, B.J., Kaplan, I.R., 1972, Early Diagenesis in a Reducing Fjord, Saanich Inlet, British Columbia - I. Chemical and Isotopic Changes in Major Components of Interstitial Water; in Geochimica et Cosmochimica Acta, vol. 36, p.1007 - 1027.

Osteryoung, J.G. and Osteryoung, R.A., 1972, Pulse Polarographic Analysis of Toxic Heavy Metals; in American Lab., July, 1972, p.1 - 8.

Pauling, L., 1970, General Chemistry; 3rd. Ed., W.H. Freeman and Company, San Francisco, Calif., 959p.

Perone, S.P., 1963, The Application of Stripping Analysis to the Determination of Silver (1), Using Graphite Electrodes; in Analytic Chemistry, Dec., 1963, vol. 35, p.2091 - 2094.

Perone, S.P. and Birk, J.R., 1965, Application of Derivative Techniques to Anodic Stripping Voltammetry; in Analytic Chemistry, Jan. - Apr., 1965, vol. 37, p.9 - 12.

Perone, S.P. and Kretlow, W.J., 1965, Anodic Stripping Voltammetry of Mercury at the Graphite Electrode; in Analytic Chemistry, Apr. - Jan., 1965, vol. 38, p.968 - 970.

Pickard, G.L., 1963, Descriptive Physical Oceanography; Pergamon Press, New York, N.Y., 200p.

Stulik, K. and Hora, V., 1976, Continuous Voltammetric Measurements with Solid Electrodes, Part I; in Journal of Electroanalytical Chemistry, vol. 70, p.253 - 263.

Stumm, W. and Morgan, J.J., 1970, Aquatic Chemistry; Wiley-Interscience, New York, N.Y., 583p.

Subramanian, G. and Prabhakara Rao, G., 1976, Evaluation of Mercury Coated Glassy Carbon Electrodes for Oscillographic Polarography; in Journal of Electroanalytical Chemistry, vol. 70, p.133 - 140.

Sverdrup, H.U., Johnson, M.W., and Fleming, R.H., 1942, The Oceans; Prentice-Hall, Inc., Englewood Cliffs, N.J., 1087p.

Tully, J.P. and Dodimead, A.J., 1957, Properties of the Water in the Strait of Georgia, British Columbia, and Influencing Factors; in Journal of Fisheries Resource Board of Canada, vol. 14, p.241 - 319.

Uhlig, H.H., 1971, Corrosion and Corrosion Control, 2nd Edition; John Wiley & Sons, Inc., New York, N.Y., 419p.

Velikov, B.L. and Dolezal, J., 1976, The Use of Complexing Agents in the Polarographic Analysis of Inorganic Compounds; in Journal of Electroanalytic Chemistry, vol. 71, p.91 - 102.

Volbrath, A., 1969, Elemental Analysis in Geochemistry A. Major Elements; Methods in Geochemistry and Geophysics; vol. 8, Elsevier Publishing Company, New York, N.Y., 373p.

West, F.K., West. P.W., and Iddings, F.A., 1966, Adsorption of Traces of Silver on Container Surfaces; in Analytical Chemistry, vol. 38, no. 11, p.1566 - 1570.

Whitfield, M., 1972, Progress Towards a Chemical Model for Sea Water; in Proceedings Royal Society of Edinburgh, sec. b, vol. 72, p.289 - 399.

Whitfield, M., 1973, A Chemical Model for the Major Electrolyte Component of Seawater Based on the Brønsted-Guggenheim Hypothesis; in Marine Chemistry, vol. I, no. 4, p.251 - 266.

Whitfield, M., 1974, A Comprehensive Specific Interaction Model for Sea Water. Calculation of the Osmotic Coefficient; in Deep Sea Research, vol. 21, p.57 - 67.

Whitfield, M., 1975, The Extension of Chemical Models for Sea Water to Include Trace Components at 25°C and 1 Atm. Pressure; in Geochemica et Cosmochimica Acta, vol. 39, p.1545 - 1557.

Whitfield, M., 1975, The Electroanalytical Chemistry of Sea Water; Chap. 20 in Chemical Oceanography, Riley, J.P. and Skirrow, G. (ed.), vol. 4, Academic Press, New York, N.Y., 362p.

Whitnack, G.C. and Sasselli, R., 1969, Application of Anodic Stripping Voltammetry to the Determination of Some Trace Elements in Sea Water; Analytica Chimica Acta, vol, 47, p.267 - 274.

Wilde, P. and Rodgers, P.W., 1970, Electrochemical Meter for Activity Measurements in Natural Environments; in the Review of Scientific Instruments, vol. 41, no. 3, p.356 - 358.

Willard, H.H., Merritt, L.L., and Dean, J.A., 1974, Instrumental Methods of Analysis, 5th Edition; Van Nostrand Company, New York, N.Y., 860p.

Wilson, E.B. Jr., 1952, An Introduction to Scientific Research; McGraw-Hill Book Company, Inc., New York, N.Y., 373p.

Wixon, B.G., Bolter, E., Gale, N.L., Jennett, J.C., and Purushothaman, 1972, The Lead Industry as a Source of Trace Metals in the Environment; from Cycling and Control of Metals, Proceedings of an Environmental Resources Conference, National Environmental Research Center, Cincinnati, Ohio, p.11 - 19.

Young, D.R., Young, C-S., and Hlavka, G.E., 1972, Sources of Trace Metals from Highly-Urbanized Southern California to the Adjacent Marine Ecosystem; from Cycling and Control of Metals, Proceedings of an Environmental Resources Conference, National Environmental Research Center, Cincinnati, Ohio, p.21 - 39.

Zbinden, C., 1931, Nouvelle Methodé du Microdosage de L'ion Cuivre; in Sociéte de Chimie Biologique, vol. 13, p.35 - 40.

Zirino, A. and Healy, M.L., 1970, Inorganic Zinc Complexes in Sea Water; in Limnology and Oceanography, vol. 15, p.956 - 958.

Zirino, A. and Healy, M.L., 1972, pH-Controlled Differential Voltammetry of Certain Trace Transition Elements in Natural Waters; in Environmental Science Tech., vol. 6, p.243 - 249.

Zirino, A. and Yamamoto, S., 1972, a pH Dependent Model for the Chemical Speciation of Copper, Zinc, Cadmium, and Lead in Sea Water; in Limnology and Oceanography, vol. 17, no. 5, p.661 - 671.

Zirino, A. and Lieberman, S.H., 1974, Automated Anodic Stripping Voltammetry for the Measurement of Copper, Zinc, Cadmium, and Lead in Sea Water; in Analytical Methods in Oceanography, T.R.P. Gibbs, Jr. (ed.), Advances in Chemistry Series #147, American Chemical Society, Washington, DC, p.82 - 98.

This report was done with support from the Department of Energy. Any conclusions or opinions expressed in this report represent solely those of the author(s) and not necessarily those of The Regents of the University of California, the Lawrence Berkeley Laboratory or the Department of Energy.

TECHNICAL INFORMATION DEPARTMENT
LAWRENCE BERKELEY LABORATORY
UNIVERSITY OF CALIFORNIA
BERKELEY, CALIFORNIA 94720